

1           **Ice, Cloud, and Land Elevation Satellite 2 (ICESat-2)**  
2  
3           **Algorithm Theoretical Basis Document (ATBD)**  
4           **for**  
5           **Land - Vegetation Along-Track Products (ATL08)**

6  
7           **Contributions by Land/Vegetation SDT Team Members**  
8           **and ICESat-2 Project Science Office**

9           **(Amy Neuenschwander, Katherine Pitts, Benjamin Jelley, John Robbins,**  
10           **Jonathan Markel, Sorin Popescu, Ross Nelson, David Harding, Dylan**  
11           **Pederson, Brad Klotz, and Ryan Sheridan)**

12  
13                   **ATBD prepared by**  
14                   **Amy Neuenschwander**

15  
16                   **15 October 2024**

17           **(This ATBD Version corresponds to release 007 of the ICESat-2 ATL08**  
18           **data)**

19  
20           **Content reviewed: technical approach, assumptions, scientific soundness,**  
21           **maturity, scientific utility of the data product**

22  
23           **This document may be cited as:**

24           Neuenschwander, A., K. Pitts, B. Jelley, J. Robbins, J. Markel, S. Popescu, R. Nelson,  
25           D. Harding, D. Pederson, B. Klotz, and R. Sheridan (2024). *Ice, Cloud, and Land*  
26           *Elevation Satellite (ICESat-2) Project Algorithm Theoretical Basis Document (ATBD) for*  
27           *Land - Vegetation Along-Track Products (ATL08), Version 7.* ICESat-2 Project, DOI:  
28           10.5067/JDZIJEU0L481.  
29

30 **ATL08 algorithm and product change history**  
31

ATBD Version	Change
2016 Nov	Product segment size changed from 250 signal photons to 100 m using five 20m segments from ATL03 (Sec 2)
2016 Nov	Filtered signal classification flag removed from classed_pc_flag (Sec 2.3.2)
2016 Nov	DRAGANN signal flag added (Sec 2.3.5)
2016 Nov	Do not report segment statistics if too few ground photons within segment (Sec 4.17 (3))
2016 Nov	Product parameters added: h_canopy_uncertainty, landsat_flag, d_flag, delta_time_beg, delta_time_end, night_flag, msw_flag (Sec 2)
2017 May	Revised region boundaries to be separated by continent (Sec 2)
2017 May	Alternative DRAGANN parameter calculation added (Sec 4.3.1)
2017 May	Set canopy flag = 0 when <i>L-km</i> segment is over Antarctica or Greenland regions (Sec 4.4 (1))
2017 May	Change initial canopy filter search radius from 3 m to 15 m (Sec 4.11 (6))
2017 May	Product parameters removed: h_rel_ph, terrain_thresh
2017 May	Product parameters added: segment_id, segment_id_beg, segment_id_end, dem_flag, surf_type (Sec 2)
2017 July	Urban flag added (Sec 2.4.20)
2017 July	Dynamic point spread function added (Sec 4.13 (6))
2017 July	Methodology for processing <i>L-km</i> segments with buffer added (Sec 4.1 (2), Sec <b>Error! Reference source not found.</b> )
2017 July	Revised alternative DRAGANN methodology ( <del>see bolded text in</del> Sec 4.3.1)
2017 July	Added post-DRAGANN filtering methodology (Sec 4.9)
2017 July	Updated SNR to be estimated from superset of ATL03 and DRAGANN found signal used for processing ATL08 (Sec 2.5.18)
2017 September	More details added to DRAGANN description (Sec 4.3), and corrections to DRAGANN implementation (Sec 3.1.1, Sec 4.3 (9))
2017 September	Added Appendix A – very detailed DRAGANN description
2017 September	Revised alternative DRAGANN methodology (see bolded text in Sec 4.3.1)
2017 September	Clarified SNR calculation (Sec 2.5.18, Sec 4.3 (18))
2017 September	Added cloud flag filtering option
2017 September	Added top of canopy median surface filter (Sec 3.5 (a), Sec 4.12 (3), Sec 4.14 (1-3))

2017 September	Modified 500 canopy photon segment filter (Sec 3.5 (c), Sec 4.14 (6))
2017 November	Added solar_azimuth, solar_elevation, and n_seg_ph to Reference Data group; parameters were already in product (Sec 2.4)
2017 November	Specified number of ground photons threshold for relative canopy product calculations (Sec 4.18 (2)); no number of ground photons threshold for absolute canopy heights (Sec 4.18.1 (1))
2017 November	Changed the ATL03 signal used in superset from all ATL03 signal (signal_conf_ph flags 1-4) to the medium-high confidence flags (signal_conf_ph flags 3-4) (Sec 3.1, Sec 4.3 (17))
2017 November	Removed Date parameter from Table 2.4 since UTC date is in file metadata
2018 March	Clarified that cloud flag filtering option should be turned off by default
2018 March	Changed h_diff_ref QA threshold from 10 m to 25 m (Table 5.2)
2018 March	Added absolute canopy height quartiles, canopy_h_quartile_abs ( <i>Later removed</i> )
2018 March	Removed psf_flag from main product; psf_flag will only be a QAQC alert (Sec 5.2)
2018 March	Added an Asmooth filter based on the reference DEM value (Sec 4.6 (4-5))
2018 March	Changed relief calculation to 95 <sup>th</sup> – 5 <sup>th</sup> signal photon heights. (Sec 4.6 (6))
2018 March	Adjusted the Asmooth smoothing methodology (Sec 4.6 (8))
2018 March	Recalculate the Asmooth surface after filtering outlying noise from signal, then detrend signal height data (Sec 4.9 (3-4))
2018 March	Added option to run alternative DRAGANN process again in high noise cases (Sec 4.3.3)
2018 March	Changed global land cover reference to MODIS Global Mosaics product (Sec 2.4.16)
2018 March	Adjusted the top of canopy median filter thresholds based on SNR (Sec 4.14 (1-2))
2018 March	Added a final photon classification QA check (Sec 4.16, Table 5.2)
2018 March	Added slope adjusted terrain parameters ( <i>Later removed</i> )
2018 June	Replaced slope adjusted terrain parameters with terrain best fit parameter (Sec 2.1.14, 4.17 (1.h))
2018 June	Clarified source for water mask (Sec 2.4.18)
2018 June	Clarified source for urban mask (Sec 2.4.20)
2018 June	Added expansion to the terrain_slope calculation (Sec 4.17)
2018 June	Removed canopy_d_quartile

2018 June	Removed canopy_quartile_heights and canopy_quartile_heights_abs, replaced with canopy_h_metrics (Secs 2.2.3, 4.18 (6), 4.18.1 (5))
2018 *** draft 1	Delta_time specified as mid-segment time, rather than mean segment time (Sec 2.4.7)
2018 *** draft 1	QA/QC products to be reported on a per orbit basis, rather than per region (Sec 5.2)
2018 *** draft 1	Added more detail to landsat_flag description
2018 *** draft 1	Added psf_flag back into ATL08 product, as it is also needed for the QA product (Sec 2.5.12)
2018 *** draft 1	Specified that the sigma_h value reported here is the mean of the ATL03 reported sigma_h values (Sec 2.5.7)
2018 *** draft 1	Removed n_photons from all subgroups
2018 *** draft 1	<p>Better defined the interpolation and smoothing methods used throughout:</p> <ul style="list-style-type: none"> <li>• 1 (3): Interpolation – nearest</li> <li>• 4.6 (5): Interpolation – PCHIP</li> <li>• 4.6 (8): Smoothing – moving average</li> <li>• 4.9 (3): Interpolation – PCHIP</li> <li>• 4.9 (3): Smoothing – moving average</li> <li>• 4.10 (10): Smoothing – moving average</li> <li>• 4.10 (11): Interpolation – linear</li> <li>• 4.10 (12): Smoothing – moving average</li> <li>• 4.10 (13): Interpolation – linear</li> <li>• 4.10 (14): Smoothing – moving average</li> <li>• 4.10 (15): Smoothing – Savitzky-Golay</li> <li>• 4.10 (16): Interpolation – linear</li> <li>• 4.10 (21): Interpolation – PCHIP</li> <li>• 4.12 (10): Interpolation – linear</li> <li>• 4.13 (all): Smoothing – moving average</li> <li>• 4.10 (6.b): Interpolation – linear</li> <li>• 4.14 (1.a): Interpolation – linear</li> <li>• 4.14 (1.c): Smoothing – lowess</li> <li>• 4.14 (4): Interpolation – PCHIP</li> <li>• 4.14 (7): Interpolation – PCHIP</li> <li>• 4.14 (9): Smoothing – moving average</li> <li>• 4.17 (1.h.i.1): Interpolation – linear</li> </ul>
2018 *** draft 1	Added ref_elev and ref_azimuth back in (it was mistakenly removed in a previous version; Secs 2.5.3, 2.5.4)
2018 *** draft 1	Clarified wording of h_canopy_quad definition (Sec 2.2.18)
2018 *** draft 1	Updated segment_snowcover description to match the ATL09 snow_ice parameter it references (Sec 2.4.19) and added product reference to Table 4.2

2018 *** draft 1	Added ph_ndx_beg (Sec 2.5.23); parameter was already on product
2018 *** draft 1	Added dem_removal_flag for QA purposes (Sec 2.4.13; Table 5.2)
2018 *** draft 2	Reformatted QA/QC trending and trigger alert list into a table for better clarification (Table 5.3)
2018 *** draft 2	Replaced n_photons in Table 5.2 with n_te_photons, n_ca_photons, and n_toc_photons
2018 *** draft 2	Removed beam_number from Table 2.5. Beam number and weak/strong designation within gtx group attributes.
2018 *** draft 2	Clarified calculation of h_te_best_fit (Sec 4.17 (1.h))
2018 *** draft 2	Changed h_canopy and h_canopy_abs to be 98 <sup>th</sup> percentile height (Table 2.2, Sec 2.2.5, Sec 2.2.6, Sec 4.18 (4), Sec 4.18.1 (3))
2018 *** draft 2	Separated h_canopy_metrics_abs from h_canopy_metrics (Table 2.2, Sec 2.2.3, Sec 4.18.1 (5))
2018 October	Removed 99 <sup>th</sup> percentile from h_canopy_metrics and h_canopy_metrics_abs (Table 2.2, Sec 2.2.3, Sec 2.2.4, Sec 4.18 (4), Sec 4.18.1 (5))
2018 December	Renamed and reworded Section 4.3.1 to better indicate that the DRAGANN preprocessing step is not optional
2018 December	Specified that DRAGANN should use along-track time, and added time rescaling step (Sec 4.3 (1 - 4))
2018 December	Added DRAGANN changes made to better capture sparse canopy in cases of low noise rates (Sec 4.3, Appendix A)
2018 December	Made corrections to DRAGANN description regarding the determination of the noise Gaussian (Sec 3.1.1, Sec 4.3)
2018 December	Removed h_median_canopy and h_median_canopy_abs, as they are equivalent to canopy_h_metrics(50) and canopy_h_metrics_abs(50) (Table 2.2, Sec 4.18 (5), Sec 4.18.1 (4))
2018 December	Removed the requirement that > 5% ground photons required to calculate relative canopy height parameters (Table 2.2, Sec 4.18 (2))
2018 December	Added canopy relative height confidence flag (canopy_rh_conf) based on the percentage of ground and canopy photons in a segment (Table 2.2, Sec 4.18 (2))
2018 December	Added ATL09 layer_flag to ATL08 output (Table 2.5, Table 4.2)
2019 February	Adjusted cloud filtering to be based on ATL09 backscatter analysis rather than cloud flags (Sec 4.1)
2019 March 5	Updated ATL09-based product descriptions reported on ATL08 product (Secs 2.5.13, 2.5.14, 2.5.15, 2.5.16)
2019 March 5	Updated cloud-based low signal filter methodology, and moved to first step of ATL08 processing (Sec 4.1)

2019 March 13	Replace canopy_closure with new landsat_perc parameter
2019 March 13	Change ATL08 product output regions to match ATL03 regions (Sec 2), but keep ATL08 regions internally and report in new parameter atl08_regions (Table 2.4, Sec 2.4.24)
2019 March 13	Add methodology for handling short ATL08 processing segments at the end of an ATL03 granule (Sec 4.2), and output distance the processing segment length is extended into new parameter last_seg_extend (Table 2.4, Sec 2.4.25)
2019 March 13	Add preprocessing step for removing atmospheric and ocean tide corrections from ATL03 heights ( <i>Later removed</i> )
2019 March 27	Remove preprocessing step for removing atmospheric and ocean tide corrections from ATL03 heights, since those values are now removed from the ATL03 photon heights.
2019 March 27	Replaced ATL03 region figure with corrected version (Figure 2.2)
2019 March 27	Specified that at least 50 classed photons are required to create the 100 m land and canopy products (Secs 2, 4.17(1), 4.18(1))
2019 March 27	Clarified that any non-extended segments would report a land_seg_extend value of 0 (Sec 4.2, Sec 2.4.25)
2019 April 30	Fixed the error in Eqn 1.4 for the sigma topo value
2019 May 13	Specified for cloud flag carry-over from ATL09 that ATL08 will report the highest cloud flag if an 08 segment straddles two 09 segments. (Section 2.5)
2019 May 13	Changed parameter cloud_flag_asr to cloud_flag_atm since the cloud_flag_asr is likely not to work over land due to varying surface reflectance (Sec, 2.5)
2019 May 13	Add ATL09 parameter cloud_fold_flag to the ATL08 data product for future qa/qc checks for low clouds. (Secs, 2.5)
2019 May 13	Clarification on the calculation of gradient for slope that feeds into the calculation of the point spread function (Sec 4.11)
2019 July 8	Changed Landsat canopy cover percentage to 3 % (from original value of 5%) (Section 4.4)
2019 July 8	Added a QA method for DRAGANN flags to help remove false positives (now Section 4.3.1)
2019 July 8	Set the window size to 9 rather than SmoothSize for the final ground finding step. (Section 4.11 and 4.12)
2019 July 8	Added a brightness flag to land segments. (Section 2.4.21)
2019 November 12	Added subset_te_flag to (Section 2.1) which indicate 100 m segments that are populated by less than 100 m worth of data

2019 November 12	Added subset_can_flag (section 2.2) which indicate 100 m segments that are populated by less than 100 m worth of data
2020 January 5	Clarified the interpolation of values (latitude, longitude, delta time) when the 100 m segments are populated by less than 100 m worth of data. (Section 2.4.3 and 2.4.4)
2020 January 13	Fine-tuned the methodology to improve ground finding by first histogramming the photons to improve detecting the ground in cases of dense canopy. (Section 4.8)
2020 January 13	Updated ATL08 HDF5 file organization figure in Section 2.1
2020 February 14	Added sentence to avoid ATL03 data having a degraded PPD flag to beginning of Section 4
2020 February 14	Added documentation for removing signal photons due to cloud contamination by checking the reference DEM to beginning of Section 4
2020 February 14	Added full saturation flag and near saturation flag from ATL03 to ATL08 data product to Section 2.
2020 February 14	Added statement to clarify handling of remaining geosegments that do not fit within a 100 m window at the end of a 10-km processing window in Section 4.2
2020 April 15	Added ph_h parameter to photon group on data structure. ph_h is the photon height above the interpolated ground surface.
2020 May 15	Added sat_flag which is derived from the ATL03 product. The saturation flag indicates that the ATL08 segment experienced some saturation which is often an indicator for water
2020 May 15	Canopy height metrics (relative and absolute heights) were expanded to every 5% ranging from 5 – 95%.
2020 May 15	The Landsat canopy cover check to determine whether the algorithm should search for both ground and canopy or just ground has been disabled. Now the ATL08 algorithm will search for both ground and canopy points everywhere.
2020 June 15	Corrected the calculation of the absolute canopy heights
2020 June 15	Changed the search radius for initial top of canopy determination (Section 4.9)
2020 September 1	Incorporate the quality_ph flag from ATL03 into the ATL08 workflow (beginning of Section 4)
2020 September 1	Added the calculation of Terrain photon rate (photon_rate_te) for each ATL08 segment to the land product (Section 2.1.16)
2020 September 1	Added the calculation of canopy photon rate (photon_rate_can) for each ATL08 segment to the land product (Section 2.2.26)



2020 September 1	Changed the k-d tree search radius for the top of canopy from 15 m to 100 m. Section 4.9.6
2020 September 15	Added new parameter for terrain heights (h_te_rh25) which represents the height of the 25% of ground cumulative distribution.
2021 March 15	Added terrain_best_fit_geosegment (h_te_best_fit_20m) parameter to the data product. 20 m estimate of best fit terrain height
2021 March 15	Added canopy_height_geosegment (h_canopy_20m) to the data product. 20 m estimate of relative canopy height
2021 March 15	Added latitude_20m to the data product.
2021 March 15	Added longitude_20m to the data product
2021 March 15	Updated the urban_flag parameter. Inclusion of the DLR Global Urban Footprint (GUF) as a potential indicator of man-made/built structures. Section 2.4.20
2021 March 15	Updated the Segment_landcover with Copernicus. Replace the MODIS landcover value with the landcover classification from the 100 m Copernicus landcover. Section 2.4.16
2021 March 15	Added the Segment_Woody_Vegetation_Fractional_cover. Inclusion of a woody vegetation fraction cover derived from the 2019 Copernicus fractional cover data products. Section 2.4.17
2021 March 15	Removed Landsat_perc (Landsat Percentage Calculation), Landsat_flag, and Canopy_flag from the ATL08 data product and from the algorithm. Removed all reference to Landsat from the ATBD.
<b>2021 September 1</b>	Added section 4.16 on quality control for the final products
<b>2021 September 1</b>	Change histogram height bin from 0.5 m to 1 m in section 4.7, step 3 and 8
<b>2021 November 1</b>	Added Final segment QA/QC Check for canopy photons that fall more than 150 m below the reference DEM. Section 4.16.1
<b>January 15, 2022</b>	Calculate number of background noise photons within canopy Section 2.2.26
<b>January 15, 2022</b>	Adjust canopy radiometry value by removing canopy noise photons from calculation Section 2.2.25
<b>January 15, 2022</b>	Add Final segment QA/QC check based on radiometric values. Section 4.16.2
<b>January 15, 2022</b>	Add Final segment QA/QC check to reassign noise photons mislabeled as canopy photons. Section 4.16.3
<b>15 April 2022</b>	Incorporate YAPC photon weights from ATL03 data product to ground finding approach. Section 4.7



<b>15 June 2022</b>	Modified the number of labeled photons required to report canopy or terrain heights within a segment for both the strong and weak beams. Section 2.2
<b>15 January 2023</b>	<b>Add parameters from ESA CCI Permafrost data parameters (probability and active layer thickness) from the year 2019 to ATL08 (Section 2.4)</b>
<b>15 January 2023</b>	<b>Add Column Optical Depth (calculated on ATL09) to ATL08 (Section 2.5)</b>
<b>15 January 2023</b>	<b>Improved ground finding over bright surfaces. Snow/ice flag we utilize the non-yapc ground finding method. Section 4.6</b>
<b>1 August 2023</b>	<b>Remove canopy finding flag in ATL08 regions 7, 8, 9, 10 (Antarctica) and 11 (Greenland)</b>
<b>1 August 2023</b>	<b>CAB Profile Cloud Filtering: Incorporate the Calibrated Atmospheric Backscatter (CAB) delineation of a ground surface to remove noise bands from the ATL03 data product prior to DRAGANN. Section 4.1</b>
<b>1 August 2023</b>	<b>Align the weak beam to the strong beam from ATL09 based on along-track distance for CAB profile cloud filtering. Section 4.2</b>
<b>1 February 2024</b>	<b>Updated description for MSW flag as described on ATL09 ATBD</b>
<b>1 February 2024</b>	<b>Incorporated a single surface search to improve ground finding (Section 4.5)</b>
<b>15 February 2024</b>	<b>Updated parameters on the quality_ph flag to allow certain photons as input into ATL08</b>
<b>15 April 2024</b>	<b>Added a terrain and canopy quality score. Values indicate potential quality of terrain and canopy heights. Section 2.1.19 and 2.2.27</b>
<b>15 April 2024</b>	<b>Added steps for identifying whether photons are from a single surface or multi-surface (i.e. canopy present)</b>
<b>6 September 2024</b>	<b>Added ground finding correction based on a priori DEM bias, section 4.6</b>
<b>9 September 2024</b>	<b>Added extension of nighttime canopy photons, above FINALGROUND surface, section 4.14</b>
<b>1 October 2024</b>	<b>Added steps to reject photons in the presence of fog or low lying clouds, section 4.7.12</b>

32  
33

34	<b>Contents</b>	
35	List of Tables .....	17
36	List of Figures .....	18
37	1 INTRODUCTION .....	20
38	1.1. Background.....	21
39	1.2 Photon Counting Lidar .....	23
40	1.3 The ICESat-2 concept.....	24
41	1.4 Height Retrieval from ATLAS.....	27
42	1.5 Accuracy Expected from ATLAS.....	29
43	1.6 Additional Potential Height Errors from ATLAS.....	31
44	1.7 Dense Canopy Cases.....	31
45	1.8 Sparse Canopy Cases.....	32
46	2 ATL08: DATA PRODUCT.....	33
47	2.1 Subgroup: Land Parameters.....	36
48	2.1.1 Georeferenced_segment_number_beg .....	37
49	2.1.2 Georeferenced_segment_number_end .....	38
50	2.1.3 Segment_terrain_height_mean .....	38
51	2.1.4 Segment_terrain_height_med.....	38
52	2.1.5 Segment_terrain_height_min.....	39
53	2.1.6 Segment_terrain_height_max .....	39
54	2.1.7 Segment_terrain_height_mode .....	39
55	2.1.8 Segment_terrain_height_skew .....	39
56	2.1.9 Segment_number_terrain_photons.....	40
57	2.1.10 Segment height_interp .....	40
58	2.1.11 Segment h_te_std .....	40
59	2.1.12 Segment_terrain_height_uncertainty.....	40
60	2.1.13 Segment_terrain_slope.....	40

61	2.1.14	Segment_terrain_height_best_fit.....	41
62	2.1.15	Segment_terrain_height_25.....	41
63	2.1.16	Subset_te_flag {1:5} .....	41
64	2.1.17	Segment Terrain Photon Rate.....	42
65	2.1.18	Terrain Best Fit GeoSegment {1:5}.....	42
66	2.1.19	Terrain Quality Score.....	42
67	2.2	Subgroup: Vegetation Parameters.....	43
68	2.2.1	Georeferenced_segment_number_beg .....	46
69	2.2.2	Georeferenced_segment_number_end .....	46
70	2.2.3	Canopy_height_metrics_abs .....	47
71	2.2.4	Canopy_height_metrics .....	47
72	2.2.5	Absolute_segment_canopy_height .....	48
73	2.2.6	Segment_canopy_height .....	48
74	2.2.7	canopy_height GeoSegment {1:5}.....	48
75	2.2.8	Absolute_segment_mean_canopy .....	49
76	2.2.9	Segment_mean_canopy .....	49
77	2.2.10	Segment_dif_canopy .....	49
78	2.2.11	Absolute_segment_min_canopy .....	49
79	2.2.12	Segment_min_canopy .....	49
80	2.2.13	Absolute_segment_max_canopy.....	50
81	2.2.14	Segment_max_canopy.....	50
82	2.2.15	Segment_canopy_height_uncertainty .....	50
83	2.2.16	Segment_canopy_openness.....	51
84	2.2.17	Segment_top_of_canopy_roughness .....	51
85	2.2.18	Segment_canopy_quadratic_height .....	51
86	2.2.19	Segment_number_canopy_photons.....	52
87	2.2.20	Segment_number_top_canopy_photons .....	52

88	2.2.21	Centroid_height.....	52
89	2.2.22	Segment_rel_canopy_conf.....	52
90	2.2.23	Subset_can_flag {1:5}.....	52
91	2.2.24	Segment Canopy Photon Rate.....	53
92	2.2.25	Segment Canopy Photon Rate Reduced.....	53
93	2.2.26	Segment Background Photons in Canopy.....	54
94	2.2.27	Canopy Quality Score.....	54
95	2.3	Subgroup: Photons .....	55
96	2.3.1	Indices_of_classed_photons .....	56
97	2.3.2	Photon_class .....	56
98	2.3.3	Georeferenced_segment_number.....	56
99	2.3.4	Photon Height .....	56
100	2.3.5	DRAGANN_flag.....	57
101	2.4	Subgroup: Reference data .....	57
102	2.4.1	Georeferenced_segment_number_beg .....	58
103	2.4.2	Georeferenced_segment_number_end.....	59
104	2.4.3	Segment_latitude .....	59
105	2.4.4	Geosegment_latitude{1:5} .....	60
106	2.4.5	Segment_longitude .....	60
107	2.4.6	Geosegment_longitude{1:5} .....	60
108	2.4.7	Delta_time .....	61
109	2.4.8	Delta_time_beg.....	61
110	2.4.9	Delta_time_end .....	61
111	2.4.10	Night_Flag .....	61
112	2.4.11	Segment_reference_DTM .....	61
113	2.4.12	Segment_reference_DEM_source.....	61
114	2.4.13	Segment_reference_DEM_removal_flag.....	62

115	2.4.14	Segment_terrain_difference.....	62
116	2.4.15	Segment_terrain flag .....	62
117	2.4.16	Segment_landcover.....	62
118	2.4.17	Segment_Woody Vegetation Fractional Cover .....	64
119	2.4.18	Segment_watermask.....	64
120	2.4.19	Segment_snowcover.....	64
121	2.4.20	Urban_flag.....	64
122	2.4.21	Permafrost_probability.....	65
123	2.4.22	Permafrost_ALT .....	65
124	2.4.23	Surface Type .....	66
125	2.4.24	ATL08_region.....	66
126	2.4.25	Last_segment_extend.....	66
127	2.4.26	Brightness_flag .....	67
128	2.5	Subgroup: Beam data.....	67
129	2.5.1	Georeferenced_segment_number_beg .....	70
130	2.5.2	Georeferenced_segment_number_end.....	70
131	2.5.3	Beam_coelevation.....	70
132	2.5.4	Beam_azimuth .....	70
133	2.5.5	ATLAS_Pointing_Angle .....	71
134	2.5.6	Reference_ground_track.....	71
135	2.5.7	Sigma_h.....	71
136	2.5.8	Sigma_along .....	71
137	2.5.9	Sigma_across .....	71
138	2.5.10	Sigma_topo .....	72
139	2.5.11	Sigma_ATLAS_LAND.....	72
140	2.5.12	PSF_flag.....	72
141	2.5.13	Layer_flag.....	72

142	2.5.14	Cloud_flag_atm.....	73
143	2.5.15	MSW .....	73
144	2.5.16	Cloud Fold Flag.....	73
145	2.5.17	Computed_Apparent_Surface_Reflectance .....	73
146	2.5.18	Column_Optical_Depth_ASR.....	74
147	2.5.19	Signal_to_Noise_Ratio .....	74
148	2.5.20	Solar_Azimuth.....	74
149	2.5.21	Solar_Elevation .....	74
150	2.5.22	Number_of_segment_photons.....	74
151	2.5.23	Photon_Index_Begin.....	75
152	2.5.24	Saturation Flag .....	75
153	3	ALGORITHM METHODOLOGY .....	76
154	3.1	Noise Filtering .....	76
155	3.1.1	DRAGANN .....	77
156	3.2	Surface Finding.....	81
157	3.2.1	De-trending the Signal Photons .....	83
158	3.2.2	Canopy Determination .....	83
159	3.2.3	Variable Window Determination .....	84
160	3.2.4	Compute descriptive statistics .....	85
161	3.2.5	Ground Finding Filter (Iterative median filtering) .....	87
162	3.3	Top of Canopy Finding Filter.....	88
163	3.4	Classifying the Photons.....	89
164	3.5	Refining the Photon Labels .....	89
165	3.6	Canopy Height Determination .....	94
166	3.7	Link Scale for Data products.....	94
167	4	ALGORITHM IMPLEMENTATION.....	95
168	4.1	Cloud based filtering.....	98

169	4.2	Preparing ATL03 data for input to ATL08 algorithm.....	101
170	4.3	Noise filtering via DRAGANN .....	102
171	4.3.1	DRAGANN Quality Assurance .....	105
172	4.3.2	Preprocessing to dynamically determine a DRAGANN parameter .....	106
173	4.3.3	Iterative DRAGANN processing.....	109
174	4.4	Compute Filtering Window.....	110
175	4.5	Identification of single surface .....	110
176	4.6	Look for potential ground photons .....	112
177	4.7	De-trend Data.....	115
178	4.8	Detect fog conditions and bypass photon classification.....	116
179	4.9	Filter outlier noise from signal.....	118
180	4.10	Finding the initial ground estimate.....	118
181	4.11	Find the top of the canopy.....	121
182	4.12	Compute statistics on de-trended (Asmooth) data .....	122
183	4.13	Refine Ground Estimates .....	123
184	4.14	Canopy Photon Filtering .....	125
185	4.15	Compute individual Canopy Heights .....	128
186	4.16	Final photon classification QA check .....	128
187	4.17	Compute segment parameters for the Land Products .....	129
188	4.18	Compute segment parameters for the Canopy Products .....	132
189	4.18.1	Canopy Products calculated with absolute heights.....	134
190	4.19	Segment Quality Check .....	134
191	4.20	Record final product without buffer .....	136
192	5	DATA PRODUCT VALIDATION STRATEGY.....	137
193	5.1	Validation Data.....	137
194	5.2	Internal QC Monitoring.....	140
195	6	REFERENCES.....	146





197	<b>List of Tables</b>	
198	Table 2.1. Summary table of land parameters on ATL08. ....	36
199	Table 2.2. Summary table of canopy parameters on ATL08. ....	44
200	Table 2.3. Summary table for photon parameters for the ATL08 product. ....	55
201	Table 2.4. Summary table for reference parameters for the ATL08 product. ....	57
202	Table 2.5. Summary table for beam parameters for the ATL08 product. ....	67
203	Table 3.1. Standard deviation ranges utilized to qualify the spread of photons within	
204	moving window. ....	86
205	Table 4.1. Input parameters to ATL08 classification algorithm. ....	96
206	Table 4.2. Additional external parameters referenced in ATL08 product. ....	97
207	Table 5.1. Airborne lidar data vertical height (Z accuracy) requirements for	
208	validation data. ....	137
209	Table 5.2. ATL08 parameter monitoring. ....	140
210	Table 5.3. QA/QC trending and triggers. ....	144
211		

212	<b>List of Figures</b>	
213	Figure 1.1. Various modalities of lidar detection. Adapted from Harding, 2009. ....	24
214	Figure 1.2. Schematic of 6-beam configuration for ICESat-2 mission. The laser	
215	energy will be split into 3 laser beam pairs – each pair having a weak spot (1X) and a	
216	strong spot (4X). ....	26
217	Figure 1.3. Illustration of off-nadir pointing scenarios. Over land (green regions) in	
218	the mid-latitudes, ICESat-2 will be pointed away from the repeat ground tracks to	
219	increase the density of measurements over terrestrial surfaces. ....	27
220	Figure 1.4. Illustration of the point spread function, also referred to as Znoise, for a	
221	series of photons about a surface. ....	29
222	Figure 2.1. HDF5 data structure for ATL08 products .....	34
223	Figure 2.2. ATL03 granule regions; graphic from ATL03 ATBD (Neumann et al.).....	35
224	Figure 2.3. ATL08 product regions. ....	36
225	Figure 2.4. Illustration of canopy photons (red dots) interaction in a vegetated area.	
226	Relative canopy heights, $H_i$ , are computed by differencing the canopy photon height	
227	from an interpolated terrain surface. ....	44
228	Figure 3.1. Combination of noise filtering algorithms to create a superset of input	
229	data for surface finding algorithms. ....	77
230	Figure 3.2. Histogram of the number of photons within a search radius. This	
231	histogram is used to determine the threshold for the DRAGANN approach. ....	79
232	Figure 3.3. Output from DRAGANN filtering. Signal photons are shown as blue. ....	81
233	Figure 3.4. Flowchart of overall surface finding method. ....	82
234	Figure 3.5. Plot of Signal Photons (black) from 2014 MABEL flight over Alaska and	
235	de-trended photons (red). ....	83
236	Figure 3.6. Shape Parameter for variable window size. ....	85
237	Figure 3.7. Illustration of the standard deviations calculated for each moving	
238	window to identify the amount of spread of signal photons within a given window.	
239	.....	87
240	Figure 3.8. Three iterations of the ground finding concept for $L$ -km segments with	
241	canopy. ....	88

242	Figure 3.9. Example of the intermediate ground and top of canopy surfaces	
243	calculated from MABEL flight data over Alaska during July 2014.....	91
244	Figure 3.10. Example of classified photons from MABEL data collected in Alaska	
245	2014. Red photons are photons classified as terrain. Green photons are classified as	
246	top of canopy. Canopy photons (shown as blue) are considered as photons lying	
247	between the terrain surface and top of canopy. ....	92
248	Figure 3.11. Example of classified photons from MABEL data collected in Alaska	
249	2014. Red photons are photons classified as terrain. Green photons are classified as	
250	top of canopy. Canopy photons (shown as blue) are considered as photons lying	
251	between the terrain surface and top of canopy. ....	93
252	Figure 3.12. Example of classified photons from MABEL data collected in Alaska	
253	2014. Red photons are photons classified as terrain. Green photons are classified as	
254	top of canopy. Canopy photons (shown as blue) are considered as photons lying	
255	between the terrain surface and top of canopy. ....	93
256	Figure 5.1. Example of <i>L-km</i> segment classifications and interpolated ground	
257	surface.....	143
258		

## 1 INTRODUCTION

This document describes the theoretical basis and implementation of the processing algorithms and data parameters for Level 3 land and vegetation heights for the non-polar regions of the Earth. The ATL08 product contains heights for both terrain and canopy in the along-track direction as well as other descriptive parameters derived from the measurements. At the most basic level, a derived surface height from the ATLAS instrument at a given time is provided relative to the WGS-84 ellipsoid. Height estimates from ATL08 can be compared with other geodetic data and used as input to higher-level ICESat-2 products, namely ATL13 and ATL18. ATL13 will provide estimates of inland water-related heights and associated descriptive parameters. ATL18 will consist of gridded maps for terrain and canopy features.

The ATL08 product will provide estimates of terrain heights, canopy heights, and canopy cover at fine spatial scales in the along-track direction. Along-track is defined as the direction of travel of the ICESat-2 satellite in the velocity vector. Parameters for the terrain and canopy will be provided at a fixed step-size of 100 m along the ground track referred to as a segment. A fixed segment size of 100 m was chosen to provide continuity of data parameters on the ATL08 data product. From an analysis perspective, it is difficult and cumbersome to attempt to relate canopy cover over variable lengths. Furthermore, a segment size of 100 m will facilitate a simpler combination of along-track data to create the gridded products.

We anticipate that the signal returned from the weak beam will be sufficiently weak and may prohibit the determination of both a terrain and canopy segment height, particularly over areas of dense vegetation. However, in more arid regions we anticipate producing a terrain height for both the weak and strong beams.

In this document, section 1 provides a background of lidar in the ecosystem community as well as describing photon counting systems and how they differ from discrete return lidar systems. Section 2 provides an overview of the Land and Vegetation parameters and how they are defined on the data product. Section 3 describes the basic methodology that will be used to derive the parameters for ATL08.

Section 4 describes the processing steps, input data, and procedure to derive the data parameters. Section 5 will describe the test data and specific tests that NASA's implementation of the algorithm should pass in order to determine a successful implementation of the algorithm.

### **1.1. Background**

The Earth's land surface is a complex mosaic of geomorphic units and land cover types resulting in large variations in terrain height, slope, roughness, vegetation height and reflectance, often with the variations occurring over very small spatial scales. Documentation of these landscape properties is a first step in understanding the interplay between the formative processes and response to changing conditions. Characterization of the landscape is also necessary to establish boundary conditions for models which are sensitive to these properties, such as predictive models of atmospheric change that depend on land-atmosphere interactions. Topography, or land surface height, is an important component for many height applications, both to the scientific and commercial sectors. The most accurate global terrain product was produced by the Shuttle Radar Topography Mission (SRTM) launched in 2000; however, elevation data are limited to non-polar regions. The accuracy of SRTM derived elevations range from 5 – 10 m, depending upon the amount of topography and vegetation cover over a particular area. ICESat-2 will provide a global distribution of geodetic measurements (of both the terrain surface and relative canopy heights) which will provide a significant benefit to society through a variety of applications including sea level change monitoring, forest structural mapping and biomass estimation, and improved global digital terrain models.

In addition to producing a global terrain product, monitoring the amount and distribution of above ground vegetation and carbon pools enables improved characterization of the global carbon budget. Forests play a significant role in the terrestrial carbon cycle as carbon pools. Events, such as management activities (Krankina et al. 2012) and disturbances can release carbon stored in forest above

ground biomass (AGB) into the atmosphere as carbon dioxide, a greenhouse gas that contributes to climate change (Ahmed et al. 2013). While carbon stocks in nations with continuous national forest inventories (NFIs) are known, complications with NFI carbon stock estimates exist, including: (1) ground-based inventory measurements are time consuming, expensive, and difficult to collect at large-scales (Houghton 2005; Ahmed et al. 2013); (2) asynchronously collected data; (3) extended time between repeat measurements (Houghton 2005); and (4) the lack of information on the spatial distribution of forest AGB, required for monitoring sources and sinks of carbon (Houghton 2005). Airborne lidar has been used for small studies to capture canopy height and in those studies canopy height variation for multiple forest types is measured to approximately 7 m standard deviation (Hall et al., 2011).

Although the spatial extent and changes to forests can be mapped with existing satellite remote sensing data, the lack of information on forest vertical structure and biomass limits the knowledge of biomass/biomass change within the global carbon budget. Based on the global carbon budget for 2015 (Quere et al., 2015), the largest remaining uncertainties about the Earth's carbon budget are in its terrestrial components, the global residual terrestrial carbon sink, estimated at  $3.0 \pm 0.8$  GtC/year for the last decade (2005-2014). Similarly, carbon emissions from land-use changes, including deforestation, afforestation, logging, forest degradation and shifting cultivation are estimated at  $0.9 \pm 0.5$  GtC /year. By providing information on vegetation canopy height globally with a higher spatial resolution than previously afforded by other spaceborne sensors, the ICESat-2 mission can contribute significantly to reducing uncertainties associated with forest vegetation carbon.

Although ICESat-2 is not positioned to provide global biomass estimates due to its profiling configuration and somewhat limited detection capabilities, it is anticipated that the data products for vegetation will be complementary to ongoing biomass and vegetation mapping efforts. Synergistic use of ICESat-2 data with other space-based mapping systems is one solution for extended use of ICESat-2 data. Possibilities include NASA's Global Ecosystems Dynamics Investigation (GEDI) lidar



planned to fly onboard the International Space Station (ISS) or imaging sensors, such as Landsat 8, or NASA/ISRO –NISAR radar mission.

## **1.2 Photon Counting Lidar**

Rather than using an analog, full waveform system similar to what was utilized on the ICESat/GLAS mission, ICESat-2 will employ a photon counting lidar. Photon counting lidar has been used successfully for ranging for several decades in both the science and defense communities. Photon counting lidar systems operate on the concept that a low power laser pulse is transmitted and the detectors used are sensitive at the single photon level. Due to this type of detector, any returned photon whether from the reflected signal or solar background can trigger an event within the detector. A discussion regarding discriminating between signal and background noise photons is discussed later in this document. A question of interest to the ecosystem community is to understand where within the canopy is the photon likely to be reflected. Figure 1.1 is an example of three different laser detector modalities: full waveform, discrete return, and photon counting. Full waveform sensors record the entire temporal profile of the reflected laser energy through the canopy. In contrast, discrete return systems have timing hardware that record the time when the amplitude of the reflected signal energy exceeds a certain threshold amount. A photon counting system, however, will record the arrival time associated with a single photon detection that can occur anywhere within the vertical distribution of the reflected signal. If a photon counting lidar system were to dwell over a surface for a significant number of shots (i.e. hundreds or more), the vertical distribution of the reflected photons will resemble a full waveform. Thus, while an individual photon could be reflected from anywhere within the vertical canopy, the probability distribution function (PDF) of that reflected photon would be the full waveform. Furthermore, the probability of detecting the top of the tree is not as great as detecting reflective surfaces positioned deeper into the canopy where the bulk of leaves and branches are located. As one might imagine, the PDF will differ according

to canopy structure and vegetation physiology. For example, the PDF of a conifer tree will look different than broadleaf trees.

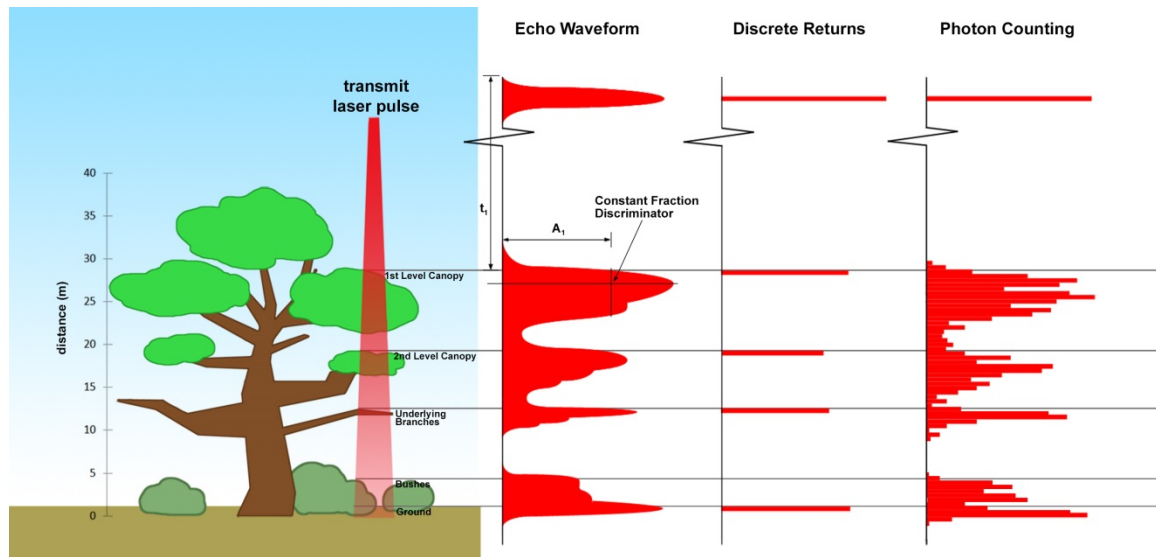


Figure 1.1. Various modalities of lidar detection. Adapted from Harding, 2009.

A cautionary note, the photon counting PDF that is illustrated in Figure 1.1 is merely an illustration if enough photons (i.e. hundreds of photons or more) were to be reflected from a target. In reality, due to the spacecraft speed, ATLAS will record 0 – 4 photons per transmit laser pulse over vegetation.

### 1.3 The ICESat-2 concept

The Advanced Topographic Laser Altimeter System (ATLAS) instrument designed for ICESat-2 will utilize a different technology than the GLAS instrument used for ICESat. Instead of using a high-energy, single-beam laser and digitizing the entire temporal profile of returned laser energy, ATLAS will use a multi-beam, micropulse laser (sometimes referred to as photon-counting). The travel time of each detected photon is used to determine a range to the surface which, when combined with satellite attitude and pointing information, can be geolocated into a unique XYZ location on or near the Earth's surface. For more information on how the photons from ICESat-2 are geolocated, refer to ATL03 ATBD. The XYZ positions from ATLAS

394 are subsequently used to derive surface and vegetation properties. The ATLAS  
395 instrument will operate at 532 nm in the green range of the electromagnetic (EM)  
396 spectrum and will have a laser repetition rate of 10 kHz. The combination of the laser  
397 repetition rate and satellite velocity will result in one outgoing laser pulse  
398 approximately every 70 cm on the Earth's surface and each spot on the surface is ~13  
399 m in diameter. Each transmitted laser pulse is split by a diffractive optical element in  
400 ATLAS to generate six individual beams, arranged in three pairs (Figure 1.2). The  
401 beams within each pair have different transmit energies ('weak' and 'strong', with an  
402 energy ratio of approximately 1:4) to compensate for varying surface reflectance. The  
403 beam pairs are separated by ~3.3 km in the across-track direction and the strong and  
404 weak beams are separated by ~2.5 km in the along-track direction. As ICESat-2 moves  
405 along its orbit, the ATLAS beams describe six tracks on the Earth's surface; the array  
406 is rotated slightly with respect to the satellite's flight direction so that tracks for the  
407 fore and aft beams in each column produce pairs of tracks – each separated by  
408 approximately 90 m.

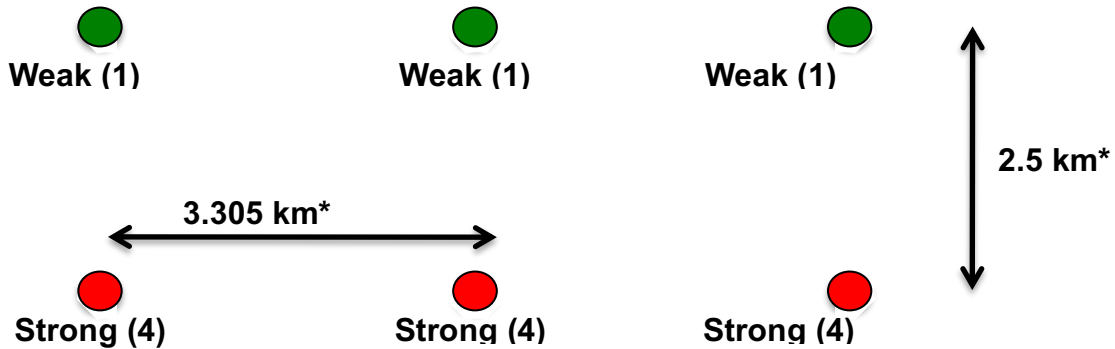
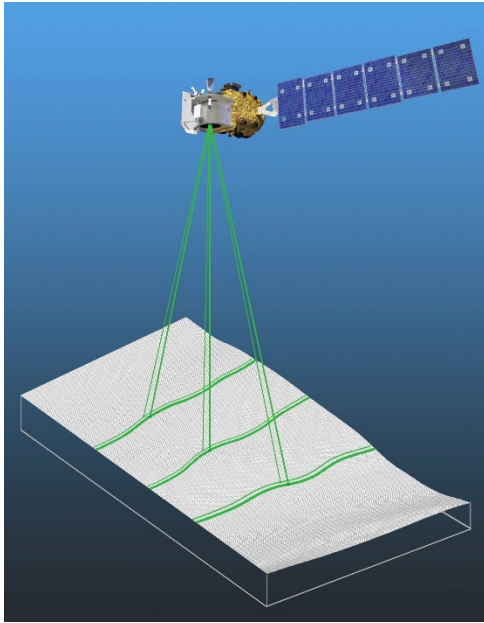


Figure 1.2. Schematic of 6-beam configuration for ICESat-2 mission. The laser energy will be split into 3 laser beam pairs – each pair having a weak spot (1X) and a strong spot (4X).

The motivation behind this multi-beam design is its capability to compute cross-track slopes on a per-orbit basis, which contributes to an improved understanding of ice dynamics. Previously, slope measurements of the terrain were determined via repeat-track and crossover analysis. The laser beam configuration as proposed for ICESat-2 is also beneficial for terrestrial ecosystems compared to GLAS as it enables a denser spatial sampling in the non-polar regions. To achieve a spatial sampling goal of no more than 2 km between equatorial ground tracks, ICESat-2 will be off-nadir pointed a maximum of 1.8 degrees from the reference ground track during the entire mission.

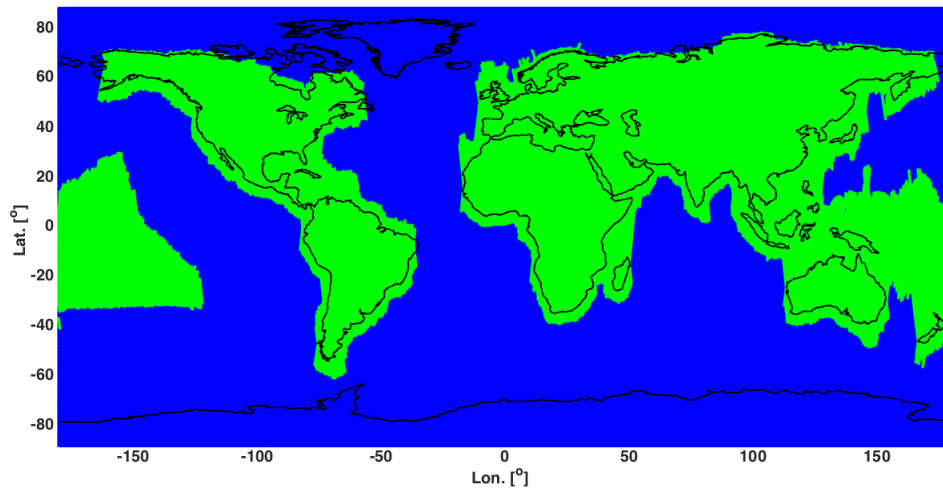


Figure 1.3. Illustration of off-nadir pointing scenarios. Over land (green regions) in the mid-latitudes, ICESat-2 will be pointed away from the repeat ground tracks to increase the density of measurements over terrestrial surfaces.

ICESat-2 is designed to densely sample the Earth's surface, permitting scientists to measure and quantitatively characterize vegetation across vast expanses, e.g., nations, continents, globally. ICESat-2 will acquire synoptic measurements of vegetation canopy height, density, the vertical distribution of photosynthetically active material, leading to improved estimates of forest biomass, carbon, and volume. In addition, the orbital density, i.e., the number of orbits per unit area, at the end of the three year mission will facilitate the production of gridded global products. ICESat-2 will provide the means by which an accurate "snapshot" of global biomass and carbon may be constructed for the mission period.

#### 1.4 Height Retrieval from ATLAS

Light from the ATLAS lasers reaches the earth's surface as flat disks of down-traveling photons approximately 50 cm in vertical extent and spread over approximately 14 m horizontally. Upon hitting the earth's surface, the photons are reflected and scattered in every direction and a handful of photons return to the

ATLAS telescope's focal plane. The number of photon events per laser pulse is a function of outgoing laser energy, surface reflectance, solar conditions, and scattering and attenuation in the atmosphere. For highly reflective surfaces (such as land ice) and clear skies, approximately 10 signal photons from a single strong beam are expected to be recorded by the ATLAS instrument for a given transmit laser pulse. Over vegetated land where the surface reflectance is considerably less than snow or ice surfaces, we expect to see fewer returned photons from the surface. Whereas snow and ice surfaces have high reflectance at 532 nm (typical Lambertian reflectance between 0.8 and 0.98 (Martino, GSFC internal report, 2010)), canopy and terrain surfaces have much lower reflectance (typically around 0.3 for soil and 0.1 for vegetation) at 532 nm. As a consequence we expect to see 1/3 to 1/9 as many photons returned from terrestrial surfaces as from ice and snow surfaces. For vegetated surfaces, the number of reflected signal photon events per transmitted laser pulse is estimated to range between 0 to 4 photons.

The time measured from the detected photon events are used to compute a range, or distance, from the satellite. Combined with the precise pointing and attitude information about the satellite, the range can be geolocated into a XYZ point (known as a geolocated photon) above the WGS-84 reference ellipsoid. In addition to recording photons from the reflected signal, the ATLAS instrument will detect background photons from sunlight which are continually entering the telescope. A primary objective of the ICESat-2 data processing software is to correctly discriminate between signal photons and background photons. Some of this processing occurs at the ATL03 level and some of it also occurs within the software for ATL08. At ATL03, this discrimination is done through a series of three steps of progressively finer resolution with some processing occurring onboard the satellite prior to downlink of the raw data. The ATL03 data product produces a classification between signal and background (i.e. noise) photons, and further discussion on that classification process can be read in the ATL03 ATBD. In addition, not all geophysical corrections (e.g. ocean tide) are applied to the position of the individual geolocated photons at the ATL03 level, but they are provided on the ATL03 data product if there

exists a need to apply them. Thus, in general, all of the heights processed in the ATL08 algorithm consists of the ATL03 heights with respect to the WGS-84 ellipsoid, with geophysical corrections applied, as specified in Chapter 6 of the ATL03 ATBD.

### 1.5 Accuracy Expected from ATLAS

There are a variety of elements that contribute to the elevation accuracy that are expected from ATLAS and the derived data products. Elevation accuracy is a composite of ranging precision of the instrument, radial orbital uncertainty, geolocation knowledge, forward scattering in the atmosphere, and tropospheric path delay uncertainty. The ranging precision seen by ATLAS will be a function of the laser pulse width, the surface area potentially illuminated by the laser, and uncertainty in the timing electronics. The requirement on radial orbital uncertainty is specified to be less than 4 cm and tropospheric path delay uncertainty is estimated to be 3 cm. In the case of ATLAS, the ranging precision for flat surfaces, is expected to have a standard deviation of approximately 25 cm. The composite of each of the errors can also be thought of as the spread of photons about a surface (see Figure 1.4) and is referred to as the point spread function or Znoise.

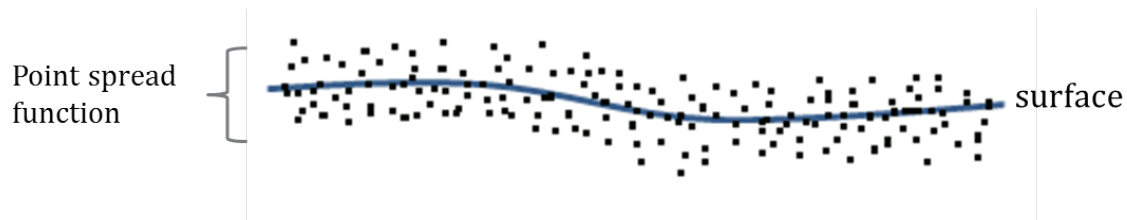


Figure 1.4. Illustration of the point spread function, also referred to as Znoise, for a series of photons about a surface.

The estimates of  $\sigma_{Orbit}$ ,  $\sigma_{troposphere}$ ,  $\sigma_{forwardscattering}$ ,  $\sigma_{pointing}$ , and  $\sigma_{timing}$  for a photon will be represented on the ATL03 data product as the final geolocated accuracy in the X, Y, and Z (or height) direction. In reality, these parameters have different temporal and spatial scales, however until ICESat-2 is on orbit, it is uncertain how these parameters will vary over time. As such, Equation 1.1 may change once the



temporal aspects of these parameters are better understood. For a preliminary quantification of the uncertainties, Equation 1.1 is valid to incorporate the instrument related factors.

$$\sigma_Z = \sqrt{\sigma_{Orbit}^2 + \sigma_{trop}^2 + \sigma_{forwardscattering}^2 + \sigma_{pointing}^2 + \sigma_{timing}^2} \quad \text{Eqn. 1.1}$$

500

Although  $\sigma_Z$  on the ATL03 product represents the best understanding of the uncertainty for each geolocated photon, it does not incorporate the uncertainty associated with local slope of the topography. The slope component to the geolocation uncertainty is a function of both the geolocation knowledge of the pointing (which is required to be less than 6.5 m) multiplied by the tangent of the surface slope. In a case of flat topography ( $\leq 1$  degree slope),  $\sigma_Z \leq 25$  cm, whereas in the case of a 10 degree surface slope,  $\sigma_Z = 119$  cm. The uncertainty associated with the local slope will be combined with  $\sigma_Z$  to produce the term  $\sigma_{AtlasLand}$ .

$$\sigma_{AtlasLand} = \sqrt{\sigma_Z^2 + \sigma_{topo}^2} \quad \text{Eqn. 1.2}$$

$$\sigma_{topo} = \sigma_{topo} = \sqrt{\left(6.5 \tan(\theta_{surface\ slope})\right)^2} \quad \text{Eqn. 1.3}$$

Ultimately, the uncertainty that will be reported on the data product ATL08 will include the  $\sigma_{AtlasLand}$  term and the local rms values of heights computed within each data parameter segment. For example, calculations of terrain height will be made on photons classified as terrain photons (this process is described in the following sections). The uncertainty of the terrain height for a segment is described in Equation 1.4, where the root mean square term of  $\sigma_{AtlasLand}$  and rms of terrain heights are normalized by the number of terrain photons for that given segment.

$$\sigma_{ATL08_{segment}} = \sqrt{\sigma_{AtlasLand}^2 + \sigma_{Zrms_{segment\_class}}^2} \quad \text{Eqn. 1.4}$$

519

## **1.6 Additional Potential Height Errors from ATLAS**

Some additional potential height errors in the ATL08 terrain and vegetation product can come from a variety of sources including:

- a. Vertical sampling error. ATLAS height estimates are based on a random sampling of the surface height distribution. Photons may be reflected from anywhere within the PDF of the reflecting surface; more specifically, anywhere from within the canopy. A detailed look at the potential effect of vertical sampling error is provided in Neuenschwander and Magruder (2016).
- b. Background noise. Random noise photons are mixed with the signal photons so classified photons will include random outliers.
- c. Complex topography. The along-track product may not always represent complex surfaces, particularly if the density of ground photons does not support an accurate representation.
- d. Vegetation. Dense vegetation may preclude reflected photon events from reaching the underlying ground surface. An incorrect estimation of the underlying ground surface will subsequently lead to an incorrect canopy height determination.
- e. Misidentified photons. The product from ATL03 combined with additional noise filtering may not identify the correct photons as signal photons.

## **1.7 Dense Canopy Cases**

Although the height accuracy produced from ICESat-2 is anticipated to be superior to other global height products (e.g. SRTM), for certain biomes photon counting lidar data as it will be collected by the ATLAS instrument present a challenge for extracting both the terrain and canopy heights, particularly for areas of dense

547 vegetation. Due to the relatively low laser power, we anticipate that the along-track  
548 signal from ATLAS may lose ground signal under dense forest (e.g. >96% canopy  
549 closure) and in situations where cloud cover obscures the terrestrial signal. In areas  
550 having dense vegetation, it is likely that only a handful of photons will be returned  
551 from the ground surface with the majority of reflections occurring from the canopy.  
552 A possible source of error can occur with both the canopy height estimates and the  
553 terrain heights if the vegetation is particularly dense and the ground photons were  
554 not correctly identified.

### 556 **1.8 Sparse Canopy Cases**

557 Conversely, sparse canopy cases also pose a challenge to vegetation height  
558 retrievals. In these cases, expected reflected photon events from sparse trees or  
559 shrubs may be difficult to discriminate between solar background noise photons. The  
560 algorithms being developed for ATL08 operate under the assumption that signal  
561 photons are close together and noise photons will be more isolated in nature. Thus,  
562 signal (in this case canopy) photons may be incorrectly identified as solar background  
563 noise on the data product. Due to the nature of the photon counting processing,  
564 canopy photons identified in areas that have extremely low canopy cover <15% will  
565 be filtered out and reassigned as noise photons.

## 2 ATL08: DATA PRODUCT

The ATL08 product will provide estimates of terrain height, canopy height, and canopy cover at fine spatial scales in the along-track direction. In accordance with the HDF-driven structure of the ICESat-2 products, the ATL08 product will characterize each of the six Ground Tracks (GT) associated with each Reference Ground Track (RGT) for each cycle and orbit number. Each ground track group has a distinct beam number, distance from the reference track, and transmit energy strength, and all beams will be processed independently using the same sequence of steps described within ATL08. Each ground track group (GT) on the ATL08 product contains subgroups for land and canopy heights segments as well as beam and reference parameters useful in the ATL08 processing. In addition, the labeled photons that are used to determine the data parameters will be indexed back to the ATL03 products such that they are available for further, independent analysis. A layout of the ATL08 HDF product is shown in Figure 2.1. The six GTs are numbered from left to right, regardless of satellite orientation.

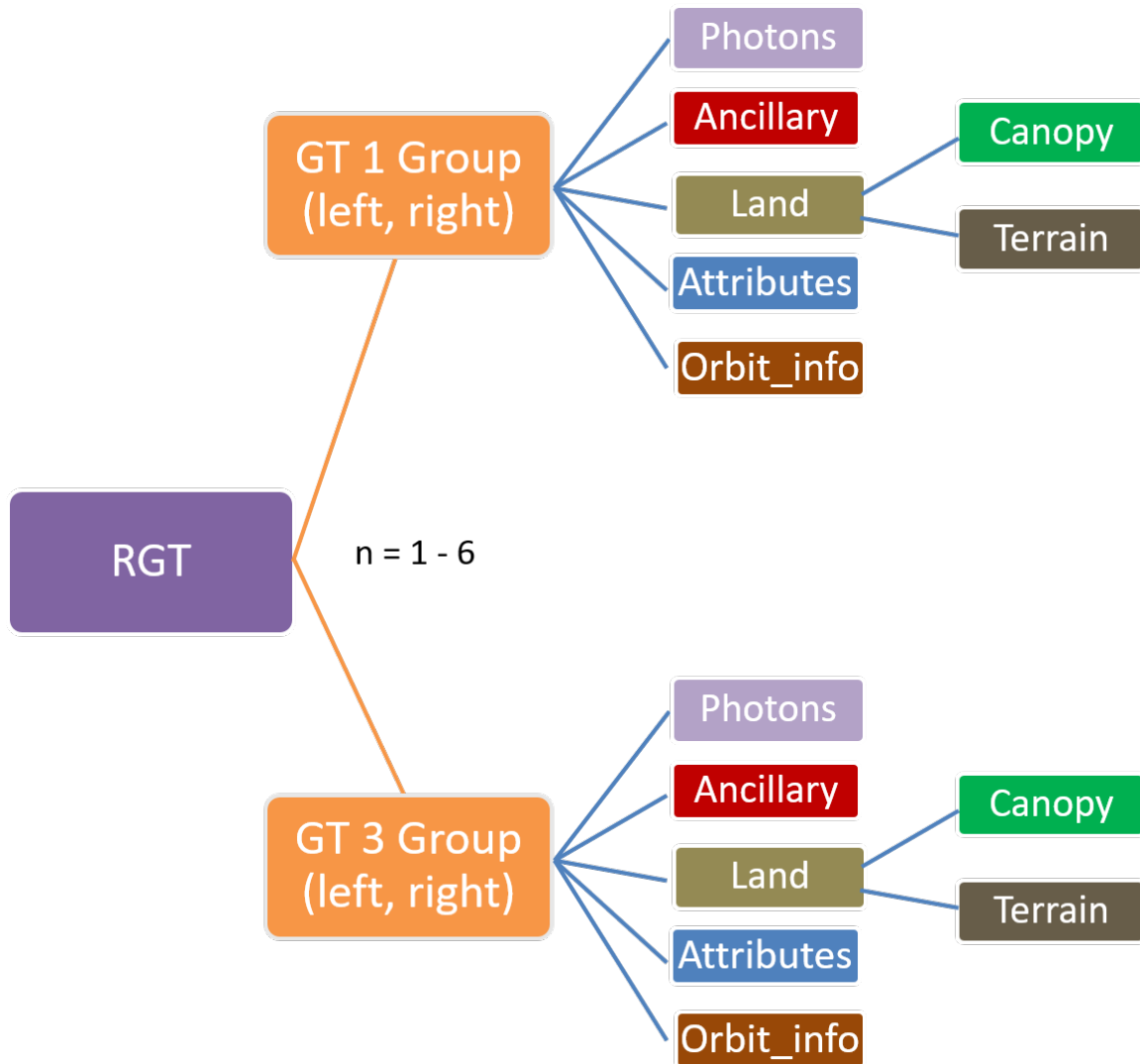


Figure 2.1. HDF5 data structure for ATL08 products

For each data parameter, terrain surface elevation and canopy heights will be provided at a fixed segment size of 100 meters along the ground track. Based on the satellite velocity and the expected number of reflected photons for land surfaces, each segment should have more than 100 signal photons, but in some instances there may be less than 100 signal photons per segment. If a segment has less than 50 classed (i.e., labeled by ATL08 as ground, canopy, or top of canopy) photons we feel this would not accurately represent the surface. Thus, an invalid value will be reported in

all height fields. In the event that there are more than 50 classed photons, but a terrain height cannot be determined due to an insufficient number of ground photons, (e.g. lack of photons penetrating through dense canopy), the only reported terrain height will be the interpolated surface height.

The ATL08 product will be produced per granule based on the ATL03 defined regions (see Figure 2.2). Thus, the ATL08 file/name convention scheme will match the file/naming convention for ATL03 –in attempt for reducing complexity to allow users to examine both data products.

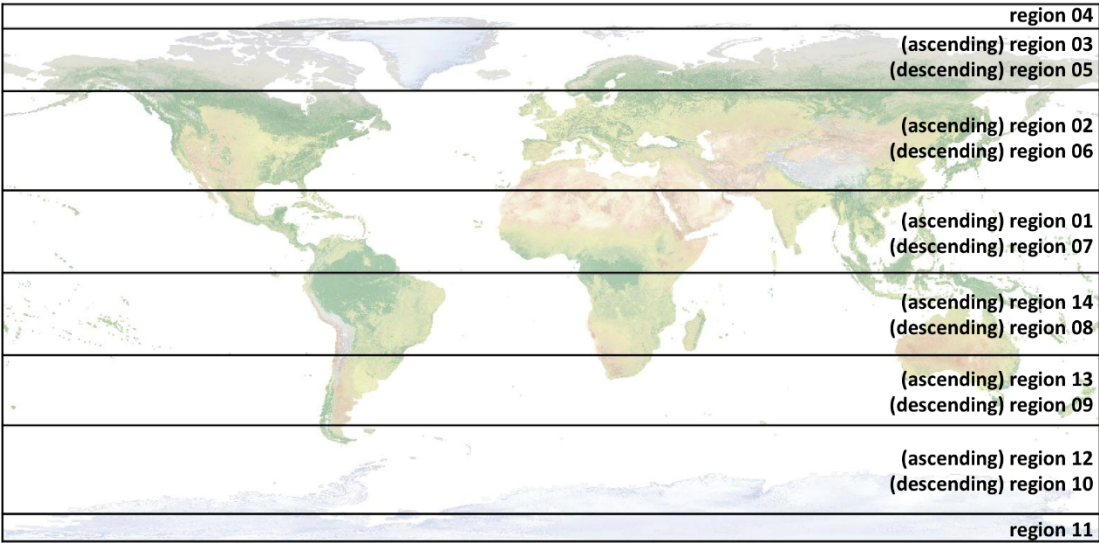


Figure 2.2. ATL03 granule regions; graphic from ATL03 ATBD (Neumann et al.).

The ATL08 product additionally has its own internal regions, which are roughly assigned by continent, as shown by Figure 2.3. For the regions covering Antarctica (regions 7, 8, 9, 10) and Greenland (region 11), the ATL08 algorithm will assume that no canopy is present. These internal ATL08 regions will be noted in the ATL08 product (see parameter atl08\_region in Section 2.4.24). Note that the regions for each ICESat-2 product are not the same.

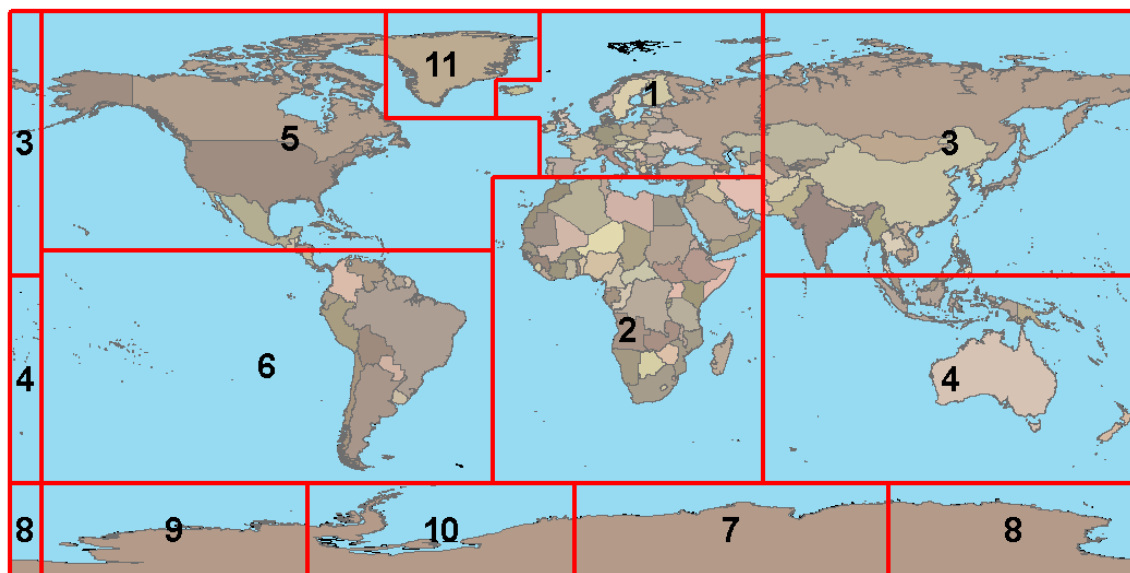


Figure 2.3. ATL08 product regions.

## 2.1 Subgroup: Land Parameters

ATL08 terrain height parameters are defined in terms of the absolute height above the reference ellipsoid.

Table 2.1. Summary table of land parameters on ATL08.

Group	Data type	Description	Source
<b>segment_id_beg</b>	Integer	First along-track segment_id number in 100-m segment	ATL03
<b>segment_id_end</b>	Integer	Last along-track segment_id number in 100-m segment	ATL03
<b>h_te_mean</b>	Float	Mean terrain height for segment	computed
<b>h_te_median</b>	Float	Median terrain height for segment	computed
<b>h_te_min</b>	Float	Minimum terrain height for segment	computed
<b>h_te_max</b>	Float	Maximum terrain height for segment	computed
<b>h_te_mode</b>	Float	Mode of terrain height for segment	computed
<b>h_te_skew</b>	Float	Skew of terrain height for segment	computed



<b>n_te_photons</b>	Integer	Number of ground photons in segment	computed
<b>h_te_interp</b>	Float	Interpolated terrain surface height at mid-point of segment	computed
<b>h_te_std</b>	Float	Standard deviation of ground heights about the interpolated ground surface	computed
<b>h_te_uncertainty</b>	Float	Uncertainty of ground height estimates. Includes all known uncertainties such as geolocation, pointing angle, timing, radial orbit errors, etc.	computed from Equation 1.4
<b>terrain_slope</b>	Float	Slope of terrain within segment	computed
<b>h_te_best_fit</b>	Float	Best fit terrain elevation at the 100 m segment mid-point location	computed
<b>h_te_best_fit_20m</b>	Float	Best fit terrain elevation at the 20 m geosegment mid-point location	computed
<b>h_te_rh25</b>	float	The relative height from classified canopy photons are sorted into a cumulative distribution, and the height associated with the 98% height above the h_te_bestfit for that segment is reported.	computed
<b>subset_te_flag</b>	Integer	Quality flag indicating the terrain photons populating the 100 m segment statistics are derived from less than 100 m worth of photons	computed
<b>photon_rate_te</b>	Float	Calculated photon rate for ground photons within each segment	computed
<b>te_quality_score</b>	Integer	Quality metric that is a composite of several parameters	computed

615

### 616 2.1.1 Georeferenced\_segment\_number\_beg

617 (parameter = segment\_id\_beg). The first along-track segment\_id in each 100-m  
618 segment. Each 100-m segment consists of five sequential 20-m segments provided  
619 from the ATL03 product, which are labeled as segment\_id. The segment\_id is a seven

digit number that uniquely identifies each along track segment, and is written at the along-track geolocation segment rate (i.e. ~20m along track). The four digit RGT number can be combined with the seven digit segment\_id number to uniquely define any along-track segment number. Values are sequential, with 0000001 referring to the first segment after the equatorial crossing of the ascending node.

#### **2.1.2 Georeferenced\_segment\_number\_end**

(parameter = segment\_id\_end). The last along-track segment\_id in each 100-m segment. Each 100-m segment consists of five sequential 20-m segments provided from the ATL03 product, which are labeled as segment\_id. The segment\_id is a seven digit number that uniquely identifies each along track segment, and is written at the along-track geolocation segment rate (i.e. ~20m along track). The four digit RGT number can be combined with the seven digit segment\_id number to uniquely define any along-track segment number. Values are sequential, with 0000001 referring to the first segment after the equatorial crossing of the ascending node.

#### **2.1.3 Segment\_terrain\_height\_mean**

(parameter = h\_te\_mean). Estimated mean of the terrain height above the reference ellipsoid derived from classified ground photons within the 100 m segment. If a terrain height cannot be directly determined within the segment (i.e. there are not a sufficient number of ground photons), only the interpolated terrain height will be reported. Required input data is classified point cloud (i.e. photons labeled as either canopy or ground in the ATL08 processing). This parameter will be derived from only classified ground photons.

#### **2.1.4 Segment\_terrain\_height\_med**

(parameter = h\_te\_median). Median terrain height above the reference ellipsoid derived from the classified ground photons within the 100 m segment. If there are not a sufficient number of ground photons, an invalid value will be reported –no interpolation will be done. Required input data is classified point cloud (i.e.

photons labeled as either canopy or ground in the ATL08 processing). This parameter will be derived from only classified ground photons.

#### **2.1.5 Segment\_terrain\_height\_min**

(parameter = h\_te\_min). Minimum terrain height above the reference ellipsoid derived from the classified ground photons within the 100 m segment. If there are not a sufficient number of ground photons, an invalid value will be reported –no interpolation will be done. Required input data is classified point cloud (i.e. photons labeled as either canopy or ground in the ATL08 processing). This parameter will be derived from only classified ground photons.

#### **2.1.6 Segment\_terrain\_height\_max**

(parameter = h\_te\_max). Maximum terrain height above the reference ellipsoid derived from the classified ground photons within the 100 m segment. If there are not a sufficient number of ground photons, an invalid value will be reported –no interpolation will be done. Required input data is classified point cloud (i.e. photons labeled as either canopy or ground in the ATL08 processing). This parameter will be derived from only classified ground photons.

#### **2.1.7 Segment\_terrain\_height\_mode**

(parameter = h\_te\_mode). Mode of the classified ground photon heights above the reference ellipsoid within the 100 m segment. If there are not a sufficient number of ground photons, an invalid value will be reported –no interpolation will be done. Required input data is classified point cloud (i.e. photons labeled as either canopy or ground in the ATL08 processing). This parameter will be derived from only classified ground photons.

#### **2.1.8 Segment\_terrain\_height\_skew**

(parameter = h\_te\_skew). The skew of the classified ground photons within the 100 m segment. If there are not a sufficient number of ground photons, an invalid value will be reported –no interpolation will be done. Required input data is classified

674 point cloud (i.e. photons labeled as either canopy or ground in the ATL08 processing).  
675 This parameter will be derived from only classified ground photons.

676       **2.1.9** Segment\_number\_terrain\_photons

677       (parameter = n\_te\_photons). Number of terrain photons identified in segment.

678       **2.1.10** Segment\_height\_interp

679       (parameter = h\_te\_interp). Interpolated terrain surface height above the  
680 reference ellipsoid from ATL08 processing at the mid-point of each segment. This  
681 interpolated surface is the FINALGROUND estimate (described in section 4.9).

682       **2.1.11** Segment\_h\_te\_std

683       (parameter = h\_te\_std). Standard deviations of terrain points about the  
684 interpolated ground surface within the segment. Provides an indication of surface  
685 roughness.

686       **2.1.12** Segment\_terrain\_height\_uncertainty

687       (parameter = h\_te\_uncertainty). Uncertainty of the mean terrain height for the  
688 segment. This uncertainty incorporates all systematic uncertainties (e.g. timing,  
689 orbits, geolocation, etc.) as well as uncertainty from errors of identified photons. This  
690 parameter is described in Section 1, Equation 1.4. If there are not a sufficient number  
691 of ground photons, an invalid value will be reported –no interpolation will be done.  
692 Required input data is classified point cloud (i.e. photons labeled as either canopy or  
693 ground in the ATL08 processing). This parameter will be derived from only classified  
694 ground photons. The  $\sigma_{segmentclass}$  term in Equation 1.4 represents the standard  
695 deviation of the terrain height residuals about the FINALGROUND estimate.

696       **2.1.13** Segment\_terrain\_slope

697       (parameter = terrain\_slope). Slope of terrain within each segment. Slope is  
698 computed from a linear fit of the terrain photons. It estimates the rise [m] in relief

699 over each segment [100 m]; e.g., if the slope value is 0.04, there is a 4 m rise over the  
700 100 m segment. Required input data are the classified terrain photons.

#### 701 **2.1.14 Segment\_terrain\_height\_best\_fit**

702 (parameter = h\_te\_best\_fit). The best fit terrain elevation at the mid-point  
703 location of each 100 m segment. The mid-segment terrain elevation is determined by  
704 selecting the best of three fits – linear, 3<sup>rd</sup> order and 4<sup>th</sup> order polynomials – to the  
705 terrain photons and interpolating the elevation at the mid-point location of the 100  
706 m segment. For the linear fit, a slope correction and weighting is applied to each  
707 ground photon based on the distance to the slope height at the center of the segment.

#### 708 **2.1.15 Segment\_terrain\_height\_25**

709 (parameter = h\_te\_rh25). The terrain elevation from the 25% height. The  
710 classified ground photons are sorted into a cumulative distribution and the height  
711 associated with the 25% height for that segment is reported.

#### 712 **2.1.16 Subset\_te\_flag {1:5}**

713 (parameter = subset\_te\_flag). This flag indicates the quality distribution of  
714 identified terrain photons within each 100 m on a geosegment basis. The purpose of  
715 this flag is to provide the user with an indication whether the photons contributing to  
716 the terrain estimate are evenly distributed or only partially distributed (i.e. due to  
717 cloud cover or signal attenuation). A 100 m ATL08 segment is comprised of 5 geo-  
718 segments and we are populating a flag for each geosegment. subset\_te\_flags:

719 -1: no data within geosegment available for analysis

720 0: indicates no ground photons within geosegment

721 1: indicates ground photons within geosegment

722 For example, an 100 m ATL08 segment might have the following  
723 subset\_te\_flags: {-1 -1 0 1 1} which would translate that no signal photons (canopy or  
724 ground) were available for processing in the first two geosegments. Geosegment 3

was found to have photons, but none were labeled as ground photons. Geosegment 4 and 5 had valid labeled ground photons. Again, the motivation behind this flag is to inform the user that, in this example, the 100 m estimate are being derived from only 40 m worth of data.

#### **2.1.17 Segment Terrain Photon Rate**

(parameter = photon\_rate\_te). This value indicates the terrain photon rate within each ATL08 segment. This value is calculated as the total number of terrain photons divided by the total number of laser shots within each ATL08 segment. The number of laser shots is defined as the number of unique Delta\_Time values within each segment.

#### **2.1.18 Terrain Best Fit GeoSegment {1:5}**

(parameter = h\_te\_best\_fit\_20m). The best fit terrain elevation at the mid-point location of each 20 m geosegment. The mid-segment terrain elevation is determined by selecting the best of three fits – linear, 3<sup>rd</sup> order and 4<sup>th</sup> order polynomials – to the terrain photons and interpolating the elevation at each 20 m along a 100 m segment. For the linear fit, a slope correction and weighting is applied to each ground photon based on the distance to the slope height at the center of the segment. For segments that do not have a sufficient number of photons, an invalid (or fill) value will be reported. Each 20 m geo-segment shall have 10 signal photons as a minimum number to be used for calculations and a minimum of 3 terrain photons are required to estimate a height.

#### **2.1.19 Terrain Quality Score**

(parameter = te\_quality\_score). The computed skill score of multiple parameters for each 100 m ATL08 segment. A score of 100 indicates a likely high quality estimate of the terrain height. Deductions for the terrain skill score are as follows.

1. Weak Beam: deduct 5 points
2. Solar Elevation: 10 – 20 degrees; deduct 5 points  
Solar Elevation > 20 degrees; deduct 10 points

- 753 3. Optical Depth  $< 0.2 - 0.3$ ; deduct 5 points  $> 0.3$  deduct 10 points  
754 4. Cloud Fold flag  $> 0$ ; deduct 10 points  
755 5. DEM\_removal\_flag  $> 0$ ; deduct 10 points  
756 6. Terrain radiometry  $< 0.2$ ; deduct 10 points; terrain radiometry between  
757 0.2 and 0.5 deduct 5 points  
758 7. Track telemetry band removal, if 40% of 10km removed, deduct 10 points  
759 for entire 10 km.  
760 8. MSW\_flag  $> 0$ ; deduct 10 points  
761 9. SNR  $< 1$ ; deduct 10 points

## 762 **2.2 Subgroup: Vegetation Parameters**

763 Canopy parameters will be reported on the ATL08 data product in terms of both  
764 the absolute height above the reference ellipsoid as well as the relative height above  
765 an estimated ground. The relative canopy height,  $H_i$ , is computed as the height from  
766 an identified canopy photon minus the interpolated ground surface for the same  
767 horizontal geolocation (see Figure 2.3). Thus, each identified signal photon above an  
768 interpolated surface (including a buffer distance based on the instrument point  
769 spread function) is by default considered a canopy photon. For strong beams, canopy  
770 parameters will only be computed for segments where more than 10 of the at least  
771 50 labeled signal photons are labeled as canopy photons. For weak beams, canopy  
772 parameters will only be computed for segments having at least 30 signal photons with  
773 6 of them being labeled as canopy photons.

774

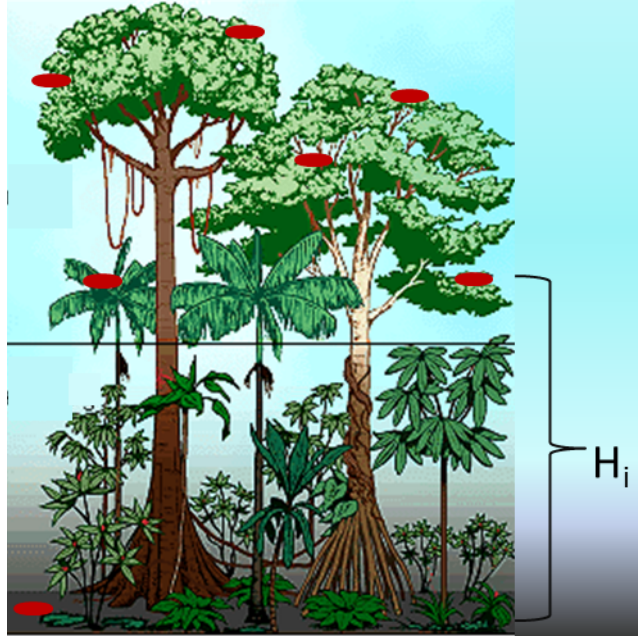


Figure 2.4. Illustration of canopy photons (red dots) interaction in a vegetated area. Relative canopy heights,  $H_i$ , are computed by differencing the canopy photon height from an interpolated terrain surface.

Table 2.2. Summary table of canopy parameters on ATL08.

Group	Data Type	Description	Source
<b>segment_id_beg</b>	Integer	First along-track segment_id number in 100-m segment	ATL03
<b>segment_id_end</b>	Integer	Last along-track segment_id number in 100-m segment	ATL03
<b>canopy_h_metrics_abs</b>	Float	Absolute (H##) canopy height metrics calculated at the following percentiles: 5, 10, 15, 20, 25, 30, 35, 40, 45, 50, 55, 60, 65, 70, 75, 80, 85, 90, 95.	computed
<b>canopy_h_metrics</b>	Float	Relative (RH##) canopy height metrics calculated at the following percentiles: 5, 10, 15, 20, 25, 30, 35, 40, 45, 50, 55, 60, 65, 70, 75, 80, 85, 90, 95.	computed
<b>h_canopy_abs</b>	Float	98% height of all the individual absolute canopy heights (height above WGS84 ellipsoid) for segment.	computed
<b>h_canopy</b>	Float	98% height of all the individual relative canopy heights (height above terrain) for segment.	computed



<b>h_canopy_20m</b>	Float	98% height of all the individual relative canopy heights (height above terrain) for 20m geosegment.	
<b>h_mean_canopy_abs</b>	Float	Mean of individual absolute canopy heights within segment	computed
<b>h_mean_canopy</b>	Float	Mean of individual relative canopy heights within segment	computed
<b>h_dif_canopy</b>	Float	Difference between h_canopy and canopy_h_metrics(50)	computed
<b>h_min_canopy_abs</b>	Float	Minimum of individual absolute canopy heights within segment	computed
<b>h_min_canopy</b>	Float	Minimum of individual relative canopy heights within segment	computed
<b>h_max_canopy_abs</b>	Float	Maximum of individual absolute canopy heights within segment. Should be equivalent to H100	computed
<b>h_max_canopy</b>	Float	Maximum of individual relative canopy heights within segment. Should be equivalent to RH100	computed
<b>h_canopy_uncertainty</b>	Float	Uncertainty of the relative canopy height (h_canopy)	computed
<b>canopy_openness</b>	Float	STD of relative heights for all photons classified as canopy photons within the segment to provide inference of canopy openness	computed
<b>toc_roughness</b>	Float	STD of relative heights of all photons classified as top of canopy within the segment	computed
<b>h_canopy_quad</b>	Float	Quadratic mean canopy height	computed
<b>n_ca_photons</b>	Integer4	Number of canopy photons within 100 m segment	computed
<b>n_toc_photons</b>	Integer4	Number of top of canopy photons within 100 m segment	computed
<b>centroid_height</b>	Float	Absolute height above reference ellipsoid associated with the centroid of all signal photons	computed
<b>canopy_rh_conf</b>	Integer	Canopy relative height confidence flag based on percentage of ground and canopy photons within a segment: 0 (<5% canopy), 1 (>5% canopy, <5% ground), 2 (>5% canopy, >5% ground)	computed
<b>subset_can_flag</b>	Integer	Quality flag indicating the canopy photons populating the 100 m segment statistics are derived from less than 100 m worth of photons	computed

<b>photon_rate_can</b>	Float	Photon rate of canopy photons within each 100 m segment	computed
<b>photon_rate_can_nr</b>	Float	Noise removed photon canopy rate within each 100 m segment	computed
<b>can_noise</b>	integer	Number of noise photons calculated that fall within the canopy height for each 100 m segment based on ATL03 background rate parameters	computed
<b>can_quality_score</b>	integer	Skill score to rate potential canopy quality based on other parameters	computed

780

### 781        2.2.1 Georeferenced\_segment\_number\_beg

782        (parameter = segment\_id\_beg). The first along-track segment\_id in each 100-m  
783 segment. Each 100-m segment consists of five sequential 20-m segments provided  
784 from the ATL03 product, which are labeled as segment\_id. The segment\_id is a seven  
785 digit number that uniquely identifies each along track segment, and is written at the  
786 along-track geolocation segment rate (i.e. ~20m along track). The four digit RGT  
787 number can be combined with the seven digit segment\_id number to uniquely define  
788 any along-track segment number. Values are sequential, with 0000001 referring to  
789 the first segment after the equatorial crossing of the ascending node.

### 790        2.2.2 Georeferenced\_segment\_number\_end

791        (parameter = segment\_id\_end). The last along-track segment\_id in each 100-m  
792 segment. Each 100-m segment consists of five sequential 20-m segments provided  
793 from the ATL03 product, which are labeled as segment\_id. The segment\_id is a seven  
794 digit number that uniquely identifies each along track segment, and is written at the  
795 along-track geolocation segment rate (i.e. ~20m along track). The four digit RGT  
796 number can be combined with the seven digit segment\_id number to uniquely define  
797 any along-track segment number. Values are sequential, with 0000001 referring to  
798 the first segment after the equatorial crossing of the ascending node.

### 2.2.3 Canopy\_height\_metrics\_abs

(parameter = canopy\_h\_metrics\_abs). The absolute height metrics (H##) of classified canopy photons (labels 2 and 3) above the ellipsoid. The height metrics are sorted based on a cumulative distribution and calculated at the following percentiles: 10, 15, 20, 25, 30, 35, 40, 45, 50, 55, 60, 65, 70, 75, 80, 85, 90, 95. These height metrics are often used in the literature to characterize vertical structure of vegetation. One important distinction of these canopy height metrics compared to those derived from other lidar systems (e.g., LVIS or GEDI) is that the ICESat-2 canopy height metrics are heights above the ground surface. These metrics do not include the ground photons. Required input data are the relative canopy heights of all canopy photons above the estimated terrain surface and the mid-segment elevation. The absolute canopy heights metrics are determined by adding the relative canopy height metric to the best-fit terrain (h\_te\_bestfit). For cases where the h\_te\_bestfit is invalid, the cumulative distribution will be calculated for the absolute canopy heights (not the relative canopy heights) and those cumulative heights will be reported.

### 2.2.4 Canopy\_height\_metrics

(parameter = canopy\_h\_metrics). Relative height metrics above the estimated terrain surface (RH##) of classified canopy photons (labels 2 and 3). The height metrics are sorted based on a cumulative distribution and calculated at the following percentiles: 10, 15, 20, 25, 30, 35, 40, 45, 50, 55, 60, 65, 70, 75, 80, 85, 90, 95. These height metrics are often used in the literature to characterize vertical structure of vegetation. One important distinction of these canopy height metrics compared to those derived from other lidar systems (e.g., LVIS or GEDI) is that the ICESat-2 canopy height metrics are heights above the ground surface. These metrics do not include the ground photons. Required input data are relative canopy heights above the estimated terrain surface for all canopy photons.

### 2.2.5 Absolute\_segment\_canopy\_height

(parameter = h\_canopy\_abs). The absolute 98% height of classified canopy photon heights (labels 2 and 3) above the ellipsoid. The relative height from classified canopy photons are sorted into a cumulative distribution, and the height associated with the 98% height above the h\_te\_bestfit for that segment is reported. For cases where the h\_te\_bestfit is invalid, the cumulative distribution will be calculated for the absolute canopy heights and the 98% absolute height will be reported.

### 2.2.6 Segment\_canopy\_height

(parameter = h\_canopy). The relative 98% height of classified canopy photon heights (labels 2 and 3) above the estimated terrain surface. Relative canopy heights have been computed by differencing the canopy photon height from the estimated terrain surface in the ATL08 processing. The relative canopy heights are sorted into a cumulative distribution, and the height associated with the 98% height is reported.

### 2.2.7 canopy\_height GeoSegment {1:5}

(parameter = h\_canopy\_20m). The relative 98% height of classified canopy photon heights (labels 2 and 3) above the estimated terrain surface in each 20 m geosegment. Relative canopy heights have been computed by differencing the canopy photon height from the estimated terrain surface in the ATL08 processing. The relative canopy heights are sorted into a cumulative distribution, and the height associated with the 98% height is reported. For segments that do not have a sufficient number of photons, an invalid (or fill) value will be reported. Each 20 m geo-segment shall have 10 signal photons as a minimum number to be used for calculations and a minimum of 3 canopy photons are required to estimate a height.

### 2.2.8 Absolute\_segment\_mean\_canopy

(parameter = h\_mean\_canopy\_abs). The absolute mean canopy height for the segment. relative canopy heights are the photons heights for canopy photons (labels 2 and 3) above the estimated terrain surface. These relative heights are averaged and then added to h\_te\_bestfit.

### 2.2.9 Segment\_mean\_canopy

(parameter = h\_mean\_canopy). The mean canopy height for the segment. Relative canopy heights have been computed by differencing the canopy photon height (labels 2 and 3) from the estimated terrain surface in the ATL08 processing. These heights are averaged.

### 2.2.10 Segment\_dif\_canopy

(parameter = h\_dif\_canopy). Difference between h\_canopy and canopy\_h\_metrics(50). This parameter is one metric used to describe the vertical distribution of the canopy within the segment.

### 2.2.11 Absolute\_segment\_min\_canopy

(parameter = h\_min\_canopy\_abs). The minimum absolute canopy height for the segment. Relative canopy heights are the photons heights for canopy photons (labels 2 and 3) above the estimated terrain surface. Required input data is classified point cloud (i.e. photons labeled as either canopy or ground in the ATL08 processing). The minimum relative canopy height for each segment is added to h\_te\_bestfit and reported as the absolute minimum canopy height.

### 2.2.12 Segment\_min\_canopy

(parameter = h\_min\_canopy). The minimum relative canopy height for the segment. Canopy heights are the photons heights for canopy photons (labels 2 and 3) differenced from the estimated terrain surface. Required input data is classified point cloud (i.e. photons labeled as either canopy or ground in the ATL08 processing).

### 2.2.13 Absolute\_segment\_max\_canopy

(parameter = h\_max\_canopy\_abs). The maximum absolute canopy height for the segment. This parameter is equivalent to H100 metric reported in the literature. This parameter, however, has the potential for error as random solar background noise may not have been fully rejected. It is recommended that h\_canopy or h\_canopy\_abs (i.e., the 98% canopy height) be considered as the top of canopy measurement. Required input data is classified point cloud (i.e. photons labeled as either canopy or ground in the ATL08 processing). The absolute max canopy height is the maximum relative canopy height added to h\_te\_bestfit.

### 2.2.14 Segment\_max\_canopy

(parameter = h\_max\_canopy). The maximum relative canopy height for the segment. Canopy heights are the photons heights for canopy photons (labels 2 and 3) differenced from the estimated terrain surface. This product is equivalent to RH100 metric reported in the literature. This parameter, however, has the potential for error as random solar background noise may not have been fully rejected. It is recommended that h\_canopy or h\_canopy\_abs (i.e., the 98% canopy height) be considered as the top of canopy measurement. Required input data is classified point cloud (i.e. photons labeled as either canopy or ground in the ATL08 processing).

### 2.2.15 Segment\_canopy\_height\_uncertainty

(parameter = h\_canopy\_uncertainty). Uncertainty of the relative canopy height for the segment. This uncertainty incorporates all systematic uncertainties (e.g. timing, orbits, geolocation, etc.) as well as uncertainty from errors of identified photons. This parameter is described in Section 1, Equation 1.4. If there are not a sufficient number of ground photons, an invalid value will be reported –no interpolation will be done. In the case for canopy height uncertainty, the parameter  $\sigma_{segmentclass}$  is comprised of both the terrain uncertainty within the segment but also the top of canopy residuals. Required input data is classified point cloud (i.e. photons labeled as either top of canopy or ground in the ATL08 processing). This parameter

will be derived from only classified top of canopy photons, label = 3. The canopy height uncertainty is derived from Equation 1.4, shown below as Equation 1.5, represents the standard deviation of the terrain points and the standard deviation of the top of canopy height photons.

$$\sigma_{ATL08_{segment\_ch}} = \frac{\sqrt{\sigma_{AtlasLand}^2 + \sigma_{Zrms_{segment\_terrain}}^2 + \sigma_{Zrms_{segment\_toc}}^2}}{n_{photons_{segment\_terrain}} + n_{photons_{segment\_toc}}} \quad \text{Eqn 1.5}$$

#### 2.2.16 Segment\_canopy\_openness

(parameter = canopy\_openness). Standard deviation of relative canopy heights within each segment. This parameter will potentially provide an indicator of canopy openness (label = 2 and 3) as a greater standard deviation of heights indicates greater penetration of the laser energy into the canopy. Required input data is classified point cloud (i.e. photons labeled as either canopy or ground in the ATL08 processing).

#### 2.2.17 Segment\_top\_of\_canopy\_roughness

(parameter = toc\_roughness). Standard deviation of relative top of canopy heights (label = 3) within each segment. This parameter will potentially provide an indicator of canopy variability. Required input data is classified point cloud (i.e. photons labeled as the top of the canopy in the ATL08 processing).

#### 2.2.18 Segment\_canopy\_quadratic\_height

(parameter = h\_canopy\_quad). The quadratic mean relative height of relative canopy heights. The quadratic mean height is computed as:

$$qmh = \sqrt{\sum_{i=1}^{n_{ca\_photons}} \frac{h_i^2}{n_{ca\_photons}}}$$

### 927       **2.2.19** Segment\_number\_canopy\_photons

928           (parameter = n\_ca\_photons). Number of canopy photons (label = 2) within  
929 each segment. Required input data is classified point cloud (i.e. photons labeled as  
930 either canopy or ground in the ATL08 processing). This parameter does not include  
931 the top of canopy photons. To determine the total number of canopy photons, add  
932 n\_ca\_photons to n\_toc\_photons within each segment.

### 933       **2.2.20** Segment\_number\_top\_canopy\_photons

934           (parameter = n\_toc\_photons). Number of top of canopy photons (label = 3)  
935 within each segment. Required input data is classified point cloud (i.e. photons  
936 labeled as top of canopy in the ATL08 processing). To determine the total number of  
937 canopy photons, add n\_ca\_photons to n\_toc\_photons within each segment.

### 938       **2.2.21** Centroid\_height

939           (parameter = centroid\_height). Optical centroid of all photons classified as  
940 either canopy or ground points (label = 1 2 or 3) within a segment. The heights used  
941 in this calculation are absolute heights above the reference ellipsoid. This parameter  
942 is equivalent to the centroid height produced on ICESat GLA14.

### 943       **2.2.22** Segment\_rel\_canopy\_conf

944           (parameter = canopy\_rh\_conf). Canopy relative height confidence flag based  
945 on percentage of ground photons and percentage of canopy photons (label 2 and 3),  
946 relative to the total classified (ground and canopy, label = 1 2 and 3) photons within  
947 a segment: 0 (<5% canopy), 1 (>5% canopy and <5% ground), 2 (>5% canopy and  
948 >5% ground). This is a measure based on the quantity, not the quality, of the  
949 classified photons in each segment.

### 950       **2.2.23** Subset\_can\_flag {1:5}

951           (parameter = subset\_can\_flag). This flag indicates the distribution of identified  
952 canopy photons (label 2 and 3) within each 100 m. The purpose of this flag is to  
953 provide the user with an indication whether the photons contributing to the canopy



954 height estimates are evenly distributed or only partially distributed (i.e. due to cloud  
955 cover or signal attenuation). A 100 m ATL08 segment is comprised of 5 geo-segments.  
956 subset\_can\_flags:

957 -1: no data within geosegment available for analysis

958 0: indicates no canopy photons within geosegment

959 1: indicates canopy photons within geosegment

960 For example, a 100 m ATL08 segment might have the following  
961 subset\_can\_flags: {-1 -1 -1 1 1} which would translate that no photons (canopy or  
962 ground) were available for processing in the first three geosegments. Geosegment 4  
963 and 5 had valid labeled canopy photons. Again, the motivation behind this flag is to  
964 inform the user that, in this example, the 100 m estimate are being derived from only  
965 40 m worth of data.

#### 966 **2.2.24 Segment Canopy Photon Rate**

967 (parameter = photon\_rate\_can). This value indicates the canopy photon rate  
968 within each ATL08 segment. This value is calculated as the total number of canopy  
969 photons (label =2 and 3) divided by the total number of unique laser shots within  
970 each ATL08 segment. The number of laser shots is defined as the number of unique  
971 Delta\_Time values within each segment.

#### 972 **2.2.25 Segment Canopy Photon Rate Reduced**

973 (parameter = photon\_rate\_can\_nr). This value indicates the canopy photon rate  
974 within each ATL08 segment where the background noise photons have been removed  
975 from the calculation. This value is calculated as the total number of canopy photons  
976 (label =2 and 3) minus the canopy noise count (can\_noise) divided by the total  
977 number of unique laser shots within each ATL08 segment. The number of laser shots  
978 is defined as the number of **unique** Delta\_Time values within each segment.

### 2.2.26 Segment Background Photons in Canopy

(parameter = can\_noise). This value represents the number of background photons that occur within the canopy height span of the 100 m ATL08 segment. Using the parameters from the ATL03 bckgrd\_atlas subgroup (bckgrd\_counts\_reduced) and (bckgrd\_in\_height\_reduced) we calculate the background noise rate (counts/m). The background noise rate is averaged across the ATL08 and finally multiplied by the ATL08 relative canopy height (h\_canopy).

Pseudocode for background noise photon removal

```
bcr = ATL03[gt + '/bckgrd_atlas/bckgrd_counts_reduced']
```

```
bihr = ATL03[gt + '/bckgrd_atlas/bckgrd_int_height_reduced']
```

```
# Calculate the Background Count Error Rate
```

```
rate = bcr / bihr
```

```
# Append the error rate from the 'Background Atlas' bins to the ATL03 Photon Level
```

```
ph_rate = rate[inds]
```

```
# Aggregate the error rate to the ATL08 rate by calculating the mean ph_rate
```

```
f08_rate = mean(ph_rate)
```

```
# Multiply the photon error rate at the ATL08 level to the h_max_canopy
```

```
canopy_noise_count = (f08_rate) * h_canopy
```

### 2.2.27 Canopy Quality Score

(Parameter = can\_quality\_score). The computed skill score of multiple parameters for each 100 m ATL08 segment. A score of 100 indicates a likely high quality estimate of canopy height. Deductions for the canopy skill score are as follows.

- 1005 1. Weak Beam: deduct 10 points
- 1006 2. Solar Elevation: 10 – 20 degrees; deduct 5 points
- 1007 Solar Elevation > 20 degrees; deduct 10 points
- 1008 3. Optical Depth <0.2 – 0.3; deduct 5 points >0.3 deduct 10 points
- 1009 4. Cloud Fold flag >0; deduct 10 points
- 1010 5. DEM\_removal\_flag > 0; deduct 10 points
- 1011 6. Total radiometry < 0.7; deduct 10 points; total radiometry < 1 deduct 5
- 1012 points
- 1013 7. Track telemetry band removal, if 40% of 10km removed, deduct 10 points
- 1014 for entire 10 km.
- 1015 8. MSW\_flag > 0; deduct 10 points
- 1016 9. SNR < 1; deduct 10 points
- 1017

### 1018 **2.3 Subgroup: Photons**

1019 The subgroup for photons contains the classified photons that were used to  
 1020 generate the parameters within the land or canopy subgroups. Each photon that is  
 1021 identified as being likely signal will be classified as: 0 = noise, 1 = ground, 2 = canopy,  
 1022 or 3 = top of canopy. The index values for each classified photon will be provided such  
 1023 that they can be extracted from the ATL03 data product for independent evaluation.

1024 Table 2.3. Summary table for photon parameters for the ATL08 product.

Group	Data Type	Description	Source
<b>classed_PC_idx</b>	Float	Indices of photons tracking back to ATL03 that surface finding software identified and used within the creation of the data products.	ATL03
<b>classed_PC_flag</b>	Integer	Classification flag for each photon as either noise, ground, canopy, or top of canopy.	computed

<b>ph_segment_id</b>	Integer	Georeferenced bin number (20-m) associated with each photon	ATL03
<b>ph_h</b>	Float	Height of photon above interpolated ground surface	computed
<b>d_flag</b>	Integer	Flag indicating whether DRAGANN labeled the photon as noise or signal	computed

1025

### 1026      **2.3.1** Indices\_of\_classed\_photons

1027          (parameter = classed\_PC\_indx). Indices of photons tracking back to ATL03 that  
1028 surface finding software identified and used within the creation of the data products  
1029 for a given segment.

### 1030      **2.3.2** Photon\_class

1031          (parameter = classed\_PC\_flag). Classification flags for a given segment. 0 =  
1032 noise, 1 = ground, 2 = canopy, 3 = top of canopy. The final ground and canopy  
1033 classification are flags 1-3. The full canopy is the combination of flags 2 and 3.

### 1034      **2.3.3** Georeferenced\_segment\_number

1035          (parameter = ph\_segment\_id). The segment\_id associated with every photon in  
1036 each 100-m segment. Each 100-m segment consists of five sequential 20-m segments  
1037 provided from the ATL03 product, which are labeled as segment\_id. The segment\_id  
1038 is a seven digit number that uniquely identifies each along track segment, and is  
1039 written at the along-track geolocation segment rate (i.e. ~20m along track). The four  
1040 digit RGT number can be combined with the seven digit segment\_id number to  
1041 uniquely define any along-track segment number. Values are sequential, with  
1042 0000001 referring to the first segment after the equatorial crossing of the ascending  
1043 node.

### 1044      **2.3.4** Photon Height

1045          (parameter = ph\_h). Height of the photon above the interpolated ground  
1046 surface at the location of the photon.

### 2.3.5 DRAGANN\_flag

(parameter = d\_flag). Flag indicating the labeling of DRAGANN noise filtering for a given photon. 0 = noise, 1=signal.

## 2.4 Subgroup: Reference data

The reference data subgroup contains parameters and information that are useful for determining the terrain and canopy heights that are reported on the product. In addition to position and timing information, these parameters include the reference DEM height, reference landcover type, and flags indicating water or snow.

Table 2.4. Summary table for reference parameters for the ATL08 product.

Group	Data Type	Description	Source
<b>segment_id_beg</b>	Integer	First along-track segment_id number in 100-m segment	ATL03
<b>segment_id_end</b>	Integer	Last along-track segment_id number in 100-m segment	ATL03
<b>latitude</b>	Float	Center latitude of signal photons within each segment	ATL03
<b>longitude</b>	Float	Center longitude of signal photons within each segment	ATL03
<b>delta_time</b>	Float	Mid-segment GPS time in seconds past an epoch. The epoch is provided in the metadata at the file level	ATL03
<b>delta_time_beg</b>	Float	Delta time of the first photon in the segment	ATL03
<b>delta_time_end</b>	Float	Delta time of the last photon in the segment	ATL03
<b>night_flag</b>	Integer	Flag indicating whether the measurements were acquired during night time conditions	computed
<b>dem_h</b>	Float4	Reference DEM elevation	external
<b>dem_flag</b>		Source of reference DEM	external
<b>dem_removal_flag</b>	Integer	Quality check flag to indicate > 20% photons removed due to large distance from dem_h	computed
<b>h_dif_ref</b>	Float4	Difference between h_te_median and dem_h	computed

<b>terrain_flg</b>	Integer	Terrain flag quality check to indicate a deviation from the reference DTM	computed
<b>segment_landcover</b>	Integer	Reference landcover for segment derived from best global landcover product available	external
<b>segment_watermask</b>	Integer	Water mask indicating inland water produced from best sources available	external
<b>segment_snowcover</b>	Integer	Daily snow cover mask derived from best sources	external
<b>urban_flag</b>	Integer	Flag indicating segment is located in an urban area	external
<b>permafrost_prob</b>	Integer4	Permafrost probability (0 – 100) derived from ESA CCI 2019 northern hemisphere permafrost dataset	external
<b>permafrost_alt</b>	Float4	Permafrost active layer thickness (m) from ESA CCI 2019 northern hemisphere permafrost dataset	external
<b>surf_type</b>	Integer1	Flags describing surface types: 0=not type, 1=is type. Order of array is land, ocean, sea ice, land ice, inland water.	ATL03
<b>atl08_region</b>	Integer	ATL08 region(s) encompassed by ATL03 granule being processed	computed
<b>last_seg_extend</b>	Float	The distance (km) that the last ATL08 processing segment in a file is either extended or overlapped with the previous ATL08 processing segment	computed
<b>brightness_flag</b>	Integer	Flag indicating that the ground surface is bright (e.g. snow-covered or other bright surfaces)	computed

1057

#### 1058      **2.4.1** Georeferenced\_segment\_number\_beg

1059      (parameter = segment\_id\_beg). The first along-track segment\_id in each 100-m  
1060 segment. Each 100-m segment consists of five sequential 20-m segments provided

from the ATL03 product, which are labeled as `segment_id`. The `segment_id` is a seven digit number that uniquely identifies each along track segment, and is written at the along-track geolocation segment rate (i.e. ~20m along track). The four digit RGT number can be combined with the seven digit `segment_id` number to uniquely define any along-track segment number. Values are sequential, with 0000001 referring to the first segment after the equatorial crossing of the ascending node.

#### **2.4.2 Georeferenced\_segment\_number\_end**

(parameter = `segment_id_end`). The last along-track `segment_id` in each 100-m segment. Each 100-m segment consists of five sequential 20-m segments provided from the ATL03 product, which are labeled as `segment_id`. The `segment_id` is a seven digit number that uniquely identifies each along track segment, and is written at the along-track geolocation segment rate (i.e. ~20m along track). The four digit RGT number can be combined with the seven digit `segment_id` number to uniquely define any along-track segment number. Values are sequential, with 0000001 referring to the first segment after the equatorial crossing of the ascending node.

#### **2.4.3 Segment\_latitude**

(parameter = `latitude`). Center latitude of signal photons within each segment. Each 100 m segment consists of 5 20m ATL03 geosegments. In most cases, there will be signal photons in each of the 5 geosegments necessary for calculating a latitude value. For instances where the 100 m ATL08 is not fully populated with photons (e.g. photons drop out due to clouds or signal attenuation), the latitude will be interpolated to the mid-point of the 100 m segment. To implement this interpolation, we confirm that each 100 m segment is comprised of at least 3 unique ATL03 geosegments IDs, indicating that data is available near the mid-point of the land segment. If less than 3 ATL03 segments are available, the coordinate is interpolated based on the ratio of delta time at the centermost ATL03 segment and that of the centermost photon, thus applying the centermost photon's coordinates to represent the land segment with a slight adjustment. In some instances, the latitude and longitude will require extrapolation to estimate a mid-100 m segment location. It is possible that in these

extremely rare cases, the latitude and longitude could not represent the true center of the 100 m segment. We encourage the user to investigate the parameters `segment_te_flag` and `segment_can_flag` which provide information as to the number and distribution of signal photons within each 100 m segment.

#### **2.4.4 Geosegment\_latitude{1:5}**

(parameter = `latitude_20m`). Interpolated center latitude of each 20 m geosegment.

#### **2.4.5 Segment\_longitude**

(parameter = `longitude`). Center longitude of signal photons within each segment. Each 100 m segment consists of 5 20m geosegments. In most cases, there will be signal photons in each of the 5 geosegments necessary for calculating a longitude value. For instances where the 100 m ATL08 is not fully populated with photons (e.g. photons drop out due to clouds or signal attenuation), the latitude will be interpolated to the mid-point of the 100 m segment. To implement this interpolation, we confirm that each 100 m segment is comprised of at least 3 unique ATL03 geosegments IDs, indicating that data is available near the mid-point of the land segment. If less than 3 ATL03 segments are available, the coordinate is interpolated based on the ratio of delta time at the centermost ATL03 segment and that of the centermost photon, thus applying the centermost photon's coordinates to represent the land segment with a slight adjustment. In some instances, the latitude and longitude will require extrapolation to estimate a mid-100 m segment location. It is possible that in these extremely rare cases, the latitude and longitude could not represent the true center of the 100 m segment. We encourage the user to investigate the parameters `segment_te_flag` and `segment_can_flag` which provide information as to the number and distribution of signal photons within each 100 m segment.

#### **2.4.6 Geosegment\_longitude{1:5}**

(parameter = `longitude_20m`). Interpolated center longitude of each 20 m geosegment.



1118

1119       **2.4.7** Delta\_time

1120           (parameter = delta\_time). Mid-segment GPS time for the segment in seconds  
1121 past an epoch. The epoch is listed in the metadata at the file level.

1122       **2.4.8** Delta\_time\_beg

1123           (parameter = delta\_time\_beg). Delta time for the first photon in the segment  
1124 in seconds past an epoch. The epoch is listed in the metadata at the file level.

1125       **2.4.9** Delta\_time\_end

1126           (parameter = delta\_time\_end). Delta time for the last photon in the segment  
1127 in seconds past an epoch. The epoch is listed in the metadata at the file level.

1128       **2.4.10** Night\_Flag

1129           (parameter = night\_flag). Flag indicating the data were acquired in night  
1130 conditions: 0 = day, 1 = night. Night flag is set when solar elevation is below 0.0  
1131 degrees.

1132       **2.4.11** Segment\_reference\_DTM

1133           (parameter = dem\_h). Reference terrain height value for segment determined  
1134 by the “best” DEM available based on data location. All heights in ICESat-2 are  
1135 referenced to the WGS 84 ellipsoid unless clearly noted otherwise. DEM is taken from  
1136 a variety of ancillary data sources: MERIT, GIMP, GMTED, MSS. The DEM source flag  
1137 indicates which source was used.

1138       **2.4.12** Segment\_reference\_DEM\_source

1139           (parameter = dem\_flag). Indicates source of the reference DEM height. Values:  
1140 0=None, 1=GIMP, 2=GMTED, 3=MSS, 4=MERIT.

1141       **2.4.13 Segment\_reference\_DEM\_removal\_flag**  
 1142           (parameter = dem\_removal\_flag). Quality check flag to indicate > 20%  
 1143 classified photons removed from land segment due to large distance from dem\_h.

1144       **2.4.14 Segment\_terrain\_difference**  
 1145           (parameter = h\_dif\_ref). Difference between h\_te\_median and dem\_h. Since the  
 1146 mean terrain height is more sensitive to outliers, the median terrain height will be  
 1147 evaluated against the reference DEM. This parameter will be used as an internal data  
 1148 quality check with the notion being that if the difference exceeds a threshold (TBD) a  
 1149 terrain quality flag (terrain\_flg) will be triggered.

1150       **2.4.15 Segment\_terrain flag**  
 1151           (parameter = terrain\_flg). Terrain flag to indicate confidence in the derived  
 1152 terrain height estimate. If h\_dif\_ref exceeds a threshold (TBD) the terrain\_flg  
 1153 parameter will be set to 1. Otherwise, it is 0.

1154       **2.4.16 Segment\_landcover**  
 1155           (parameter = segment\_landcover). Updating the segment landcover with the  
 1156 2019 Copernicus Landcover 100 m discrete landcover product which incorporates 23  
 1157 discrete landcover classes which follow the UN-FAO's Land Cover Classification  
 1158 System. The ATL08 landcover segment will be the Copernicus Landcover value at the  
 1159 segment                      latitude/longitude                      (255=Undetermined).  
 1160 <https://land.copernicus.eu/global/products/lc>  
 1161 (<https://doi.org/10.5281/zenodo.3939050>).

Map Code	Landcover Class	Definition according to UN LCCS
0	No data	
111	Closed forest, evergreen needle leaf	Tree canopy >70%, almost all needle leaf trees remain green all year. Canopy is never without green foliage
113	Closed forest, deciduous needle leaf	Tree canopy >70%, consists of seasonal needle leaf communities with an annual cycle of leaf-on and leaf-off periods.

112	Closed forest, evergreen broad leaf	Tree canopy >70%, almost all broadleaf trees remain green year round. Canopy is never without green foliage
114	Closed forest, deciduous broad leaf	Tree canopy >70%, consists of seasonal broad leaf communities with an annual cycle of leaf-on and leaf-off periods.
115	Closed forest, mixed	Closed forest, mix of types
116	Closed forest, unknown	Closed forest, not matching any of the other definitions
121	Open forest, evergreen needle leaf	Top layer- trees 15-70% and second layer mixed of shrubs and grassland, almost all needle leaf trees remain green all year. Canopy is never without green foliage
123	Open forest, deciduous needle leaf	Top layer- trees 15-70% and second layer mixed of shrubs and grassland, consists of seasonal needle leaf tree communities with an annual cycle of leaf-on and leaf-off
122	Open forest, evergreen broad leaf	Top layer- trees 15-70% and second layer mixed of shrubs and grassland, almost all broad leaf trees remain green all year. Canopy is never without green foliage
124	Open forest, deciduous broad leaf	Top layer- trees 15-70% and second layer mixed of shrubs and grassland, consists of seasonal broad leaf tree communities with an annual cycle of leaf-on and leaf-off
125	Open forest, mixed	Open forest, mix of types
126	Open forest, unknown	Open forest, not matching any of the other definitions
20	Shrubs	Woody perennial plants with persistent and woody stems and without a main stem being less than 5m. The shrub foliage can be either evergreen or deciduous.
30	Herbaceous	Plants without persistent stems or shoots above ground and lacking firm structure. Tree and shrub cover is less than 10%
90	Herbaceous Wetland	Lands with a permanent mixture of water and herbaceous or woody vegetation. The vegetation can be present in salt, brackish, or fresh water.
100	Moss and lichen	Moss and lichen
60	Bare/sparse vegetation	Lands with exposed soil, sand, or rocks and never has more than 10% vegetation cover during any time of the year
40	Cultivated and managed vegetation/agriculture	Lands covered with temporary crops followed by harvest and a bare soil period.
50	Urban/built up	Land covered by buildings or other man-made structures
70	Snow and ice	Land under snow or ice throughout the year
80	Permanent water bodies	Lakes, reservoirs, and rivers. Can be either fresh or salt-water bodies
200	Open sea	Oceans, seas. Can be either fresh or salt-water bodies.

1162

1163

1164

1165       **2.4.17 Segment\_Woody Vegetation Fractional Cover**

1166           (parameter = segment\_cover). Woody vegetation fractional cover derived  
1167 from the 2019 Copernicus 100 m shrub and forest fractional cover data products. The  
1168 woody cover fractional cover is the simple addition of the forest fractional cover with  
1169 the shrub fractional cover. The ATL08 woody vegetation fractional cover value shall  
1170 be the pixel value at the segment latitude/longitude. The Copernicus data products  
1171 can be found at <https://lcviewer.vito.be/download>

1172       **2.4.18 Segment\_watermask**

1173           (parameter = segment\_watermask). Water mask (i.e., flag) indicating inland  
1174 water as referenced from the Global Raster Water Mask at 250 m spatial resolution  
1175 (Carroll et al, 2009; available online at <http://glcf.umd.edu/data/watermask/>). 0 =  
1176 no water; 1 = water; 255 = Undetermined.

1177       **2.4.19 Segment\_snowcover**

1178           (parameter = segment\_snowcover). Daily snowcover mask (i.e., flag)  
1179 indicating a likely presence of snow or ice within each segment produced from best  
1180 available source used for reference. The snow mask will be the same snow mask as  
1181 used for ATL09 Atmospheric Products: NOAA snow-ice flag. 0=ice free water;  
1182 1=snow free land; 2=snow; 3=ice; 255=Undetermined.

1183       **2.4.20 Urban\_flag**

1184           (parameter = urban\_flag). Segment estimated urban cover flag as derived from  
1185 the Global Urban Footprint (GUF) data product. GUF is a global mapping of urban  
1186 areas derived from the TerraSAR-X and TanDEM-X satellites. The GUF maps at a  
1187 resolution of ~12 m (0.4 arcseconds). Due to differences in resolution, the ATL08  
1188 GUF value is set based upon a 4x4 block of pixels about the 100 m segment  
1189 latitude/longitude . If ANY of the pixels the GUF pixels are labeled as urban, the  
1190 ATL08 GUF value is set to urban. The GUF urban flag is set as -1 = undetermined, 0 =

not urban, 1 = urban. The GUF data are available from DLR  
[https://www.dlr.de/eoc/en/desktopdefault.aspx/tabid-9628/16557\\_read-40454/](https://www.dlr.de/eoc/en/desktopdefault.aspx/tabid-9628/16557_read-40454/)

#### **2.4.21 Permafrost\_probability**

(parameter = permafrost\_prob). Segment estimated permafrost probability derived from the ESA CCI 2019 Permafrost data product version 3 (Obu et al, 2021). Probability values range from 0 to 100 and are reported as integers. Should an ATL08 segment straddle two 1 km pixels, the maximum probability will be reported at the 100 m segment level. Permafrost probability is defined as the fraction of Mean Annual Ground Temperature < 0 C. The permafrost products are defined as the yearly fraction of permafrost-underlain and permafrost-free area within a pixel. The classification of permafrost zones are: isolated (0 – 10%), sporadic (10-50%), discontinuous (50-90%) and continuous (90-100%). The permafrost probability maps are produced at a 1 km resolution for the northern hemisphere and data from 2019 is reported here. The ESA CCI data products are available from <https://climate.esa.int/en/projects/permafrost/>. If no value can be determined, a value of 255 will be reported.

#### **2.4.22 Permafrost\_ALT**

(parameter = permafrost\_alt). Segment estimated active layer thickness (m) derived from the ESA CCI Permafrost data product (Obu et al, 2021). At the segment level, the CCI ALT value is divided by 100 to provide a depth value in meters. Should a 100 m segment cross a 1 km pixel value, the maximum ALT value will be reported. Active layer thickness is the depth of the seasonally unfrozen soil for 2019 based on MODIS land surface temperatures merged with downscaled ERA5 reanalysis near-surface air temperature. The active layer thickness can vary from year to year as it is dependent upon air temperature, soil type, snow cover, among others. The permafrost ALT maps are produced at a 1 km resolution for the northern hemisphere and represent the maximum depth of seasonal thaw. All of the permafrost datasets are published through ESA Climate Archive available at

<https://catalogue.ceda.ac.uk/uuid/8239d5f6263f4551bf2bd100d3ecbead>. If no value can be determined, a value of 255 will be reported.

#### **2.4.23 Surface Type**

(parameter = surf\_type). The surface type for a given segment is determined at the major frame rate (every 200 shots, or ~140 meters along-track) and is a two-dimensional array surf\_type(n, nsurf), where n is the major frame number, and nsurf is the number of possible surface types such that surf\_type(n, isurf) is set to 0 or 1 indicating if surface type isurf is present (1) or not (0), where isurf = 1 to 5 (land, ocean, sea ice, land ice, and inland water) respectively.

#### **2.4.24 ATL08\_region**

(parameter = atl08\_region). The ATL08 regions that encompass the ATL03 granule being processed through the ATL08 algorithm. The ATL08 regions are shown by Figure 2.3.

#### **2.4.25 Last\_segment\_extend**

(parameter = last\_seg\_extend). The distance (km) that the last ATL08 10 km processing segment is either extended beyond 10 km or uses data from the previous 10 km processing segment to allow for enough data for processing the ATL03 photons through the ATL08 algorithm. If the last portion of an ATL03 granule being processed would result in a segment with less than 3.4 km (170 geosegments) worth of data, that last portion is added to the previous 10 km processing window to be processed together as one extended ATL08 processing segment. The resulting last\_seg\_extend value would be a positive value of distance beyond 10 km that the ATL08 processing segment was extended by. If the last ATL08 processing segment would be less than 10 km but greater than 3.4 km, a portion extending from the start of current ATL08 processing segment backwards into the previous ATL08 processing segment would

1246 be added to the current ATL08 processing segment to make it 10 km in length. The  
 1247 distance of this backward data gathering would be reported in last\_seg\_extend as a  
 1248 negative distance value. Only new 100 m ATL08 segment products generated from  
 1249 this backward extension would be reported. All other segments that are not extended  
 1250 will report a last\_seg\_extend value of 0.

#### 1251 **2.4.26 Brightness\_flag**

1252 (parameter = brightness\_flag). Based upon the classification of the photons  
 1253 within each 100 m, this parameter flags ATL08 segments where the mean number of  
 1254 ground photons per shot exceed a value of 3. This calculation can be made as the total  
 1255 number of ground photons divided by the number of ATLAS shots within the 100 m  
 1256 segment. A value of 0 = indicates non-bright surface, value of 1 indicates bright  
 1257 surface, and a value of 2 indicates “undetermined” due to clouds or other factors. The  
 1258 brightness is computed initially on the 10 km processing segment. If the ground  
 1259 surface is determined to be bright for the entire 10 km segment, the brightness is then  
 1260 calculated at the 100 m segment size.

1261

### 1262 **2.5 Subgroup: Beam data**

1263 The subgroup for beam data contains basic information on the geometry and  
 1264 pointing accuracy for each beam.

1265 Table 2.5. Summary table for beam parameters for the ATL08 product.

Group	Data Type	Units	Description	Source
segment_id_beg	Integer		First along-track segment_id number in 100-m segment	ATL03
segment_id_end	Integer		Last along-track segment_id number in 100-m segment	ATL03
ref_elev	Float		Elevation of the unit pointing vector for the reference photon in the	ATL03

		local ENU frame in radians. The angle is measured from East-North plane and positive towards up	
<b>ref_azimuth</b>	Float	Azimuth of the unit pointing vector for the reference photon in the ENU frame in radians. The angle is measured from North and positive toward East.	ATL03
<b>atlas_pa</b>	Float	Off nadir pointing angle of the spacecraft	ATL03
<b>rgt</b>	Integer	The reference ground track (RGT) is the track on the earth at which the vector bisecting laser beams 3 and 4 is pointed during repeat operations	ATL03
<b>sigma_h</b>	Float	Total vertical uncertainty due to PPD and POD	ATL03
<b>sigma_along</b>	Float	Total along-track uncertainty due to PPD and POD knowledge	ATL03
<b>sigma_across</b>	Float	Total cross-track uncertainty due to PPD and POD knowledge	ATL03
<b>sigma_topo</b>	Float	Uncertainty of the geolocation knowledge due to local topography (Equation 1.3)	computed
<b>sigma_atlas_land</b>	Float	Total uncertainty that includes sigma_h plus the geolocation uncertainty due to local slope Equation 1.2	computed
<b>psf_flag</b>	integer	Flag indicating sigma_atlas_land (aka PSF) as computed in Equation 1.2 exceeds a value of 1m.	computed
<b>layer_flag</b>	Integer	Cloud flag indicating presence of clouds or blowing snow	ATL09



<b>cloud_flag_atm</b>	Integer	Cloud confidence flag from ATL09 indicating clear skies	ATL09
<b>msw_flag</b>	Integer	Multiple scattering warning product produced on ATL09	ATL09
<b>cloud_fold_flag</b>	integer	Cloud flag to indicate potential of high clouds that have “folded” into the lower range bins	ATL09
<b>asr</b>	Float	Apparent surface reflectance (ASR)	ATL09
<b>column_od_asr</b>	Float	Column optical depth from ASR.	ATL09
<b>snr</b>	Float	Background signal to noise level	Computed
<b>solar_azimuth</b>	Float	The azimuth (in degrees) of the sun position vector from the reference photon bounce point position in the local ENU frame. The angle is measured from North and is positive towards East.	ATL03g
<b>solar_elevation</b>	Float	The elevation of the sun position vector from the reference photon bounce point position in the local ENU frame. The angle is measured from the East-North plane and is positive Up.	ATL03g
<b>n_seg_ph</b>	Integer	Number of photons within each land segment	computed
<b>ph_ndx_beg</b>	Integer	Photon index begin	computed
<b>sat_flag</b>	Integer	Flag derived from full_sat_fract and near_sat_fract on the ATL03 data product	computed

1266

### 2.5.1 Georeferenced\_segment\_number\_beg

(parameter = segment\_id\_beg). The first along-track segment\_id in each 100-m segment. Each 100-m segment consists of five sequential 20-m segments provided from the ATL03 product, which are labeled as segment\_id. The segment\_id is a seven digit number that uniquely identifies each along track segment, and is written at the along-track geolocation segment rate (i.e. ~20m along track). The four digit RGT number can be combined with the seven digit segment\_id number to uniquely define any along-track segment number. Values are sequential, with 0000001 referring to the first segment after the equatorial crossing of the ascending node.

### 2.5.2 Georeferenced\_segment\_number\_end

(parameter = segment\_id\_end). The last along-track segment\_id in each 100-m segment. Each 100-m segment consists of five sequential 20-m segments provided from the ATL03 product, which are labeled as segment\_id. The segment\_id is a seven digit number that uniquely identifies each along track segment, and is written at the along-track geolocation segment rate (i.e. ~20m along track). The four digit RGT number can be combined with the seven digit segment\_id number to uniquely define any along-track segment number. Values are sequential, with 0000001 referring to the first segment after the equatorial crossing of the ascending node.

### 2.5.3 Beam\_coelevation

(parameter = ref\_elev). Elevation of the unit pointing vector for the reference photon in the local ENU frame in radians. The angle is measured from East-North plane and positive towards up.

### 2.5.4 Beam\_azimuth

(parameter = ref\_azimuth). Azimuth of the unit pointing vector for the reference photon in the ENU frame in radians. The angle is measured from North and positive toward East.

### 2.5.5 ATLAS\_Pointing\_Angle

(parameter = atlas\_pa). Off nadir pointing angle (in radians) of the satellite to increase spatial sampling in the non-polar regions.

### 2.5.6 Reference\_ground\_track

(parameter = rgt). The reference ground track (RGT) is the track on the earth at which the vector bisecting laser beams 3 and 4 (or GT2L and GT2R) is pointed during repeat operations. Each RGT spans the part of an orbit between two ascending equator crossings and are numbered sequentially. The ICESat-2 mission has 1387 RGTs, numbered from 0001xx to 1387xx. The last two digits refer to the cycle number.

### 2.5.7 Sigma\_h

(parameter = sigma\_h). Total vertical uncertainty due to PPD (Precise Pointing Determination), POD (Precise Orbit Determination), and geolocation errors. Specifically, this parameter includes radial orbit error,  $\sigma_{orbit}$ , tropospheric errors,  $\sigma_{Trop}$ , forward scattering errors,  $\sigma_{forwardscattering}$ , instrument timing errors,  $\sigma_{timing}$ , and off-nadir pointing geolocation errors. The component parameters are pulled from ATL03 and ATL09. Sigma\_h is the root sum of squares of these terms as detailed in Equation 1.1. The sigma\_h reported here is the mean of the sigma\_h values reported within the five ATL03 geosegments that are used to create the 100 m ATL08 segment.

### 2.5.8 Sigma\_along

(parameter = sigma\_along). Total along-track uncertainty due to PPD and POD knowledge. This parameter is pulled from ATL03.

### 2.5.9 Sigma\_across

(parameter = sigma\_across). Total cross-track uncertainty due to PPD and POD knowledge. This parameter is pulled from ATL03.

#### **2.5.10 Sigma\_topo**

(parameter = sigma\_topo). Uncertainty in the geolocation due to local surface slope as described in Equation 1.3. The local slope is multiplied by the 6.5 m geolocation uncertainty factor that will be used to determine the geolocation uncertainty. The geolocation error will be computed from a 100 m sample due to the local slope calculation at that scale.

#### **2.5.11 Sigma\_ATLAS\_LAND**

(parameter = sigma\_atlas\_land). Total vertical geolocation error due to ranging, and local surface slope. The parameter is computed for ATL08 as described in Equation 1.2. The geolocation error will be computed from a 100 m sample due to the local slope calculation at that scale.

#### **2.5.12 PSF\_flag**

(parameter = psf\_flag). Flag indicating that the point spread function (computed as sigma\_atlas\_land) has exceeded 1m.

#### **2.5.13 Layer\_flag**

(parameter = layer\_flag). Flag is a combination of multiple ATL09 flags and takes daytime/nighttime into consideration. A value of 1 means clouds or blowing snow is likely present. A value of 0 indicates the likely absence of clouds or blowing snow. If no ATL09 product is available for an ATL08 segment, an invalid value will be reported. Since the cloud flags from the ATL09 product are reported at an along-track distance of 250 m, we will report the highest value of the ATL09 flags at the ATL08 resolution (100 m). Thus, if a 100 m ATL08 segment straddles two values from ATL09, the highest cloud flag value will be reported on ATL08. This reporting strategy holds for all the cloud flags reported on ATL08.

1341       **2.5.14** Cloud\_flag\_atm

1342       (parameter = cloud\_flag\_atm). Cloud confidence flag from ATL09 that indicates  
1343 the number of cloud or aerosol layers identified in each 25Hz atmospheric profile. If  
1344 the flag is greater than 0, aerosols or clouds could be present.

1345       **2.5.15** MSW

1346       (parameter = msw\_flag). Multiple scattering warning flag with values from -1 to  
1347 5 as computed in the ATL09 atmospheric processing and delivered on the ATL09 data  
1348 product. A value of 127 indicates that the signal to noise of the data was too low to  
1349 reliably ascertain the presence of cloud or blowing snow. We expect values of 127 to  
1350 occur only during daylight. If no ATL09 product is available for an ATL08 segment,  
1351 an invalid value will be reported. MSW flags:

1352	127 = signal to noise ratio too low to determine presence of
1353	cloud or blowing snow
1354	0 = no_scattering is detected
1355	1 = clouds/scattering at > 3 km
1356	2 = clouds/scattering at 1-3 km
1357	3 = clouds/scattering at < 1 km
1358	4 = blowing snow at < 0.5 optical depth
1359	5 = blowing snow at >= 0.5 optical depth

1360       **2.5.16** Cloud Fold Flag

1361       (parameter = cloud\_fold\_flag). Clouds occurring higher than 14 to 15 km in the  
1362 atmosphere will be folded down into the lower portion of the atmospheric profile.

1363       **2.5.17** Computed\_Apparent\_Surface\_Reflectance

1364       (parameter = asr). Apparent surface reflectance computed in the ATL09  
1365 atmospheric processing and delivered on the ATL09 data product. If no ATL09  
1366 product is available for an ATL08 segment, an invalid value will be reported.

#### **2.5.18 Column\_Optical\_Depth\_ASR**

(parameter = column\_od\_asr). The particulate total column optical depth calculated on ATL09. This parameter is only valid when a ground return is detectable. Optical depth values >3 indicate that the ground return was not found and the optical depth calculation is invalid. A value of 0 indicates a totally clear atmosphere with no cloud or aerosols present. The column optical depth parameter does not include the OD of the molecular atmosphere: only particulate. The optical depth parameter reported on the ATL08 data product shall be the maximum observed OD from ATL09 within each 100 m segment. If no ATL09 product is available for an ATL08 segment, an invalid value will be reported.

#### **2.5.19 Signal\_to\_Noise\_Ratio**

(parameter = snr). The Signal to Noise Ratio of geolocated photons as determined by the ratio of the superset of ATL03 signal and DRAGANN found signal photons used for processing the ATL08 segments to the background photons (i.e., noise) within the same ATL08 segments.

#### **2.5.20 Solar\_Azimuth**

(parameter = solar\_azimuth). The azimuth (in degrees) of the sun position vector from the reference photon bounce point position in the local ENU frame. The angle is measured from North and is positive towards East.

#### **2.5.21 Solar\_Elevation**

(parameter = solar\_elevation). The elevation of the sun position vector from the reference photon bounce point position in the local ENU frame. The angle is measured from the East-North plane and is positive up.

#### **2.5.22 Number\_of\_segment\_photons**

(parameter = n\_seg\_ph). Number of photons in each land segment.

1392        **2.5.23 Photon\_Index\_Begin**

1393            (parameter = ph\_ndx\_beg). Index (1-based) within the photon-rate data of  
1394 the first photon within this each land segment.

1395        **2.5.24 Saturation Flag**

1396            (parameter = sat\_flag) Saturation flag derived from the ATL03 saturation  
1397 flags full\_sat\_frac. The saturation flags on the ATL03 data product (full\_sat\_frac)  
1398 are the percentage of photons determined to be saturated within each geosegment.  
1399 For the ATL08 saturation flag, a value of 0 will indicate no saturation. A value of 1  
1400 will indicate the average of all 5 geosegment full\_sat\_frac values was over 0.2. This  
1401 value of 1 is an indication of standing water or saturated soils. If an ATL08 segment  
1402 is not fully populated with 5 values for full\_sat\_frac, a value of -1 will be set.

1403            sat\_flag:        -1 indicates not enough valid data to make determination

1404                            0 indicates no saturation in ATL08 segment

1405                            1 indicates saturation in ATL08 segment

1406

1407

1408

1409

### 3 ALGORITHM METHODOLOGY

For the ecosystem community, identification of the ground and canopy surface is by far the most critical task, as meeting the science objective of determining global canopy heights hinges upon the ability to detect both the canopy surface and the underlying topography. Since a space-based photon counting laser mapping system is a relatively new instrument technology for mapping the Earth's surface, the software to accurately identify and extract both the canopy surface and ground surface is described here. The methodology adopted for ATL08 establishes a framework to potentially accept multiple approaches for capturing both the upper and lower surface of signal photons. One method used is an iterative filtering of photons in the along-track direction. This method has been found to preserve the topography and capture canopy photons, while rejecting noise photons. An advantage of this methodology is that it is self-parameterizing, robust, and works in all ecosystems if sufficient photons from both the canopy and ground are available. For processing purposes, along-track data signal photons are parsed into  $L$ -km segment of the orbit which is recommended to be 10 km in length.

#### 3.1 Noise Filtering

Solar background noise is a significant challenge in the analysis of photon counting laser data. Range measurement data created from photon counting lidar detectors typically contain far higher noise levels than the more common photon integrating detectors available commercially in the presence of passive, solar background photons. Given the higher detection sensitivity for photon counting devices, a background photon has a greater probability of triggering a detection event over traditional integral measurements and may sometimes dominate the dataset. Solar background noise is a function of the surface reflectance, topography, solar elevation, and atmospheric conditions. Prior to running the surface finding algorithms used for ATL08 data products, the superset of output from the GSFC medium-high confidence classed photons (ATL03 signal\_conf\_ph: flags 3-4) and the



output from DRAGANN will be considered as the input data set. ATL03 input data requirements include the latitude, longitude, height, segment delta time, segment ID, and a preliminary signal classification for each photon. The motivation behind combining the results from two different noise filtering methods is to ensure that all of the potential signal photons for land surfaces will be provided as input to the surface finding software. The description of the methodology for the ATL03 classification is described separately in the ATL03 ATBD. The methodology behind DRAGANN is described in the following section.

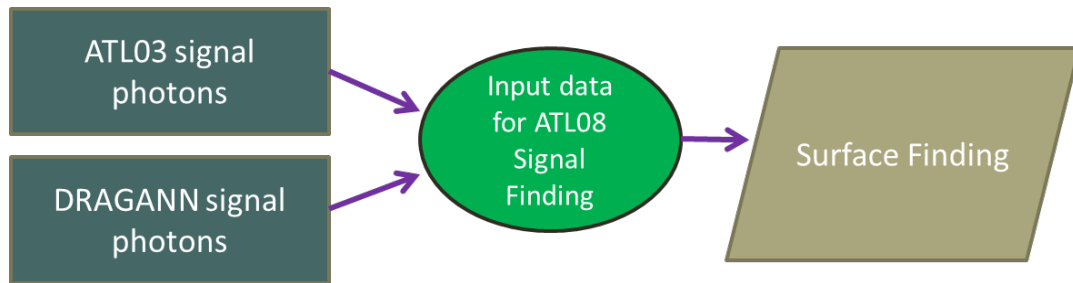


Figure 3.1. Combination of noise filtering algorithms to create a superset of input data for surface finding algorithms.

### 3.1.1 DRAGANN

The Differential, Regressive, and Gaussian Adaptive Nearest Neighbor (DRAGANN) filtering technique was developed to identify and remove noise photons from the photon counting data point cloud. DRAGANN utilizes the basic premise that signal photons will be closer in space than random noise photons. The first step of the filtering is to implement an adaptive nearest neighbor search. By using an adaptive method, different thresholds can be applied to account for variable amounts of background noise and changing surface reflectance along the data profile. This search finds an effective radius by computing the probability of finding P number of points within a search area. For MABEL and mATLAS, P=20 points within the search area

was empirically derived but found to be an effective and efficient number of neighbors.

There may be cases, however, where the value of  $P$  needs to be changed. For example, during night acquisitions it is anticipated that the background noise rate will be considerably low. Since DRAGANN is searching for two distributions in neighborhood searching space, the software could incorrectly identify signal photons as noise photons. The parameter  $P$ , however, can be determined dynamically from estimations of the signal and noise rates from the photon cloud. In cases of low background noise (night),  $P$  would likely be changed to a value lower than 20. Similarly, in cases of high amounts of solar background,  $P$  may need to be increased to better capture the signal and avoid classifying small, dense clusters of noise as signal. In this case, however, it is likely that noise photons near signal photons will also be misclassified as signal. The method for dynamically determining a  $P$  value is explained further in section 4.3.1.

After  $P$  is defined, a histogram of the number of neighbors within a search radius for each point is generated. The distribution of neighbor radius occurrences is analyzed to determine the noise threshold.

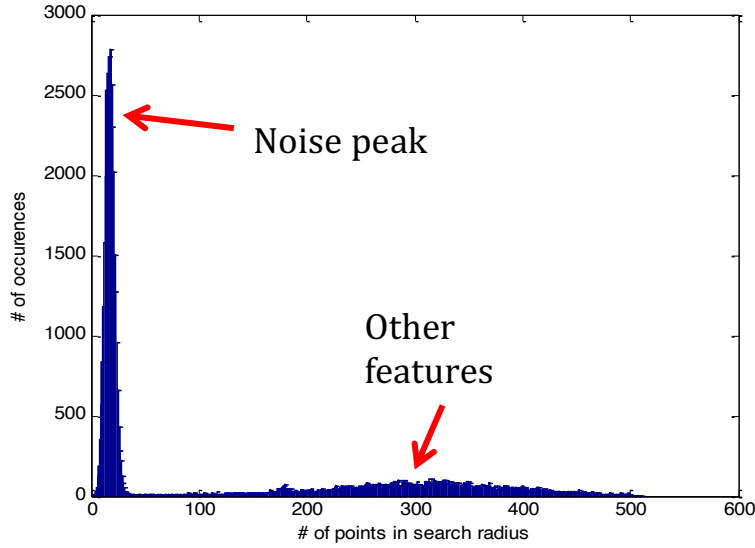
$$\frac{P}{N_{total}} = \frac{V}{V_{total}} \quad \text{Eqn. 3.1}$$

where  $N_{total}$  is the total number of photons in the point cloud,  $V$  is the volume of the nearest neighborhood search, and  $V_{total}$  is the bounding volume of the enclosed point cloud. For a 2-dimensional data set,  $V$  becomes

$$V = \pi r^2 \quad \text{Eqn. 3.2}$$

where  $r$  is the radius. A good practice is to first normalize the data set along each dimension before running the DRAGANN filter. Normalization prevents the algorithm from favoring one dimension over the others in the radius search (e.g., when the latitude and longitude are in degrees and height is in meters).

1491



1492

1493 Figure 3.2. Histogram of the number of photons within a search radius. This histogram is  
1494 used to determine the threshold for the DRAGANN approach.

1495

1496 Once the radius has been computed, DRAGANN counts the number of points  
1497 within the radius for each point and histograms that set of values. The distribution of  
1498 the number of points, Figure 3.2, reveals two distinct peaks; a noise peak and a signal  
1499 peak. The motivation of DRAGANN is to isolate the signal photons by determining a  
1500 threshold based on the number of photons within the search radius. The noise peak  
1501 is characterized as having a large number of occurrences of photons with just a few  
1502 neighboring photons within the search radius. The signal photons comprise the broad  
1503 second peak. The first step in determining the threshold between the noise and signal  
1504 is to implement Gaussian fitting to the number of photons distribution (i.e., the  
1505 distribution shown in Figure 3.2). The Gaussian function has the form

1506

1507 
$$g(x) = ae^{\frac{-(x-b)^2}{2c^2}}$$
 Eqn. 3.3

1508

where  $a$  is the amplitude of the peak,  $b$  is the center of the peak, and  $c$  is the standard deviation of the curve. A first derivative sign crossing method is one option to identify peaks within the distribution.

To determine the noise and signal Gaussians, up to ten Gaussian curves are fit to the histogram using an iterative process of fitting and subtracting the maximum amplitude peak component from the histogram until all peaks have been extracted. Then, the potential Gaussians pass through a rejection process to eliminate those with poor statistical fits or other apparent errors (Goshtasby and O'Neill, 1994; Chauve et al. 2008). A Gaussian with an amplitude less than  $1/5$  of the previous Gaussian and within two standard deviations of the previous Gaussian should be rejected. Once the errant Gaussians are rejected, the final two remaining are assumed to represent the noise and signal. These are separated based on the remaining two Gaussian components within the histogram using the logic that the leftmost Gaussian is noise (low neighbor counts) and the other is signal (high neighbor counts).

The intersection of these two Gaussians (noise and signal) determines a data threshold value. The threshold value is the parameter used to distinguish between noise points and signal points when the point cloud is re-evaluated for surface finding. In the event that only one curve passes the rejection process, the threshold is set at  $1 \sigma$  above the center of the noise peak.

An example of the noise filtered product from DRAGANN is shown in Figure 3.3. The signal photons identified in this process will be combined with the coarse signal finding output available on the ATL03 data product.

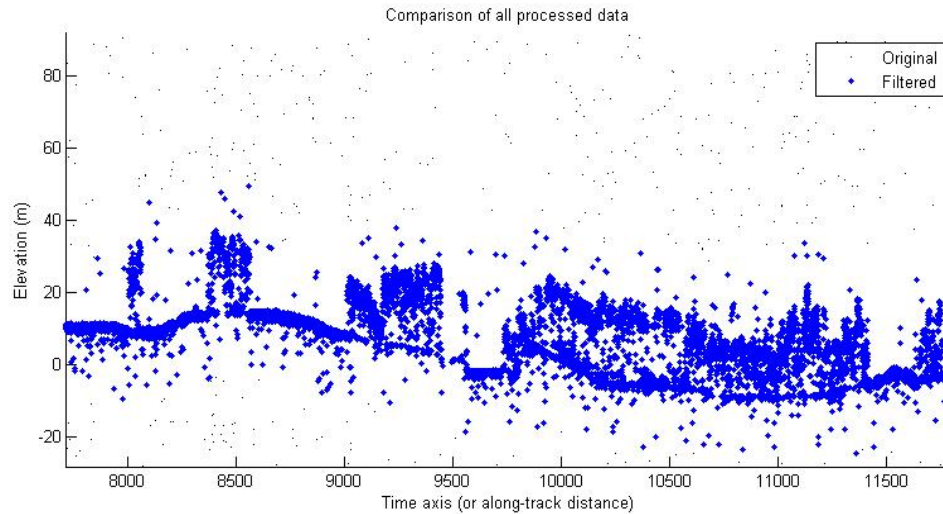


Figure 3.3. Output from DRAGANN filtering. Signal photons are shown as blue.

Figure 3.3 provides an example of along-track (profiling) height data collected in September 2012 from the MABEL (ICESat-2 simulator) over vegetation in North Carolina. The photons have been filtered such that the signal photons returned from vegetation and the ground surface are remaining. Noise photons that are adjacent to the signal photons are also retained in the input dataset; however, these should be classified as noise photons during the surface finding process. It is possible that some additional outlying noise may be retained during the DRAGANN process when noise photons are densely grouped, and these photons should be filtered out before the surface finding process. Estimates of the ground surface and canopy height can then be derived from the signal photons.

### 3.2 Surface Finding

Once the signal photons have been determined, the objective is to find the ground and canopy photons from within the point cloud. With the expectation that one algorithm may not work everywhere for all biomes, we are employing a framework that will allow us to combine the solutions of multiple algorithms into one final composite solution for the ground surface. The composite ground surface solution will then be utilized to classify the individual photons as ground, canopy, top

of canopy, or noise. Currently, the framework described here utilizes one algorithm for finding the ground surface and canopy surface. Additional methods, however, could be integrated into the framework at a later time. Figure 3.4 below describes the framework.

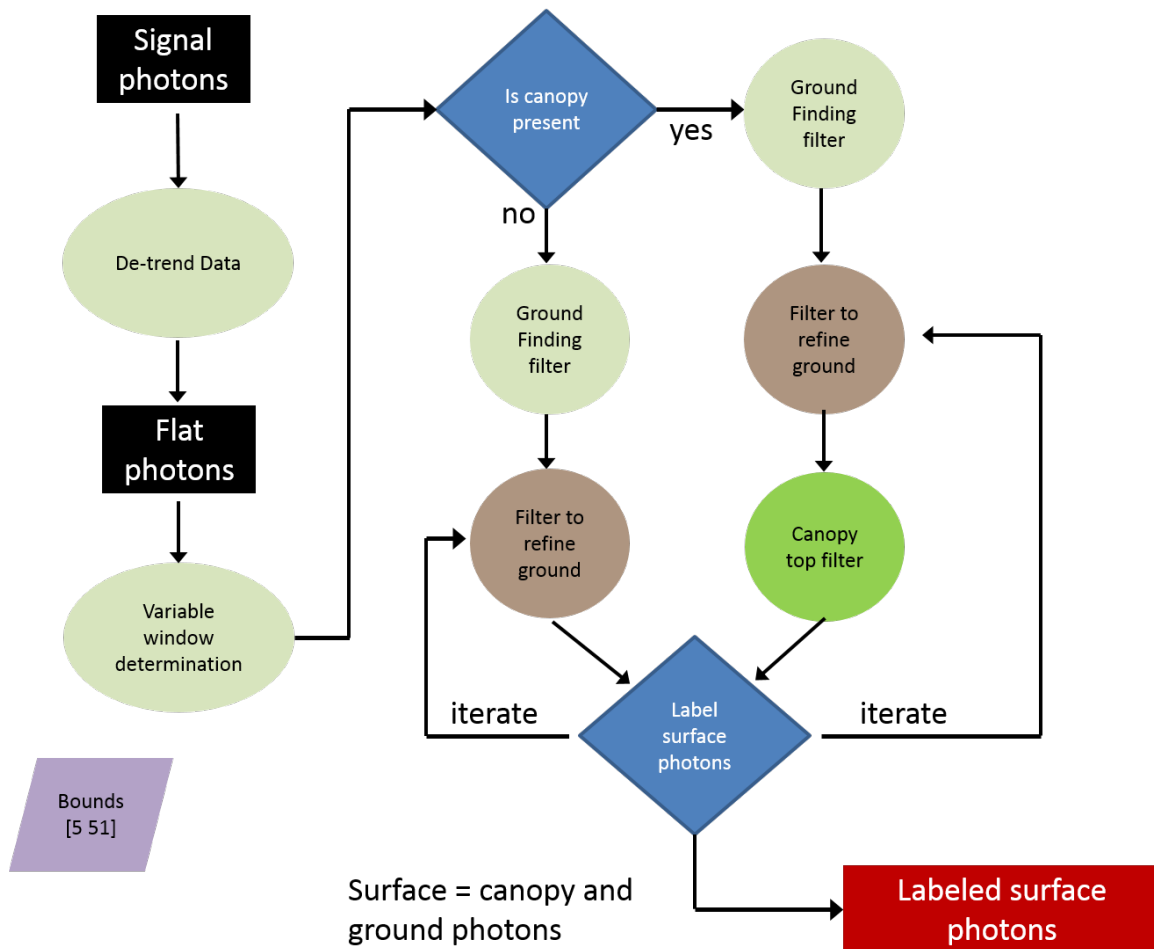


Figure 3.4. Flowchart of overall surface finding method.

### 3.2.1 De-trending the Signal Photons

An important step in the success of the surface finding algorithm is to remove the effect of topography on the input data, thus improving the performance of the algorithm. This is done by de-trending the input signal photons by subtracting a heavily smoothed “surface” that is derived from the input data. Essentially, this is a low pass filter of the original data and most of the analysis to detect the canopy and ground will subsequently be implemented on the high pass data. The amount of smoothing that is implemented in order to derive this first surface is dependent upon the relief. For segments where the relief is high, the smoothing window size is decreased so topography isn’t over-filtered.

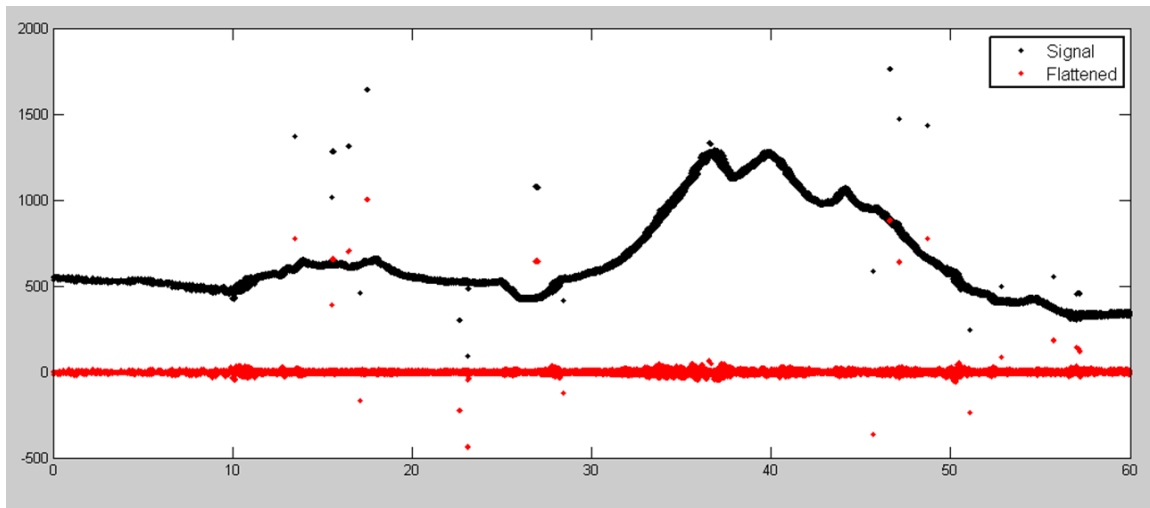


Figure 3.5. Plot of Signal Photons (black) from 2014 MABEL flight over Alaska and de-trended photons (red).

### 3.2.2 Canopy Determination

A key factor in the success of the surface finding algorithm is for the software to automatically **account for the presence of canopy** along a given  $L$ -km segment. Due to the large volume of data, this process has to occur in an automated fashion, allowing the correct methodology for extracting the surface to be applied to the data. In the absence of canopy, the iterative filtering approach to finding ground works

1580 extremely well, but if canopy does exist, we need to accommodate for that fact when  
1581 we are trying to recover the ground surface.

1582 For ATL08 product regions over Antarctica (regions 7, 8, 9, 10) and Greenland  
1583 (region 11), the algorithm will assume only ground photons (canopy flag = 0) (see  
1584 Figure 2.2).

1585

### 1586 3.2.3 Variable Window Determination

1587 The method for generating a best estimated terrain surface will vary depending  
1588 upon whether canopy is present. *L-km segments* without canopy are much easier to  
1589 analyze because the ground photons are usually continuous. *L-km segments* with  
1590 canopy, however, require more scrutiny as the number of signal photons from ground  
1591 are fewer due to occlusion by the vegetation.

1592 There are some common elements for finding the terrain surface for both cases  
1593 (canopy/no canopy) and with both methods. In both cases, we will use a variable  
1594 windowing span to compute statistics as well as filter and smooth the data. For  
1595 clarification, the window size is variable for each *L-km segment*, but it is constant  
1596 within the *L-km segment*. For the surface finding algorithm, we will employ a  
1597 Savitzky-Golay smoothing/median filtering method. Using this filter, we compute a  
1598 variable smoothing parameter (or window size). It is important to bound the filter  
1599 appropriately as the output from the median filter can lose fidelity if the scan is over-  
1600 filtered.

1601 We have developed an empirically-determined shape function, bound between  
1602 [5 51], that sets the window size (*Sspan*) based on the number of photons within each  
1603 *L-km segment*.

$$1604 \quad Sspan = \text{ceil}[5 + 46 * (1 - e^{-a*length})] \quad \text{Eqn. 3.4}$$

$$1605 \quad a = \frac{\log\left(1 - \frac{21}{51-5}\right)}{-28114} \approx 21 \times 10^{-6} \quad \text{Eqn. 3.5}$$



where  $a$  is the shape parameter and length is the total number of photons in the  $L$ -km segment. The shape parameter,  $a$ , was determined using data collected by MABEL and is shown in Figure 3.6. It is possible that the model of the shape function, or the filtering bounds, will need to be adjusted once ICESat-2/ATLAS is on orbit and collecting data.

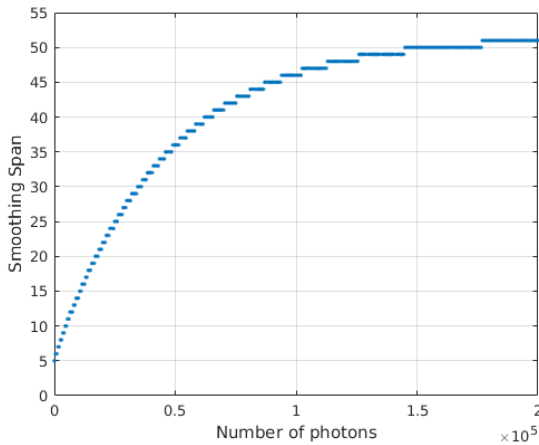


Figure 3.6. Shape Parameter for variable window size.

### 3.2.4 Compute descriptive statistics

To help characterize the input data and initialize some of the parameters used in the algorithm, we employ a moving window to compute descriptive statistics on the de-trended data. The moving window's width is the smoothing span function computed in Equation 5 and the window slides  $\frac{1}{4}$  of its size to allow of overlap between windows. By moving the window with a large overlap helps to ensure that the approximate ground location is returned. The statistics computed for each window step include:

- Mean height
- Min height
- Max height
- Standard deviation of heights

1626

1627           Dependent upon the amount of vegetation within each window, the estimated  
1628 ground height is estimated using different statistics. A standard deviation of the  
1629 photon elevations computed within each moving window are used to classify the  
1630 vertical spread of photons as belonging to one of four classes with increasing amounts  
1631 of variation: open, canopy level 1, canopy level 2, canopy level 3. The canopy indices  
1632 are defined in Table 3.1.

1633

1634 Table 3.1. Standard deviation ranges utilized to qualify the spread of photons within  
1635 moving window.

Name	Definition	Lower Limit	Upper Limit
Open	Areas with little or no spread in signal photons determined due to low standard deviation	N/A	Photons falling within 1 <sup>st</sup> quartile of Standard deviation
Canopy Level 1	Areas with small spread in signal photons	1 <sup>st</sup> quartile	Median
Canopy Level 2	Areas with a medium amount of spread	Median	3 <sup>rd</sup> quartile
Canopy Level 3	Areas with high amount of spread in signal photons	3 <sup>rd</sup> quartile	N/A

1636

1637

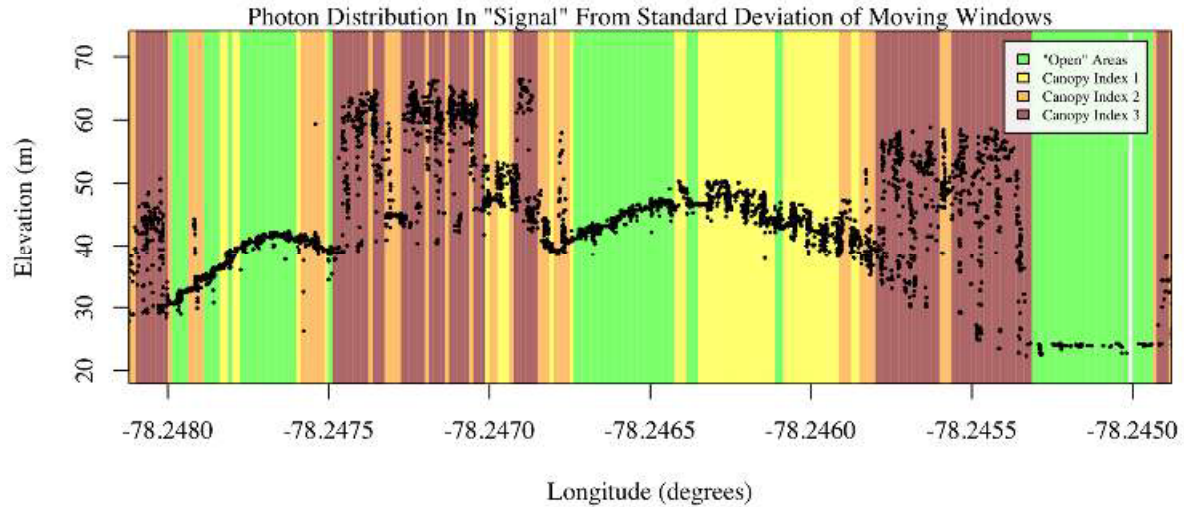
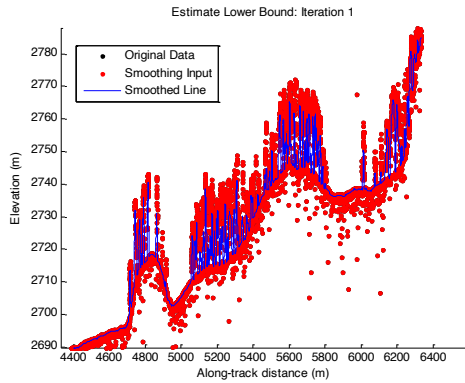


Figure 3.7. Illustration of the standard deviations calculated for each moving window to identify the amount of spread of signal photons within a given window.

### 3.2.5 Ground Finding Filter (Iterative median filtering)

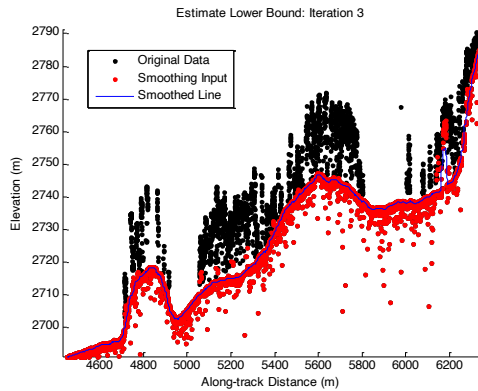
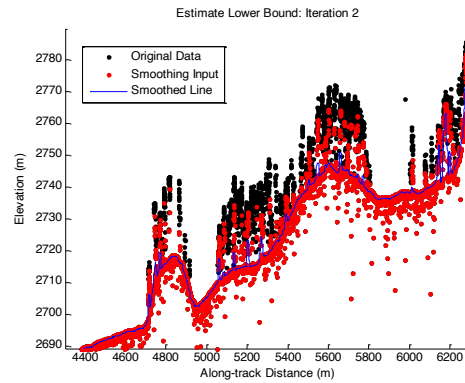
A combination of an iterative median filtering and smoothing filter approach will be employed to derive the output solution of both the ground and canopy surfaces. The input to this process is the set of de-trended photons. Finding the ground in the presence of canopy often poses a challenge because often there are fewer ground photons underneath the canopy. The algorithm adopted here uses an iterative median filtering approach to retain/eliminate photons for ground finding in the presence of canopy. When canopy exists, a smoothed line will lay somewhere between the canopy top and the ground. This fact is used to iteratively label points above the smoothed line as canopy. The process is repeated five times to eliminate canopy points that fall above the estimated surface as well as noise points that fall below the ground surface. An example of iterative median filtering is shown in Figure 3.8. The final median filtered line is the preliminary surface estimate. A limitation of this approach, however, is in cases of dense vegetation and few photons reaching the ground surface. In these instances, the output of the median filter may lie within the canopy.

1658



1659

1660



1661

1662 Figure 3.8. Three iterations of the ground finding concept for  $L$ -km segments with canopy.

1663

### 1664 3.3 Top of Canopy Finding Filter

1665 Finding the top of the canopy surface uses the same methodology as finding  
1666 the ground surface, except now the de-trended data are “flipped” over. The “flip”  
1667 occurs by multiplying the photons heights by -1 and adding the mean of all the heights  
1668 back to the data. The same procedure used to find the ground surface can be used to  
1669 find the indices of the top of canopy points.

1670

### 3.4 *Classifying the Photons*

Once a composite ground surface is determined, photons falling within the point spread function of the surface are labeled as ground photons. Based on the expected performance of ATLAS, the point spread function should be approximately 35 cm rms. Signal photons that are not labeled as ground and are below the ground surface (buffered with the point spread function) are considered noise, but keep the signal label.

The top of canopy photons that are identified can be used to generate an upper canopy surface through a shape-preserving surface fitting method. All signal photons that are not labeled ground and lie above the ground surface (buffered with the point spread function) and below the upper canopy surface are considered to be canopy photons (and thus labeled accordingly). Signal photons that lie above the top of canopy surface are considered noise, but keep the signal label.

FLAGS,	0 = noise
	1 = ground
	2 = canopy
	3 = TOC (top of canopy)

The final ground and canopy classifications are flags 1 – 3. The full canopy is the combination of flags 2 and 3.

### 3.5 *Refining the Photon Labels*

During the first iteration of the algorithm, it is possible that some photons are mislabeled; most likely this would be noise photons mislabeled as canopy. To reject these mislabeled photons, we apply three criteria:

- a) If top of canopy photons are 2 standard deviations above a smoothed median top of canopy surface
- b) If there are less than 3 canopy indices within a 15m radius

1700 c) If, for 500 signal photon segments, the number of canopy photons  
1701 is < 5% of the total (when SNR > 1), or < 10% of the total (when SNR  
1702 <= 1). This minimum number of canopy indices criterion implies a  
1703 minimum amount of canopy cover within a region.

1704 There are also instances where the ground points will be redefined. This  
1705 reassigning of ground points is based on how the final ground surface is determined.  
1706 Following the “iterate” steps in the flowchart shown in Figure 3.4, if there are no  
1707 canopy indices identified for the *L-km* segment, the final ground surface is  
1708 interpolated from the identified ground photons and then will undergo a final round  
1709 of median filtering and smoothing.

1710 If canopy photons are identified, the final ground surface is interpolated based  
1711 upon the level/amount of canopy at that location along the segment. The final ground  
1712 surface is a composite of various intermediate ground surfaces, defined thusly:

**ASmooth** heavily smoothed surface used to de-trend the signal data

**Interp\_Aground** interpolated ground surface based upon the identified ground  
photons

**AgroundSmooth** median filtered and smoothed version of Interp\_Aground

1713

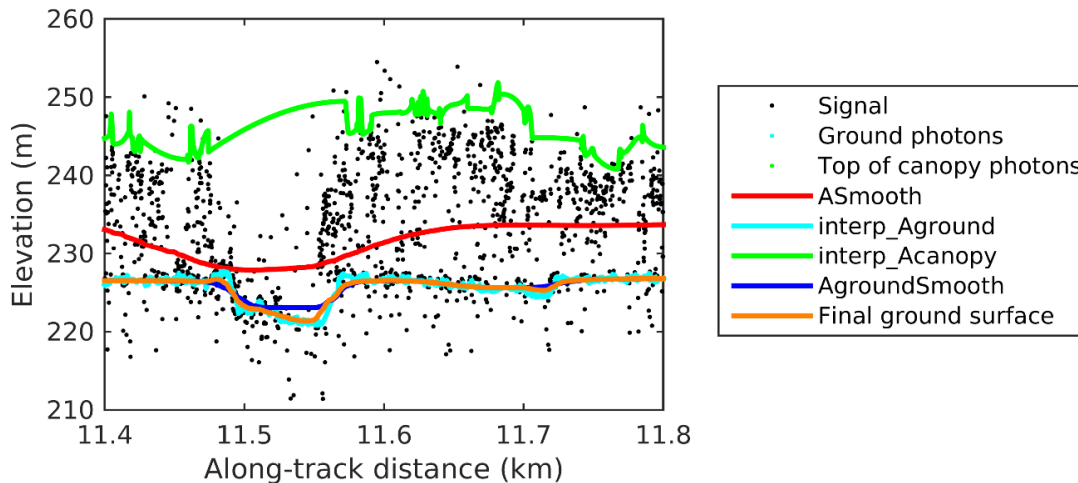


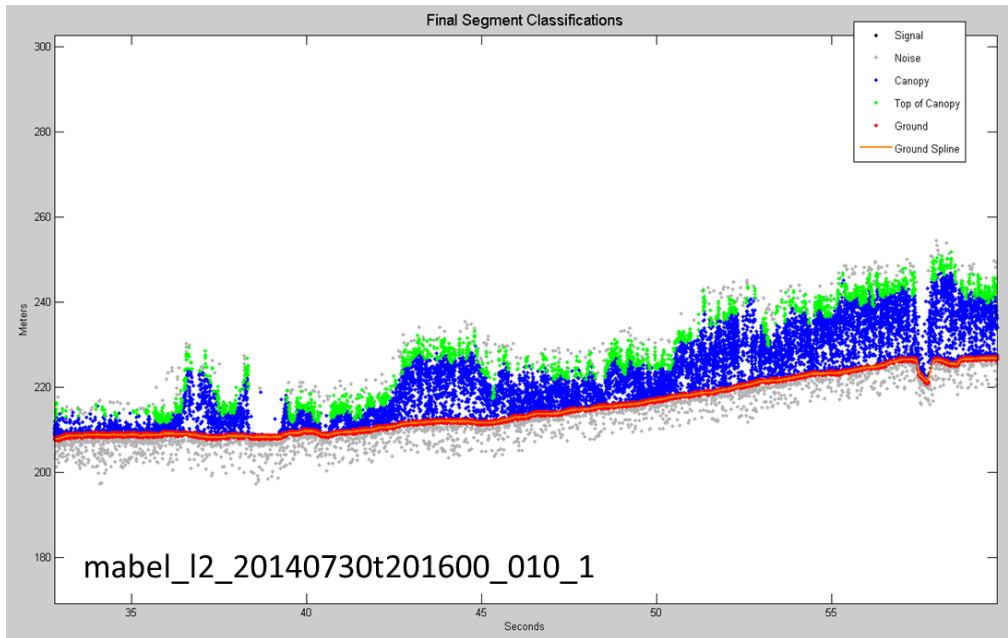
Figure 3.9. Example of the intermediate ground and top of canopy surfaces calculated from MABEL flight data over Alaska during July 2014.

During the first round of ground surface refinement, where there are canopy photons identified in the segment, the ground surface at that location is defined by the smoothed ground surface (AgroundSmooth) value. Else, if there is a location along-track where the standard deviation of the ground-only photons is greater than the 75% quartile for all signal photon standard deviations (i.e., canopy level 3), then the ground surface at that location is a weighted average between the interpolated ground surface ( $\text{Interp\_Aground} \times 1/3$ ) and the smoothed interpolated ground surface ( $\text{AgroundSmooth} \times 2/3$ ). For all remaining locations long the segment, the ground surface is the average of the interpolated ground surface (Interp\_Aground) and the heavily smoothed surface (ASmooth).

The second round of ground surface refinement is simpler than the first. Where there are canopy photons identified in the segment, the ground surface at that location is defined by the smoothed ground surface (AgroundSmooth) value again. For all other locations, the ground surface is defined by the interpolated ground surface (Interp\_Aground). This composite ground surface is run through the median and smoothing filters again.

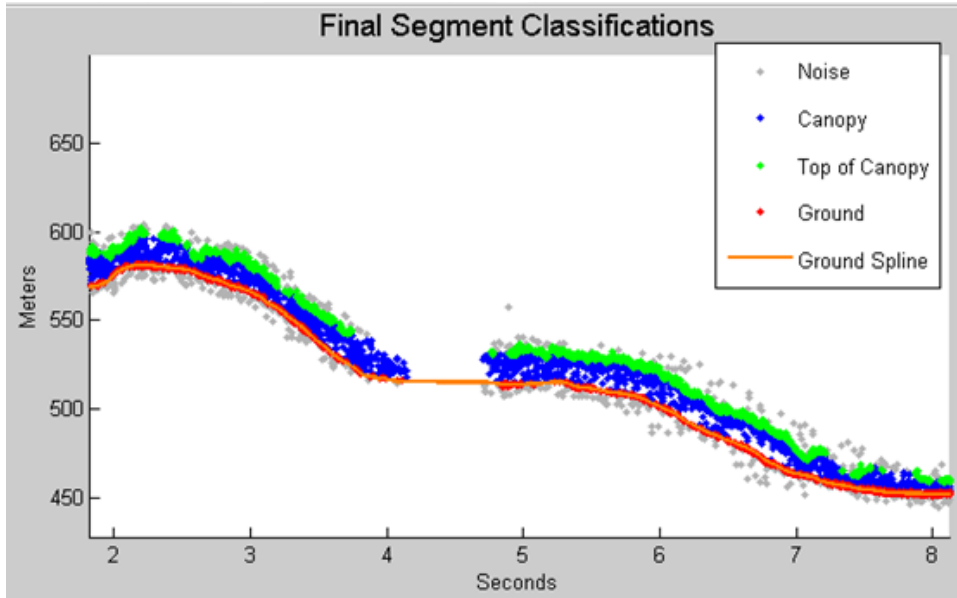
1734 The pseudocode for this surface refining process can be found in section 4.13.

1735 Examples of the ground and canopy photons for several MABEL lines are  
1736 shown in Figures 3.10 – 3.12.



1737  
1738 Figure 3.10. Example of classified photons from MABEL data collected in Alaska 2014.  
1739 Red photons are photons classified as terrain. Green photons are classified as top of canopy.  
1740 Canopy photons (shown as blue) are considered as photons lying between the terrain  
1741 surface and top of canopy.





1742

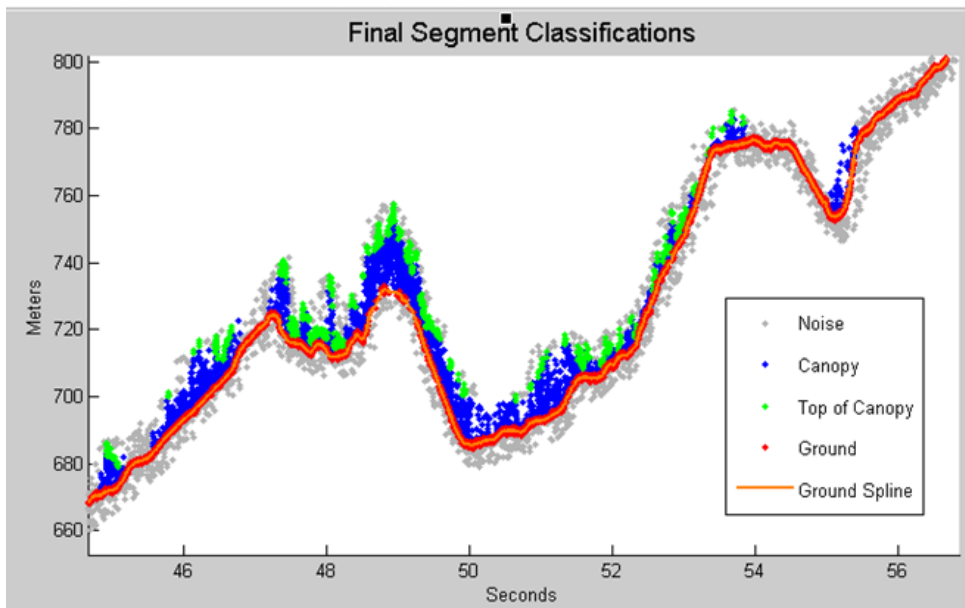
1743 Figure 3.11. Example of classified photons from MABEL data collected in Alaska 2014.

1744 Red photons are photons classified as terrain. Green photons are classified as top of canopy.

1745 Canopy photons (shown as blue) are considered as photons lying between the terrain

1746 surface and top of canopy.

1747



1748

1749 Figure 3.12. Example of classified photons from MABEL data collected in Alaska 2014.

1750 Red photons are photons classified as terrain. Green photons are classified as top of canopy.

1751 Canopy photons (shown as blue) are considered as photons lying between the terrain  
1752 surface and top of canopy.

1753

### 1754 **3.6 Canopy Height Determination**

1755 Once a final ground surface is determined, canopy heights for individual  
1756 photons are computed by removing the ground surface height for that photon's  
1757 latitude/longitude. These relative canopy height values will be used to compute the  
1758 canopy statistics on the ATL08 data product.

1759

### 1760 **3.7 Link Scale for Data products**

1761 The link scale for each segment within which values for vegetation parameters  
1762 will be derived will be defined over a fixed distance of 100 m. A fixed segment length  
1763 ensures that canopy and terrain metrics are consistent between segments, in addition  
1764 to increased ease of use of the final products. A size of 100 m was selected as it should  
1765 provide approximately 140 photons (a statistically sufficient number) from which to  
1766 make the calculations for terrain and canopy height.

1767

## 4 ALGORITHM IMPLEMENTATION

Prior to running the surface finding algorithms used for ATL08 data products, the superset of output from the GSFC medium-high confidence classed photons (ATL03 signal\_conf\_ph: flags 3-4) and the output from DRAGANN will be considered as the input data set. ATL03 input data requirements include the along-track time, latitude, longitude, height, and classification for each photon. The motivation behind combining the results from two different noise filtering methods is to ensure that all of the potential signal photons for land surfaces will be provided as input to the surface finding software. Prior to running DRAGANN, reject telemetry bins that occur 150m above or below the reference DEM. Rejection of these noise blocks will ensure a better parameterization of DRAGANN.

Some additional quality checks are also described here prior to implementing the ATL08 software. The first check utilizes the POD\_PPD flag on ATL03. In instances where the satellite is maneuvering or the pointing/ranging solutions are suspect, ATL08 will not use those data. Thus, data will only flow to the ATL08 algorithm when the POD\_PPD flag is set to 0 which indicates ‘nominal’ conditions.

A second quality check pertains to the flags set on the ATL03 photon quality flag (quality\_ph). Currently, ATL03 quality\_ph flags are described as:

0 = nominal conditions

1 = possible after-pulse (this identifies the after pulses that occur between 2.3 and 5 m below the surface)

2 = possible late impulse response effect (this flag identifies additional detector effects 5 – 50 m below the surface).

3 = possible TEP crossing.

10 = partially saturated geosegment identified on ATL03

20 = fully saturated geosegment identified on ATL03

For this release of the software, we want to mention that there are cases of after-pulsing that occur 0.5 – 2.3 m below the surface that have been flagged with a value of 10 or 20. For this release of the software, we have determined that we will include saturated photons. Thus, the output from the DRAGANN algorithm (i.e. the DRAGANN flag) will be set to a value of 0 when ATL03 quality\_ph flags photons with values other than 0, 10, or 20 such that they are ignored in the ATL08 algorithm.

A third quality check pertains to the signal photons (DRAGANN + ATL03 signal confidence photons) and whether those heights are near the surface heights. To pass this check, signal photons that lie 120 m above the reference DEM will be disregarded. Signal photons lying below the reference DEM will be allowed to continue for additional ATL08 processing. The motivation for this quality check is to eliminate ICESat-2 photons that are reflecting from clouds rather than the true surface.

Table 4.1. Input parameters to ATL08 classification algorithm.

Name	Data Type	Long Name	Units	Description	Source
<b>delta_time</b>	DOUBLE	GPS elapsed time	seconds	Elapsed GPS seconds since start of the granule for a given photon. Use the metadata attribute granule_start_seconds to compute full gps time.	ATL03
<b>lat_ph</b>	FLOAT	latitude of photon	degrees	Latitude of each received photon. Computed from the ECEF Cartesian coordinates of the bounce point.	ATL03
<b>lon_ph</b>	FLOAT	longitude of photon	degrees	Longitude of each received photon. Computed from the ECEF Cartesian coordinates of the bounce point.	ATL03
<b>h_ph</b>	FLOAT	height of photon	meters	Height of each received photon, relative to the WGS-84 ellipsoid.	ATL03
<b>sigma_h</b>	FLOAT	height uncertainty	m	Estimated height uncertainty (1-sigma) for the reference photon.	ATL03
<b>signal_conf_ph</b>	UINT_1_LE	photon signal confidence	counts	Confidence level associated with each photon event selected as signal (0-noise. 1- added to allow for buffer but algorithm classifies as background, 2-low, 3-med, 4-high).	ATL03

<b>segment_id</b>	UNIT_32	along-track segment ID number	unitless	A seven-digit number uniquely identifying each along-track segment. These are sequential, starting with one for the first segment after an ascending equatorial crossing node.	ATL03
<b>cab_prof</b>	FLOAT	Calibrated Attenuated Backscatter	unitless	Calibrated Attenuated Backscatter from 20 to -1 km with vertical resolution of 30m	ATL09
<b>dem_h</b>	FLOAT	DEM Height	meters	Best available DEM (in priority of GIMP/ANTARCTIC/GMTED/MSS) value at the geolocation point. Height is in meters above the WGS84 Ellipsoid.	ATL09

1806

1807 Table 4.2. Additional external parameters referenced in ATL08 product.

Name	Data Type	Long Name	Units	Description	Source
<b>atlas_pa</b>				Off nadir pointing angle of the spacecraft	
<b>ground_track</b>				Ground track, as numbered from left to right: 1 = 1L, 2 = 1R, 3 = 2L, 4 = 2R, 5 = 3L, 6 = 3R	
<b>dem_h</b>				Reference DEM height	ANC06
<b>ref_azimuth</b>	FLOAT	azimuth	radians	Azimuth of the unit pointing vector for the reference photon in the local ENU frame in radians. The angle is measured from north and positive towards east.	ATL03
<b>ref_elev</b>	FLOAT	elevation	radians	Elevation of the unit pointing vector for the reference photon in the local ENU frame in radians. The angle is measured from east-north plane and positive towards up.	ATL03
<b>rgt</b>	INTEGER_2	reference ground track	unitless	The reference ground track (RGT) is the track on the Earth at which a specified unit vector within the observatory is pointed. Under nominal operating conditions, there will be no data collected along the	ATL03

				RGT, as the RGT is spanned by GT2L and GT2R. During slews or off-pointing, it is possible that ground tracks may intersect the RGT. The ICESat-2 mission has 1,387 RGTs.	
<b>sigma_along</b>	DOUBLE	along-track geolocation uncertainty	meters	Estimated Cartesian along-track uncertainty (1-sigma) for the reference photon.	ATL03
<b>sigma_across</b>	DOUBLE	across-track geolocation uncertainty	meters	Estimated Cartesian across-track uncertainty (1-sigma) for the reference photon.	ATL03
<b>surf_type</b>	INTEGER_1	surface type	unitless	Flags describing which surface types this interval is associated with. 0=not type, 1=is type. Order of array is land, ocean, sea ice, land ice, inland water.	ATL03 , Section 4
<b>layer_flag</b>	Integer	Consolidated cloud flag	unitless	Flag indicating the presence of clouds or blowing snow with good confidence	ATL09
<b>cloud_flag_asr</b>	Integer(3)	Cloud probability from ASR	unitless	Cloud confidence flag, from 0 to 5, indicating low, med, or high confidence of clear or cloudy sky	ATL09
<b>msw_flag</b>	Byte(3)	Multiple scattering warning flag	unitless	Flag with values from 0 to 5 indicating presence of multiple scattering, which may be due to blowing snow or cloud/aerosol layers.	ATL09
<b>asr</b>	Float(3)	Apparent surface reflectance	unitless	Surface reflectance as modified by atmospheric transmission	ATL09
<b>snow_ice</b>	INTEGER_1	Snow Ice Flag	unitless	NOAA snow-ice flag. 0=ice free water; 1=snow free land; 2=snow; 3=ice	ATL09

1808

#### 1809 **4.1 Cloud based filtering**

1810 It is possible for the presence of clouds to affect the number of surface photon  
1811 returns through signal attenuation, or to cause false positive classifications of  
1812 ground or canopy photons on low cloud returns. Either of these cases would reduce  
1813 the accuracy of the ATL08 product. To improve the performance of the ATL08

algorithm, ideally all clouds would be identified prior to processing through the ATL08 algorithm. There will be instances, however, where low lying clouds (e.g. <800 m above the ground surface) may be difficult to identify. Currently, ATL08 provides an ATL09 derived cloud flag (`layer_flag`) on its 100 m product and encourages the user to make note of the presence of clouds when using ATL08 output. Unfortunately at present, a review of on-orbit data from ATL03 and ATL09 indicate that the cloud layer flag is not being set correctly in the ATL09 algorithm. Ultimately, the final cloud based filtering process used in the ATL08 algorithm will most likely be derived from parameters/flag on the ATL09 data product. Until the ATL09 cloud flags are proven reliable, however, a preliminary cloud screening method is presented below. This methodology utilizes the calibrated attenuated backscatter on the ATL09 data product to identify (and subsequently remove for processing) clouds or other problematic issues (i.e. incorrectly telemetered windows). Using this new method, telemetered windows identified as having either low or no surface signal due to the presence of clouds (likely situated above the telemetered band), as well as photon returns suspected to be clouds instead of surface returns, will be omitted from the ATL08 processing. This process, however, will not identify the extremely low clouds (i.e. <800 m). The steps are as follows:

1. Match up the ATL09 calibrated attenuated backscatter (`cab_prof`) columns to the ATL03 granule being processed using segment ID.
2. Flip the matching `cab_prof` vertical columns so that the elevation bins go from low to high.
3. For each of the matching ATL09 `cab_prof` vertical columns, perform a cubic Savitsky-Golay smoothing filter with a span size of 15 vertical bins. Call this `cab_smooth`.
4. Perform the same smoothing filter on each horizontal row of the `cab_smooth` output, this time using a span size of 7 horizontal bins. Call this `cab_smoother`.
5. Create a `low_signal` logical array the length of the number of matching ATL09 columns and set to false.

1844 6. For each column of cab\_smoother:

1845     a. Set any values below 0 to 0.

1846     b. Set a logical array of cab\_smoother bins that are below 15 km in

1847         elevation to true. Call this cab15.

1848     c. Using the ATL09 dem\_h value for that column, find the ATL09

1849         cab\_smoother bins that are 240 m above and 240 m below (~8 ATL09

1850         vertical bins each direction) the dem\_h value. The bins found here that

1851         are also within cab15 are designated as sfc\_bins.

1852     d. Find the maximum peak value of cab\_smoother within the sfc\_bins, if

1853         any. This will represent the surface peak.

1854     e. Find the maximum value of cab\_smoother that is higher in elevation

1855         than the sfc\_bins and within cab15, if any. This will represent the

1856         cloud peak.

1857     f. If there is no surface peak, set the low\_signal flag to true.

1858     g. If there are both surface and cloud peak values returned, determine a

1859         surface peak / cloud peak ratio. If that ratio is less than or equal to 0.4,

1860         set low\_signal flag for that column to true.

1861 7. After each matching ATL09 column of cab\_smoother has been analyzed for

1862     low signal, assign the low\_signal flag to an ATL03 photon resolution logical

1863     array by matching up the ATL03 photon segment\_id values to the ATL09

1864     range of segment IDs for each ATL09 cab\_prof column.

1865 8. For each ATL09 cab\_prof column where the low\_signal flag was not set, check

1866     for any ATL03 photons greater than 800 meters in elevation away (higher or

1867     lower) from the ATL09 dem\_h value. Assign an ATL03 photon resolution

1868     too\_far\_signal flag to true when this conditional is met.

1869 9. A logical array mask is created for any ATL03 photons that have either the

1870     low\_signal flag or the too\_far\_signal flag set to true such that those photons

1871     will not be further processed by the ATL08 function.

1872 10. Filtering due to ATL09 no ground detection or ATL03 has low confidence

1873     photons



1874

1875 **4.2 Preparing ATL03 data for input to ATL08 algorithm**

- 1876 1. Alignment of weak and strong beam against to the ATL09 data product to aid  
1877 in noise photon rejection based on segment distance (along-track distance  
1878 from equator) within ATL08.
- 1879 2. At times, cloud attenuation will lead to a reduced L-km with a length that is  
1880 not a multiple of 100 meters. If the last 100m land segment of the L-km  
1881 segment contains fewer than 5 ATL03 20m geosegments and the current L-  
1882 km segment is not the last one of the granule, do not report output for this  
1883 last 100m land segment. Retain the starting geosegment of this land segment  
1884 and begin the next L-km segment here.
- 1885 3. Break up data into *L-km* segments. Segments equivalent of 10 km in along-  
1886 track distance of an orbit would be appropriate.
- 1887 a. If the last portion of an ATL03 granule being processed would result  
1888 in an *L-km* segment with less than 3.4 km (170 geosegments) worth of  
1889 data, that last portion is added to the previous *L-km* processing  
1890 window to be processed together as one extended *L-km* processing  
1891 segment.
- 1892 i. The resulting **last\_seg\_extend** value would be reported as a  
1893 positive value of distance beyond 10 km that the ATL08  
1894 processing segment was extended by.
- 1895 b. If the last *L-km* segment would be less than 10 km but greater than 3.4  
1896 km, a portion extending from the start of current *L-km* processing  
1897 segment backwards into the previous *L-km* processing segment would  
1898 be added to the current ATL08 processing segment to make it 10 km  
1899 in length. Only new 100 m ATL08 segment products generated from  
1900 this backward extension would be reported.
- 1901 i. The distance of this backward data gathering would be  
1902 reported in **last\_seg\_extend** as a negative distance value.

- 1903           c. All other segments that are not extended will report a last\_seg\_extend  
1904           value of 0.
- 1905       4. Add a buffer of 200 m (or 10 segment\_id's) to both ends of each *L-km*  
1906       segment. The total processing segment length is  $(L-km + 2*buffer)$ , but will  
1907       be referred to as *L-km* segments for simplicity.
- 1908           a. The first *L-km* segment from an ATL03 granule would only have a  
1909           buffer at the end, and the last *L-km* segment from an ATL03 granule  
1910           would only have a buffer at the beginning.
- 1911       5. The input data for ATL08 algorithm is X, Y, Z, T (where T is time).

1912

### 1913   **4.3 Noise filtering via DRAGANN**

1914   DRAGANN will use ATL03 photons with all signal classification flags (0-4). These  
1915   will include both signal and noise photons. This section give a broad overview of the  
1916   DRAGANN function. See Appendix A for more details.

- 1917       1. Determine the relative along-track time, ATT, of each geolocated photon  
1918       from the beginning of each *L-km* segment.
- 1919       2. Rescale the ATT with equal-time spacing between each data photon, keeping  
1920       the relative beginning and end time values the same.
- 1921       3. Normalize the height and rescaled ATT data from 0 – 1 for each *L-km*  
1922       segment based on the min/max of each field. So,  $normtime = (time -$   
1923        $mintime)/(maxtime - mintime)$ .
- 1924       4. Build a kd-tree based on normalized Z and normalized and rescaled ATT.
- 1925       5. Determine the search radius starting with Equation 3.1.  $P=[$ determined by  
1926       preprocessor; see Sec 4.3.1], and  $V_{total}=1$ .  $N_{total}$  is the number of photons  
1927       within the data *L-km* segment. Solve for V.
- 1928       6. Now that you know V, determine the radius using Equation 3.2.
- 1929       7. Compute the number of neighbors for each photon using this search radius.

1930 8. Generate a histogram of the neighbor count distribution. As illustrated in  
1931 Figure 3.2, the noise peak is the first peak (usually with the highest  
1932 amplitude).

1933 9. Determine the 10 highest peaks of the histogram.

1934 10. Fit Gaussians to the 10 highest peaks. For each peak,

1935 a. Compute the amplitude,  $a$ , which is located at peak position  $b$ .

1936 b. Determine the width,  $c$ , by stepping one bin at a time away from  $b$  and  
1937 finding the last histogram value that is  $> \frac{1}{2}$  the amplitude,  $a$ .

1938 c. Use the amplitude and width to fit a Gaussian to the peak of the  
1939 histogram, as described in Equation 3.3.

1940 d. Subtract the Gaussian from the histogram, and move on to calculate  
1941 the next highest peak's Gaussian.

1942 e. Reject Gaussians that are too near ( $< 2$  standard deviations) and  
1943 amplitude too low ( $< 1/5$  previous amplitude) from the previous  
1944 signal Gaussian.

1945 11. Reject any of the returned Gaussians with imaginary components.

1946 12. Determine if there is a narrow noise Gaussian at the beginning of the  
1947 histogram. These typically occur when there is little noise, such as during  
1948 nighttime passes.

1949 a. Search for the Gaussian with the highest amplitude,  $a$ , in the first 5%  
1950 of the histogram

1951 b. Check if the highest amplitude is  $\geq 1/10$  of the maximum of all  
1952 Gaussian amplitudes

1953 c. Check if the width,  $c$ , of the Gaussian with the highest amplitude is  $\leq$   
1954 4 bins

1955 d. If these three conditions are met, save the  $[a,b,c]$  values as  $[a_0,b_0,c_0]$ .

1956 e. If the three conditions are not met, search again within the first 10%.  
1957 Repeat the process, incrementing the percentage of histogram  
1958 searched by 5% up to 30%. As soon as the conditions are met, save  
1959 the  $[a_0,b_0,c_0]$  values and break out of the percentage histogram search  
1960 loop.

1961 13. If a narrow noise peak was found, sort the remaining Gaussians from largest  
1962 to smallest area, estimated by  $a \cdot c$ , then append  $[a_0, b_0, c_0]$  to the beginning of  
1963 the sorted  $[a, b, c]$  arrays. If a narrow noise peak was not found, sort all  
1964 Gaussians by largest to smallest area.

- 1965 a. If a narrow noise peak was not found, check in sorted order if one of
- 1966 the Gaussians are in the first 10% of the histogram. If so, it becomes
- 1967 the first Gaussian.
- 1968 b. Reject any Gaussians that are fully contained within another.
- 1969 c. Reject Gaussians whose centers are within 3 standard deviations of
- 1970 another, unless only two Gaussians remain

1971 14. If there are two or more Gaussians remaining, they are referred to as  
1972 Gaussian 1 and Gaussian 2, assumed to be the noise and signal Gaussians.

1973 15. Determine the threshold value that will define the cutoff between noise and  
1974 signal.

- 1975 a. If the absolute difference of the two Gaussians becomes near zero,
- 1976 defined as  $< 1e-8$ , set the first bin index where that occurs, past the
- 1977 first Gaussian peak location, as the threshold. This would typically be
- 1978 set if the two Gaussians are far away from each other.
- 1979 b. Else, the threshold value is the intersection of the two Gaussians,
- 1980 which can be estimated as the first bin index past the first Gaussian
- 1981 peak location and before the second Gaussian where there is a
- 1982 minimum absolute difference between the two Gaussians.
- 1983 c. If there is only one Gaussian, it is assumed to be the noise Gaussian,
- 1984 and the threshold is set to  $b + c$ .

1985 16. Label all photons having a neighbor count above the threshold as signal.

1986 17. Label all photons having a neighbor count below the threshold as noise.

1987 18. Reject noise photons.

1988 19. Retain signal photons for feeding into next step of processing.

1989 20. Use Logical OR to combine DRAGANN signal photons with ATL03 medium-  
1990 high confidence signal photons (flags 3-4) as ATL08 signal photons.

1991           21. Calculate a signal to noise ratio (SNR) for the *L-km* segment by dividing the  
1992           number of ATL08 signal photons by the number of noise (i.e., all – signal)  
1993           photons.

#### 1994           **4.3.1 DRAGANN Quality Assurance**

1995           Based upon on-orbit data, there are instances where only noise photons are selected  
1996           as signal photons following running through DRAGANN. These instances usually  
1997           occur to telemetered windows with low signal, signal attenuation near the surface  
1998           due to fog, haze (or other atmospheric properties). If any d\_flag results in the 10 km  
1999           = 1

- 2000           1. For each 20 m segment\_id that has a d\_flag = 1, build a histogram of 5 m  
2001           height bins using the height of only the DRAGANN-flagged photons  
2002           (d\_flag=1)
- 2003           2. If the number of bins indicates that all d\_flag photons fall within the same  
2004           vertical 60 m, do nothing and move to the next geosegment.
- 2005           3. If the d\_flag photons fall outside of 60 m, calculate the median and  
2006           standard deviation of the histogram counts.
- 2007           4. If the maximum value of the histogram counts is greater than the median  
2008           + 3\*standard deviation, a surface peak has been detected based on the  
2009           relative photon density within the 5 meter steps. Else, set all d\_flag = 0  
2010           for this geosegment.
- 2011           5. Set all d\_flag = 0 from 3 height bins below the detected peak to the bottom  
2012           of the telemetry window.
- 2013           6. Starting with the peak count bin (surface), step upwards bin by bin and  
2014           check if 12 bin counts (60 meters of height bins) above surface are less  
2015           than 0.5 \* histogram median. If so, for all photons above current height in  
2016           loop + 60 meters, set all d\_flag = 0 and exit bin-by-bin loop.
- 2017           7. Starting with one bin above the peak count bin (surface), again step  
2018           upwards bin by bin. For each iteration, calculate the standard deviation of  
2019           the bin counts including only the current bin to the highest height bin and  
2020           call this noise standard deviation. If all remaining vertical height bins

2021 from current bin to highest height bin are less than  $2 \times$  histogram  
 2022 standard deviation, or if the noise standard deviation is less than 1.0, or if  
 2023 this bin and the next 2 higher bins each have counts less than the peak bin  
 2024 count (entire histogram)  $- 3 \times$  histogram standard deviation, then set all  
 2025  $d\_flag = 0$  for all heights above this level and exit bin-by-bin loop  
 2026 8. For a final check, construct a new histogram, with median and standard  
 2027 deviation, using the corrected  $d\_flag$  results and only where  $d\_flag = 1$ . If  
 2028 the histogram median is greater than 0.0 and the standard deviation is  
 2029 greater than  $0.75 \times$  median, set all  $d\_flag$  in this geosegment = 0. This  
 2030 indicates results not well constrained about a detectable surface.  
 2031

#### 2032 **4.3.2 Preprocessing to dynamically determine a DRAGANN parameter**

2033 While a default value of  $P=20$  was found to work well when testing with MABEL  
 2034 flight data, further testing with simulated data showed that  $P=20$  is not sufficient in  
 2035 cases of very low or very high noise. Additional testing with real ATL03 data have  
 2036 shown the ground signal to be much stronger, and the canopy signal to be much  
 2037 weaker, than originally anticipated. Therefore, a preprocessing step for dynamically  
 2038 calculating  $P$  and running the core DRAGANN function is described in this  
 2039 subsection. This assumes  $L$ -km to be 10 km (with additional  $L$ -km buffering).

- 2040 1. Define a DRAGANN processing window of 170 segments ( $\sim 3.4$  km),  
 2041 and a buffer of 10 segments ( $\sim 200$  m).
- 2042 2. The buffer is applied to both sides of each DRAGANN processing  
 2043 window to create buffered DRAGANN processing windows  
 2044 (referenced as “buffered window” for the rest of this section) that will  
 2045 overlap the DRAGANN processing windows next to them.
- 2046 3. For each buffered window within the  $L$ -km segment, calculate a  
 2047 histogram of points with 1 m elevation bins.
- 2048 4. For each buffered window histogram, calculate the median counts.
- 2049 5. Bins with counts below the buffered window median count value are  
 2050 estimated to be noise. Calculate the mean count of noise bins.

2051 6. Bins with counts above the buffered window median count value are  
2052 estimated to be signal. Calculate the mean count of signal bins.  
2053 7. Determine the time elapsed over the buffered window.  
2054 8. Calculate estimated noise and signal rates for each buffered window  
2055 by multiplying each window's mean counts of noise bins and signal  
2056 bins, determined from steps 5 and 6 above, by 1/(elapsed time) to  
2057 return the rates in terms of points/meter[elevation]/second[across].  
2058 9. Calculate a noise ratio for each window by dividing the noise rate by  
2059 the signal rate.  
2060 10. If, for all the buffered windows in the *L-km* segment, the noise rate is  
2061 less than 20 and the noise ratio is less than 0.15; OR any noise rate is  
2062 0; OR any signal rate is greater than 1000: re-calculate steps 3-9  
2063 using the entire *L-km* segment. Continue with the following steps  
2064 using results from the one *L-km* window (instead of multiple buffered  
2065 windows).  
2066 11. Now, determine the DRAGANN parameter, *P*, for each buffered  
2067 window based on the following conditionals:  
2068 a. If the signal rate is NaN (i.e., an invalid value), set the signal  
2069 index array to empty and move on to the next buffered  
2070 window.  
2071 b. If noise rate < 20 || noise ratio < 0.15:  
2072  $P = \text{signal rate}$   
2073 If signal rate is < 5,  $P = 5$ ; if signal rate > 20,  $P = 20$   
2074 c. Else  $P = 20$ .  
2075 12. Run DRAGANN on the buffered window points using the calculated *P*.  
2076 13. If DRAGANN fails to find a signal (i.e., only one Gaussian found), run  
2077 DRAGANN again with  $P = 10$ .  
2078 14. If DRAGANN still fails to find a signal, try to determine *P* a second time  
2079 using the following conditionals:  
2080 a. If (noise rate >= 20) ...  
2081 && (signal rate > 100) ...

```

2082         && (signal rate < 250),
2083         P = (signal rate)/2
2084     b. Else if signal rate >= 250,
2085         if noise rate >= 250,
2086             P = (noise rate)*1.1
2087         else,
2088             P = 250
2089     c. Else, P = mean(noise rate, signal rate)
2090 15. Run DRAGANN on the buffered window points using the newly
2091     calculated P.
2092     a. If still no signal points are found, set a dragannError flag.
2093 16. If signal points were found by DRAGANN, for each buffered window
2094     calculate a signal check by dividing the number of signal points found
2095     via DRAGANN by the number of total points in the buffered window.
2096 17. If dragannError has been set, or there are suspect signal statistics, the
2097     following snippet of pseudocode will check those conditionals and try
2098     to iteratively find a better P value to run DRAGANN with:
2099
2100     try_count = 0
2101
2102     While dragannError ...
2103     || ( (noise rate >= 30) ...
2104         && (signal check > noise ratio) ...
2105         && (noise ratio >= 0.15) ) ...
2106     || (signal check < 0.001):
2107
2108         if P < 3,
2109             break
2110         else,
2111             P = P*0.75
2112         end
2113
2114     if try_count < 2
2115         Clear out signal index results from previous DRAGANN run
2116         Re-run DRAGANN with new P value
2117         Recalculate the signal check
2118     end
2119
2120     if no signal index results are returned

```



```

2121         P = P*0.75
2122     end
2123
2124     try_count = try_count + 1
2125
2126 end
2127
2128 18. If no signal photons are found by DRAGANN because only one
2129     Gaussian was found, set the threshold as  $b+c$  (i.e., one standard
2130     deviation away from the Gaussian peak location) for a final DRAGANN
2131     run. Otherwise, set the signal index array to empty and move on to the
2132     next buffered window.
2133
2134 19. Assign the signal values found from DRAGANN for each buffered
2135     window to the original DRAGANN processing window range of points.
2136
2137 20. Combine signal points from each DRAGANN processing window back
2138     into one  $L\text{-km}$  array of signal points for further processing.

```

2137

### 2138 **4.3.3 Iterative DRAGANN processing**

2139 It is possible in processing segments with high noise rates that DRAGANN will  
2140 incorrectly identify clusters of noise as signal. One way to reduce these false positive  
2141 noise clusters is to run the alternative DRAGANN process (Sec 4.3.1) again with the  
2142 input being the signal output photons from the first run through alternative  
2143 DRAGANN. Note that this methodology is still being tested, so by default this option  
2144 should not be set.

- 2145 1. If  $\text{SNR} < 1$  (TBD) from alternative DRAGANN run, run alternative DRAGANN  
2146 process again using the output signal photons from first DRAGANN run as the  
2147 input to the second DRAGANN run.
- 2148 2. Recalculate SNR based on output of second DRAGANN run.

2149

2150

#### 4.4 Compute Filtering Window

1. Next step is to run a surface filter with a variable window size (variable in that it will change from  $L$ -km segment to  $L$ -km segment). The window-size is denoted as Window.
2.  $Sspan = \text{ceil}[5 + 46 * (1 - e^{-a*length})]$ , where  $length$  is the number of photons in the segment.
3.  $a = \frac{\log\left(1 - \frac{21}{51-5}\right)}{-28114} \approx 21 \times 10^{-6}$ , where  $a$  is the shape parameter for the window span.

#### 4.5 Identification of single surface

Through development of a successful strategy for ground finding, an initial strategy to undertake is to determine whether a segment contains a single surface (i.e. just ground) or if it is a combination of multiple surfaces (i.e. ground and vegetation). To make this determination, we will utilize the Copernicus vegetation fraction estimate. A minimum of 2 signal photons are required to be present in any 20 m geosegment for the following steps to be successful.

To initiate the process, a linear regression of photon heights in each 20m segment utilizing only heights from signal photons is built. For the X dimension, use photon times relative to the first photon time in the geosegment. Populate an array at each photon time, again relative to the first photon time in the segment, with heights along a line dictated by the linear regression heights. If Copernicus vegetation fraction for the 20 m geosegment (by nearest 100 m value to center of geosegment) is valid and  $\leq 50\%$ , and the linear regression standard deviation is  $< 2\text{m}$ , and the Copernicus land cover type is either no\_data (code: 0), bare/sparse\_vegetation (code: 60), snow/ice (code: 70), permanent\_water\_bodies (code: 80), moss/lichen (code: 100), or open\_sea (code: 200) assume the potential for a single terrain surface is high and execute the following:

1. Difference the linear regression heights from photon heights, yielding a residual
2. Build a histogram with 1.5 m bin heights with the residual, "hhist1"

- 2179 3. Build another histogram one half a bin height below the first one, "hhist2"
- 2180 4. If either histogram contains only a single populated bin, track the photons falling
- 2181 within as likely ground and that a single surface has been found. Skip further
- 2182 single surface analysis.
- 2183 5. If the maximum histogram count, for either histogram "hhist1" or "hhist2"
- 2184 exceeds the sum of all other bin counts greater than background neighbor
- 2185 density as a bin count provided in section titled: "Finding Initial Ground
- 2186 Estimate:", track that a single surface has been found. (This noise density can be
- 2187 computed early, ahead of other steps.)
- 2188 6. For both histograms, if the sum of two bin counts below the bin with maximum
- 2189 count differ from the sum of two bin counts above the bin containing the
- 2190 maximum count by less than three, second surface (terrain or vegetation)
- 2191 detection is unlikely. Track that a single surface has been found.
- 2192 7. If a single surface deemed present, use the single highest histogram count from
- 2193 either "hhist1" and "hhist2" for all following steps.
- 2194 8. If a single surface has not been deemed present, but vegetation fraction < 5% or
- 2195 invalid, land cover type is not agriculture (code:40), and linear regression root
- 2196 mean square error is < 0.5m, assume that a single surface has been found.
- 2197 9. If signal photon classification is available from ATL03 and/or DRAGANN
- 2198 processes, choose photons with residual heights within the maximum count
- 2199 histogram bin and classified as signal in a mask of initial ground photons to be
- 2200 considered by YAPC in following steps. Otherwise, choose all photons with
- 2201 residual heights within maximum count histogram bin.
- 2202 10. For all of the above, track which photons come from segments with a detected
- 2203 single surface.
- 2204 11. For segments with 5 or less signal photons, assume all signal photons are
- 2205 appropriate for the initial ground "guess". Linear regression and histogramming
- 2206 would not have reliably succeeded, further analysis steps will cull errors.
- 2207

#### 2208 **4.6 Look for potential ground photons**

2209 For each 20m segment, develop a mask of likely ground photons to use for limiting  
2210 those returned by YAPC analysis by executing the following.

2211 Using variable histogram bin heights, step through geosegments to analyze the  
2212 lowest bins with populations higher than noise to build an initial ground “guess”  
2213 mask.

- 2214 1. If any geosegment does not provide at least 2 signal photons, bypass all remaining  
2215 steps for this section for that geosegment.
- 2216 2. If the vegetation fraction < 50%, and the single surface linear regression standard  
2217 deviation < 2.0m, difference the linear regression applied to all photon times from the  
2218 photon heights yielding a residual to use for all remaining steps. Otherwise, the  
2219 following is carried out with the original photon heights.
- 2220 3. Build histograms of heights of all photons with 0.5m bin size
- 2221 4. If fewer than 3 bins, and expanded to 6m bin size, assume all signal photons apply to  
2222 initial ground “guess”; YAPC and filtering will separate canopy, if any, from ground.
- 2223 5. Using only the 0.5m bin size histograms, determine noise bin count via 25th  
2224 percentile of lowest 10% of bin count
- 2225 6. If the above doesn't produce a valid number, such as in the case of few histogram  
2226 bins, recalculate via median of lowest 10% of bin count
- 2227 7. Enforce a minimum noise count of 1
- 2228 8. If max histogram count is less than  $1.25 \times \text{noise count}$ , cycle, add 0.5m to bin size,  
2229 cycle back to start of histograms, to a maximum bin size of 6m
- 2230 9. If maximum histogram count  $\leq \text{noise count} \times 3$ , assume no well-captured surface,  
2231 expand bin size by 0.5 and cycle to back to building histograms
- 2232 10. Starting at lowest histogram step through bins, lowest to DEM+10m, until the sum of  
2233 2 bin counts exceeds  $\text{noise count} \times 1.25$  or regardless of distance to DEM height, the  
2234 sum of 2 bin count exceeds  $\text{noise count} \times 4$  and  $> 0.25 \times \text{max histogram count}$ .
- 2235 11. If any DRAGANN/signal\_conf photons are present, set only those photons with  
2236 heights within the 2 height bins as initial ground “guess”

2237 12. If no DRAGANN/signal\_conf photons are present, set all photons within the 2 height  
 2238 bins as initial ground “guess”

2239 13. Determine a DEM bias for each segment with a valid initial ground “guess”  
 2240 consisting of at least 2 photons via DEM – mean(heights of initial ground guess)  
 2241

2242 Check results of initial ground “guess” for unrealistic slopes, discontinuities, or behaviors  
 2243 in individual segments not supported by information from DEM and neighboring  
 2244 segments. Conduct this analysis for each geosegment 3 times; once forward in segment  
 2245 id, once backward, and again forward. Once complete, if any anomalies were detected,  
 2246 the steps below will adjust the above results, reassigning photons as an initial ground  
 2247 “guess”.

2248 14. Bypass all remaining steps if reference data indicates urban surfaces are present  
 2249 in the 20m geosegment.

2250 15. Reduce outliers by comparing histogram bin height changes against expected local  
 2251 topography. If any segment histogram results, segment by segment, change by more  
 2252 than 75% of the difference of highest and lowest DEM heights within 240m of the  
 2253 segment in question, reset those bin heights to a mean of immediate neighbor bin  
 2254 heights.

2255 16. Determine a terrain variability for each geosegment exhibited by the neighboring  
 2256 240m of initial ground “guess” via the 90<sup>th</sup> – 10<sup>th</sup> percentiles for 240m before and  
 2257 after the geosegment in question, then average them.

2258 17. Determine median bias for each geosegment consisting of the median bias of 10  
 2259 segments before and 10 segments after, excluding the single highest and lowest of  
 2260 DEM bias for each before and after. Also exclude the present segment of interest.  
 2261 Require a minimum of 3 valid DEM bias calculations for both before and after,  
 2262 otherwise store invalid for median bias.

2263 18. If the terrain variability less than 30m, and the nearest 10 segments' second highest  
 2264 bias minus second lowest bias less than 20m, and the absolute value of the second  
 2265 highest and lowest is less than 22m, then check for this segments ground “guess” to

2266       reside within 0.75m of the segment DEM-bias median determined above. If so, skip  
 2267       all further steps, ground already found in appropriate height window.

2268   19. If this segment's minimum height ground "guess" is above the DEM+bias median,  
 2269       and the current segment has fewer than 35 photons in ground "guess", and has either:  
 2270       a. less than 3 ground "guess" photons, or b. less than half the average of the  
 2271       neighboring 6 closest segments ground "guess" photons, then this segment likely has  
 2272       ground "guess" photons too high, likely in the canopy. Reset this segment's ground  
 2273       "guess" photons and skip to step 24.

2274   20. If this segment's ground "guess" photon count is less than 15, look for single segment  
 2275       ground misses as compared to immediate neighbors, one segment before and after:  
 2276       a. If this segment's DEM bias (not median of neighbors) is positive and more  
 2277       than 2 times that of both immediate neighbor segments, reset this segment's  
 2278       ground "guess" and skip to step 24.  
 2279       b. If this segment's DEM bias is negative and falls below 2 times the value of  
 2280       both immediate neighbors, reset this segment's ground "guess" and skip to  
 2281       step 24.

2282   21. If any ground "guess" exists within segment in question, and for both 60m before and  
 2283       after, check if mean heights of ground "guess" for this segment fall in between those  
 2284       before and after, indicating the presence of a slope. If so, skip remaining steps and  
 2285       keep this segment's ground "guess".

2286   22. If the mean height difference of the previous or following 60m and this  
 2287       segment's ground "guess" photon heights exceeds 2 times the terrain variability,  
 2288       this discontinuity indicates a ground finding issue. Reset this segment's ground  
 2289       "guess" photons and skip to step 24.

2290   23. If the segment's ground "guess" has been reset, also invalidate the segment's  
 2291       DEM bias as the analysis indicates it would be unreliable.

2292   24. Set a new ground guess for this segment using all signal photons within 1 meter  
 2293       of the DEM-median bias of 10 neighbors before and after, determined above. If  
 2294       no photons satisfy this requirement, this is acceptable. Excess photons in the 2  
 2295       vertical meters of ground guess will be culled in outlier removal and smoothing  
 2296       steps, below.

#### 4.7 De-trend Data

In this next phase of the ATL08 process, we will utilize signal photons identified by DRAGANN and the ATL03 classification (signal\_conf\_ph) values of 3 and 4 as well as the YAPC photon weights on the ATL03 data product. In lieu of the steps presented in 4.5.2 through 4.5.3, we are now using the photon weights from the YAPC algorithm provided on the ATL03 data product as a better initial estimate of the ground surface. Early results indicate that the highest 5-10% of photon weights correspond to the ground surface except in areas of dense vegetation. We have found that in areas of high topographic change, the utilization of the yapc photons weights out-performs the previous approach of iterative filtering to estimate the initial ground line.

Evaluate YAPC weights, inclusive of DEM, DRAGANN, signal\_conf, initial ground “guess”, and median DEM bias via:

1. Obtain snow\_ice flag results from ATL09, mapped to each 20m geosegment

For each 20m segment:

2. Normalize YAPC weights for each segment via ATL03 YAPC weight\*sqrt(segment\_ph\_cnt), while setting zero for any photons beyond 10m above DEM elevation, minus DEM bias median, if valid. Divide these values by the maximum value of the same for normalization. Limit to a maximum value of 1.0
3. Calculate the segment specific signal threshold using the maximum change in percentiles of normalized weights from 0.005 to 1.0, in steps of 0.005. The largest change in the range of percentiles indicates the change from noise the signal and should be used in the follow steps involving normalized weights. A maximum threshold value of 0.95 should be enforced
4. For any segment with snow\_ice > 1 (both snow and ice results), ignore initial ground “guess” and track all photons with DRAGANN/signal\_conf positive, with normalized weights >= calculated threshold and skip the following steps
5. Track all photons in the segment included in initial ground “guess”, with normalized weights >= calculated threshold, and DRAGANN/signal\_conf positive

6. If less than 2 photons result in any 20m segment, track photons that are DRAGANN/signal\_conf positive and included in initial ground “guess”
7. If still less than 2 photons present, track photons that are included in the initial ground “guess”, within 10m of DEM (minus DEM bias median, if valid)
8. In situations where the maximum weights were zero, thereby making normalization and threshold determination impossible, track photons that are DRAGANN/signal\_conf positive and included in initial ground “guess”
9. For better resolution of attenuated ground surfaces, duplicate twice all tracked photons, with a monotonically increasing temporary along track distance. This yields 3 ground “starting” photons for each photon passing all tests
10. These photons are provided to ATL08 filtering, smoothing functions for initial ground surface finding

#### ***4.8 Detect fog conditions and bypass photon classification***

12. Track segments where mean photon heights included via weights, indirectly including ground “guess” results above, exceed 30 meters above the provided DEM height, as provided by the ancillary data. Conduct this check for processing windows with dem\_flag indicating DEM ancillary data sourced from the global DEM (MERIT) and/or sea level. Thus, segments within the 10km have the dem\_flag = 2 (MERIT) or dem\_flag = 3 (sea level). This intentionally excludes Antarctica and Greenland as those regions’ surface dynamics, and DEM errors, may lead to false positives for this check. If the count of segments with the condition of initial ground over 30 meters above reference DEM exceeds 5 for the 10km processing window, discard all classifications of photons in the processing window as ground or canopy candidates and cycle to the next window. This test will be implemented for every spatially coincident granule as the DEM is temporally static.

The output of these steps is a set of masked photons referred to here as Asmooth\_yapc\_weights.



2354

- 2355 1. The input data are the signal photons identified by DRAGANN and the ATL03  
2356 classification (signal\_conf\_ph) values of 3-4 further focused by YAPC weight  
2357 analysis.
- 2358 2. Generate a rough surface by connecting all photons to each other. Let's call this  
2359 surface interp\_A.
- 2360 3. Run a median filter through Asmooth\_yapc\_weights using the window size set by  
2361 the software. Output = Asmooth.
- 2362 4. Define a reference DEM limit (ref\_dem\_limit) as 120 m (TBD).
- 2363 5. Remove any Asmooth values further than the ref\_dem\_limit threshold from the  
2364 reference DEM, and interpolate the Asmooth surface based on the remaining  
2365 Asmooth values. The interpolation method to use is the shape preserving  
2366 piecewise cubic Hermite interpolating polynomial – hereafter labeled as “pchip”  
2367 (Fritsch & Carlson, 1980).
- 2368 6. Compute the approximate relief of the *L-km* segment using the 95<sup>th</sup> - 5<sup>th</sup>  
2369 percentile heights of the signal photons. We are going to filter Asmooth again  
2370 and the smoothing is a function of the relief.
- 2371 7. Define the SmoothSize using the conditional statements below. The SmoothSize  
2372 will be used to detrend the data as well as to create an interpolated ground  
2373 surface later.

2374       SmoothSize = 2 \* Window

- 2375       • If relief >= 900, SmoothSize = round(SmoothSize/4)
- 2376       • If relief >= 400 && <= 900, SmoothSize = round(SmoothSize/3)
- 2377       • If relief >= 200 && <= 400, SmoothSize = round(SmoothSize/2)
- 2378 8. Greatly smooth Asmooth by first running Asmooth 10 times through a median  
2379 filter then a smoothing filter with a moving average method on the result. Both  
2380 the median filter and the smoothing filter use a window size of SmoothSize.
- 2381 9. Create a second smooth line (Asmooth2) that roughly follows the ground and  
2382 Asmooth2 will be used only for detrending data during initial ground estimation.

2383 Asmooth2 is created by running five iterations of a median filter and smoothing  
2384 using SmoothSize defined in 4.6.7. The threshold for removing photons is 1 m  
2385 above each iteration.

#### 2386 **4.9 Filter outlier noise from signal**

- 2387 1. If there are any signal data that are 150 meters above Asmooth\_yapc, remove  
2388 them from the signal data set.
- 2389 2. If the standard deviation of the detrended signal is greater than 10 meters,  
2390 remove any signal value from the signal data set that is 2 times the standard  
2391 deviation of the detrended signal below Asmooth\_yapc or Asmooth2.
- 2392 3. Calculate a new Asmooth surface by interpolating (pchip method) a surface  
2393 from the remaining signal photons and median filtering using the Window  
2394 size, then median filter and smooth (moving average method) 10 times again  
2395 using the SmoothSize.
- 2396 4. Calculate a new Asmooth2 surface by interpolating a surface from remaining  
2397 signal photons and repeat **step 4.6**.
- 2398 5. Detrend the signal photons by subtracting the signal height values from the  
2399 Asmooth2 surface height values. Use the Asmooth2 detrended heights for the  
2400 initial ground estimate surface finding.
- 2401 6. Other calculations for canopy and ground finding will utilize detrended from  
2402 the original Asmooth.

2403

#### 2404 **4.10 Finding the initial ground estimate**

- 2405 1. At this point, the initial signal photons have been noise filtered and de-trended  
2406 and should have the following format: X, Y, detrended Z, T (T=time). From this,  
2407 the input data into the ground finding will be the ATD (along track distance)  
2408 metric (such as time) and the detrended Z height values.
- 2409 2. Define a medianSpan as round (Window\*2/3).
- 2410 3. Calculate the background neighbor density of the subsurface photons using ALL  
2411 available photons (the non-detrended data). This step is run on all photons

2412 including noise photons. Histogram the photons in 1 m vertical bins and a 60 m  
 2413 horizontal bin.

2414 4. To avoid including zero population bins in the histogram signal tracking process,  
 2415 identify the bin with the maximum bin count among bins 2 – 4 (starting at the  
 2416 lowest height) across each 60 m within the 10-km processing window.

2417 5. Calculate the mean of those maximum bin values to represent the noise count for  
 2418 the 10-km window.

2419 6. The following steps are run on the detrended signal photons.

2420 7. Calculate the brightness of the surface for each 60 m to be histogrammed via the  
 2421 calculation in Section 2.4.21. If a bright surface is detected, skip steps 8 and 9

2422 8. Determine the lowest 1 m histogram height bin for each 60 m along track, in the  
 2423 detrended heights where:

2424       a. The neighbor density is 10 x greater than the background density  
 2425       AND

2426       b. The neighbor density is greater than the histogram population median  
 2427       plus 1/3 of the population standard deviation

2428       c. OR if yapc analysis was successful, the height bin includes the  
 2429       maximum height found among YAPC-tracked photons

2430 9. The photons with detrended heights above this bin are masked from  
 2431 consideration in the initial ground height estimate. Detrended signal photons  
 2432 implies that the d\_flag photons.

2433 10. Identifying the ground surface is an iterative process. Start by assuming that all  
 2434 the input signal height photons are the ground. The first goal is the cut out the  
 2435 lower height excess photons in order to find a lower bound for potential ground  
 2436 photons. This process is done 5 times and an offset of 4 meters is subtracted  
 2437 from the resulting lower bound. The smoothing filter uses a moving average  
 2438 again:

2439       for j=1:5

2440               cutOff = median filter (ground, medianSpan)

2441               cutOff = smooth filter (cutOff, Window)

```

2442         ground = ground( (cutOff - ground) > -1 )
2443     end
2444     lowerbound = median filter (ground, medianSpan*3)
2445     middlebound = smooth filter (lowerbound, Window)
2446     lowerbound = smooth filter (lowerbound, Window) - 4
2447 end;
2448 11. Create a linearly interpolated surface along the lower bound points and only
2449     keep input photons above that line as potential ground points:
2450
2451         top = input( input > interp(lowerbound) )
2452
2453 12. The next goal is to cut out excess higher elevation photons in order to find an
2454     upper bound to the ground photons. This process is done 3 times and an offset of
2455     1 meter is added to the resulting upper bound. The smoothing filter uses a
2456     moving average:
2457
2458     for j = 1:3
2459         cutOff = median filter (top, medianSpan)
2460         cutOff = smooth filter (cutOff, Window)
2461         top = top( (cutOff - top) > -1 )
2462     end
2463     upperbound = median filter (top, medianSpan)
2464     upperbound = smooth filter (upperbound, Window) + 1
2465
2466 13. Create a linearly interpolated surface along the upper bound points and extract
2467     the points between the upper and lower bounds as potential ground points:
2468
2469         ground = input( ( input > interp(lowerbound) ) & ...
2470             ( input < interp(upperbound) ) )
2471
2472 14. Refine the extracted ground points to cut out more canopy, again using the
2473     moving average smoothing:
2474
2475     For j = 1:2

```

```

2469         cutOff = median filter (ground, medianSpan)
2470         cutOff = smooth filter (cutOff, Window)
2471         ground = ground( (cutOff - ground) > -1 )
2472     end

2473 15. Run the ground output once more through a median filter using window side
2474     medianSpan and a smoothing filter using window size Window, but this time
2475     with the Savitzky-Golay method.
2476 16. Finally, linearly interpolate a surface from the ground points.
2477 17. The first estimate of canopy points are those indices of points that are between 2
2478     and 150 meters above the estimated ground surface. Save these indices for the
2479     next section on finding the top of canopy.
2480 18. The output from the final iteration of ground points is temp_interpA – an
2481     interpolated ground estimate.
2482 19. Find ground indices that lie within 10 m below and 0.5 m above of
2483     temp_interpA . Now, find ground indices that lie <=6 m above the refDEM
2484 20. Apply the ground indices to the original heights (i.e., not the de-trended data) to
2485     label ground photons.
2486 21. Interpolate a ground surface using the pchip method based on the ground
2487     photons. Output is interp_Aground.
2488 22. All initial ground results (interp_Aground) must lie within 6m or below the
2489     reference DEM height.

```

2490

#### 2491 ***4.11 Find the top of the canopy***

2492 The top of canopy filtering and all canopy finding shall only occur in ATL08  
2493 regions 1 – 6. ATL08 regions 7-11 include Antarctica and Greenland and we are  
2494 assuming there is no canopy there, thus a canopy value will not reported in these  
2495 regions.

- 2496 1. The input values include the ATD metric (i.e., time), and the de-trended Z  
2497 values indexed by the canopy indices extracted from step 4.7(17).  
2498 2. Flip this data over so that we can find a canopy “surface” by multiplying the  
2499 de-trended canopy heights by -1.0 and adding the mean(heights).  
2500 3. Finding the top of canopy is also an iterative process. Follow the same steps  
2501 described in 4.7(2) – 4.7(16), but use the canopy indexed and flipped Z  
2502 values in place of the ground input. Do not include any photons from  
2503 segments deemed to have only a single surface in initial ground finding steps.  
2504 4. Final retained photons are considered top of canopy photons. Use the indices  
2505 of these photons to define top of canopy photons in the original (not de-  
2506 trended) Z values.  
2507 5. Build a kd-tree on canopy indices using elevation data detrended with  
2508 Asmooth.  
2509 6. If there are less than three canopy indices within a 100m radius, reassign  
2510 these photons to noise photons. Initially, a value of 15 m was used for the  
2511 search radius. In Release 004 of the algorithm, this value was increased to  
2512 100 m to include more top of canopy photons that were not captured in the  
2513 initial canopy spline estimate.

2514

#### 2515 ***4.12 Compute statistics on de-trended (Asmooth) data***

- 2516 1. The input data have been noise filtered and de-trended (Asmooth) and  
2517 should have the following input format: X, Y, detrended Z, T.  
2518 2. The input data will contain signal photons as well as a few noise photons  
2519 near the surface.  
2520 3. Compute statistics of heights in the along-track direction using a sliding  
2521 window. Using the window size (window), compute height statistics for all  
2522 photons that fall within each window. These include max height, median  
2523 height, mean height, min height, and standard deviation of all photon heights.  
2524 Additionally, in each window compute the median height and standard

2525 deviation of just the initially classified top of canopy photons, and the  
 2526 standard deviation of just the initially classified ground photon heights.  
 2527 Currently only the median top of canopy, and all STD variables are being  
 2528 utilized, but it's possible that other statistics may be incorporated as  
 2529 changes/improvements are made to the code.

- 2530 4. Slide the window  $\frac{1}{4}$  of the window span and recompute statistics along the  
 2531 entire  $L$ -km segment. This results in one value for each statistic for each  
 2532 window.
- 2533 5. Determine canopy index categories for each window based upon the total  
 2534 distribution of STD values for all signal photons along the  $L$ -km segment  
 2535 based on STD quartiles.
- 2536 6. Open canopy have STD values falling within the 1<sup>st</sup> quartile.
- 2537 7. Canopy Level 1 has STD values falling from 1<sup>st</sup> quartile to median STD value.
- 2538 8. Canopy Level 2 has STD values falling from median STD value to 3<sup>rd</sup> quartile.
- 2539 9. Canopy Level 3 has STD values falling from 3<sup>rd</sup> quartile to max STD.
- 2540 10. Linearly interpolate the window STD values (both for all photons and  
 2541 ground-only photons) back to the native along-track resolution and calculate  
 2542 the interpolated all-photon STD quartiles to create an interpolated canopy  
 2543 level index. This will be used later for interpolating a ground surface.  
 2544

#### 2545 **4.13 Refine Ground Estimates**

- 2546 1. Detrend the interpolated ground surface using Asmooth. Smooth the  
 2547 detrended interpolated ground surface 10 times. All further ground surface  
 2548 smoothing use the moving average method:

2549 For j= 1:10

2550           AgroundSmooth = median filter (interp\_Aground, SmoothSize\*3)

2551           AgroundSmooth = smooth filter (AgroundSmooth, SmoothSize)

2552 End

```

2553
2554 2. This output (AgroundSmooth) from the filtering/smoothing function is an
2555 intermediate ground solution and it will be used to estimate the final
2556 solution.
2557 3. If there are no canopy indices identified along the entire segment AND relief
2558 >400 m
2559     FINALGROUND = median filter (Asmooth, SmoothSize)
2560     FINALGROUND = smooth filter (FINALGROUND, SmoothSize)
2561 Else
2562     FINALGROUND = AgroundSmooth
2563 end
2564 4. If there are canopy indices identified along the segment:
2565 If there is a canopy photon identified at a location along-track above the
2566 ground surface, then at that location along-track
2567     FINALGROUND = AgroundSmooth
2568 else if there is a location along-track where the interpolated ground STD has
2569 an interpolated canopy level>=3
2570     FINALGROUND = Interp_Aground*1/3 + AgroundSmooth*2/3
2571 else
2572     FINALGROUND = Interp_Aground*1/2 + Asmooth*1/2
2573 end
2574 5. Smooth the resulting interpolated ground surface (FINALGROUND) once
2575 using a median filter with window size of 9 then a smoothing filter twice with
2576 window size of 9. Select ground photons that lie within the point spread
2577 function (PSF) of FINALGROUND.
2578 6. PSF is determined by sigma_atlas_land (Eq. 1.2) calculated at the photon
2579 resolution and thresholded between 0.5 to 1 m.

```



2580           a. Estimate the terrain slope by taking the gradient of FINALGROUND.  
 2581                Gradient is reported at the center of  $((\text{finalground}(n+1)-$   
 2582                 $\text{finalground}(n-1))/(\text{dist\_x}(n+1)-\text{dist\_x}(n-1)))/2$   
 2583           b. Linearly interpolate the sigma\_h values to the photon resolution.  
 2584           c. Calculate sigma\_topo (Eq. 1.3) at the photon resolution.  
 2585           d. Calculate sigma\_atlas\_land at the photon resolution using the sigma\_h  
 2586                and sigma\_topo values at the photon resolution.  
 2587           e. Set PSF equal to sigma\_atlas\_land.  
 2588                i. Any PSF < 0.5 m is set to 0.5 m as the minimum PSF.  
 2589                ii. Any PSF > 1 m is set to 1 m as the maximum PSF. Set psf\_flag to  
 2590                true.

2591

#### 2592   **4.14 Canopy Photon Filtering**

2593       1. The first canopy filter will remove photons classified as top of canopy that  
 2594       are significantly above a smoothed median top of canopy surface. To  
 2595       calculate the smoothed median top of canopy surface:  
 2596           a. Linearly interpolate the median and standard deviation canopy  
 2597                window statistics, calculated from 4.12 (3), to the top of canopy  
 2598                photon resolution. Output variables: interpMedianC, interpStdC.  
 2599           b. Calculate a canopy window size using Eq. 3.4, where *length* = number  
 2600                of top of canopy photons. Output variable: winC.  
 2601           c. Create the median filtered and smoothed top of canopy surface,  
 2602                smoothedC, using a locally weighted linear regression smoothing  
 2603                method, “lowess” (Cleveland, 1979):

2604                       smoothedC = median filter ( interpMedianC, winC )

2605

2606                       if SNR > 1, canopySmoothSpan = winC\*2;

2607                       else, canopySmoothSpan = smoothSpan;

```

2608
2609             smoothedC = smooth filter ( smoothedC, canopySmoothSpan )
2610
2610         d. Add the detrended heights back into the smoothedC surface:
2611
2611             smoothedC = smoothedC + Asmooth
2612
2612     2. Set canopy height thresholds based on the interpolated top of canopy STD:
2613
2613         If SNR > 1, canopySTDthresh = 3; else, canopySTDthresh = 2;
2614         canopy_height_thresh = canopySTDthresh*interpStdC
2615
2615         high_cStd = canopy_height_thresh > 10
2616
2616         low_cStd = canopy_height_thresh < 3
2617
2617         canopy_height_thresh(high_cStd) =
2618         canopy_height_thresh(high_cStd)/2
2619
2619         canopy_height_thresh(low_cStd) = 3
2620
2620     3. Relabel as noise any top of canopy photons that are higher than smoothedC +
2621         canopy_height_thresh.
2622
2622     4. Next, interpolate a top of canopy surface using the remaining top of canopy
2623         photons (here we are trying to create an upper bound on canopy points). The
2624         interpolation method used is pchip. This output is named interp_Acanopy.
2625
2625     5. Photons falling below interp_Acanopy and above FINALGROUND+PSF are
2626         labeled as canopy points.
2627
2627     6. For 500 signal photon segments, if number of all canopy photons (i.e., canopy
2628         and top of canopy) is:
2629
2629         < 5% of the total (when SNR > 1), OR
2630         < 10% of the total (when SNR <= 1),
2631         relabel the canopy photons as noise.
2632
2632     7. Interpolate, using the pchip method, a new top of canopy surface from the
2633         filtered top of canopy photons. This output is again named interp_Acanopy.

```

2634 8. Again, label photons that lie between interp\_Acanopy and  
2635 FINALGROUND+PSF as canopy photons.

2636 9. Since the canopy points have been relabeled, we need to do a final  
2637 refinement of the ground surface:

2638 If canopy is present at any location along-track

2639         FINALGROUND = AgroundSmooth (at that location)

2640 Else if canopy is not present at a location along-track

2641         FINALGROUND = interp\_Aground

2642 Smooth the resulting interpolated ground surface (FINALGROUND) once  
2643 using a median filter with window size of SmoothSize (SmoothSize = 9), then  
2644 a moving average smoothing filter twice with window size of SmoothSize  
2645 (SmoothSize = 9)

2646 10. Relabel ground photons based on this new (and last) FINALGROUND solution  
2647 +/- a recalculated PSF (via steps in 4.13 (6)). Points falling below the buffer  
2648 are labeled as noise.

2649 11. Using Interp\_Acanopy and this last FINALGROUND solution + PSF buffer,  
2650 label all photons that lie between the two as canopy photons.

2651 12. Repeat the canopy cover filtering: For 500 signal photon segments, if  
2652 number of all canopy photons (i.e., canopy and top of canopy) is:

2653         < 5% of the total (when SNR > 1), OR  
2654         < 10% of the total (when SNR <= 1),

2655 relabel the canopy photons as noise. This is the last canopy labeling step.

2656 13. Reset any canopy labeled photons residing in a segment deemed to have a  
2657 single surface during initial ground finding to noise.

2658

#### 2659 **4.15 Compute individual Canopy Heights**

- 2660 1. At this point, each photon will have its final label assigned in  
2661 **classed\_pc\_flag**: 0 = noise, 1 = ground, 2 = canopy, 3 = top of canopy.
- 2662 2. For each individual photon labeled as canopy or top of canopy, subtract the Z  
2663 height value from the interpolated terrain surface, FINALGROUND, at that  
2664 particular position in the along-track direction.
- 2665 3. The relative height for each individual canopy or top of canopy photon will  
2666 be used to calculate canopy products described in Section 4.18. Additional  
2667 canopy products will be calculated using the absolute heights, as described in  
2668 Section 4.18.1.
- 2669 4. When processing windows during night passes, with solar elevation angles  
2670 less than 5 degrees, calculate a relative canopy mean height for the 10km  
2671 processing window relative to the FINALGROUND interpolated ground  
2672 surface height. Use canopy and top of canopy classed photons, only. Limit  
2673 results to where the optical depth is less than or equal to 0.05. This value is  
2674 the relative 10 km canopy mean and will be used in Step 5.
- 2675 5. Reassign noise photons to top of canopy class if:
  - 2676 a. DRAGANN indicates signal ( $d\_flag = 1$ )
  - 2677 b. Optical depth  $\leq 0.05$
  - 2678 c. Quality\_ph = 0, 10, or 20
  - 2679 d. Photon is not already classed ground nor canopy
  - 2680 e. Photon is not in a detected single surface segment, as determine in  
2681 early ground finding steps
  - 2682 f. Photon height is  $\leq 3 \times$  relative 10 km canopy mean (calculated above)  
2683 over FINALGROUND height.

#### 2685 **4.16 Final photon classification QA check**

- 2686 1. Find any ground, canopy, or top of canopy photons that have elevations  
2687 further than the ref\_dem\_limit from the reference DEM elevation value.  
2688 Convert these to the noise classification.

- 2689        2. Find any relative heights of canopy or top of canopy photons that are greater  
2690            than 150 m above the interpolated ground surface, FINALGROUND. Convert  
2691            these to the noise classification.
- 2692        3. Find any FINALGROUND elevations that are further than the ref\_dem\_limit  
2693            from the reference DEM elevation value. Convert those FINALGROUND  
2694            elevations to an invalid value, and convert any classified photons at the same  
2695            indices to noise.
- 2696        4. If more than 50% of photons are removed in a segment, set ph\_removal\_flag  
2697            to true.

2698

2699    **4.17 Compute segment parameters for the Land Products**

- 2700        1. For each 100 m segment, determine the classed photons (photons classified  
2701            as ground, canopy, or top of canopy).
- 2702            a. If there are fewer than 50 classed photons (strong beam) or < 30  
2703                classed photons (weak beam) in a 100 m segment, do not calculate  
2704                land or canopy products.
- 2705            b. If there are 50 or more classed photons in a 100 m segment (strong  
2706                beam) or 30 or more classed photons in a 100 m segment (weak beam),  
2707                then calculate terrain statistics on all ground photons.
- 2708            c. If the number of ground photons > 5% of the total number of classed  
2709                photons within the segment (this control value of 5% can be modified  
2710                once on orbit):
- 2711                d. Compute statistics on the ground photons: mean, median, min, max,  
2712                        standard deviation, mode, and skew. These heights will be reported  
2713                        on the product as **h\_te\_mean**, **h\_te\_median**, **h\_te\_min**, **h\_te\_max**,  
2714                        **h\_te\_mode**, and **h\_te\_skew** respectively described in Table 2.1.
- 2715                e. Compute the standard deviation of the ground photons about the  
2716                        interpolated terrain surface, FINALGROUND. This value is reported as  
2717                        **h\_te\_std** in Table 2.1.

2718 f. Compute the residuals of the ground photon Z heights about the  
2719 interpolated terrain surface, FINALGROUND. The product is the root  
2720 sum of squares of the ground photon residuals combined with the  
2721 **sigma\_atlas\_land** term in Table 2.5 as described in Equation 1.4. This  
2722 parameter reported as **h\_te\_uncertainty** in Table 2.1.

2723 g. Compute a linear fit on the ground photons and report the slope. This  
2724 parameter is **terrain\_slope** in Table 2.1.

2725 h. Calculate a best fit terrain elevation at the mid-point location of the  
2726 100 m segment:

2727 i. Calculate each terrain photon's distance along-track into the  
2728 100 m segment using the corresponding ATL03 20 m products  
2729 segment\_length and dist\_ph\_along, and determine the mid-  
2730 segment distance (expected to be 50 m  $\pm$  0.5 m).

2731 1. Use the mid-segment distance to linearly interpolate a  
2732 mid-segment time (**delta\_time** in Table 2.4). Use the  
2733 mid-segment time to linearly interpolate other mid-  
2734 segment parameters: interpolated terrain surface,  
2735 FINALGROUND, as **h\_te\_interp** (Table 2.1); **latitude**  
2736 and **longitude** (Table 2.4).

2737 ii. Calculate a linear fit, as well as 3<sup>rd</sup> and 4<sup>th</sup> order polynomial fits  
2738 to the terrain photons in the segment.

2739 iii. Create a slope-adjusted and weighted mid-segment variable,  
2740 weightedZ, from the linear fit: Use terrain\_slope to apply a  
2741 slope correction to each terrain photon by subtracting the  
2742 terrain photon heights from the linear fit. Determine the mid-  
2743 segment location of the linear fit, and add that height to the  
2744 slope corrected terrain photons. Apply a linear weighting to  
2745 each photon based on its distance to the mid-segment location:  
2746  $1 / \sqrt{(\text{photon distance along} - \text{mid-segment distance})^2}$ .  
2747 Calculate the weighted mid-segment terrain height, weightedZ:

2748                               sum( each adjusted terrain height \* its weight ) / sum(all  
2749                               weights).

2750                               iv. Determine which of the three fits is best by calculating the  
2751                               mean and standard deviation of the fit errors. If one of the fits  
2752                               has both the smallest mean and standard deviations, use that  
2753                               fit. Else, use the fit with the smallest standard deviation. If  
2754                               more than one fit has the same smallest mean and/or standard  
2755                               deviation, use the fit with the higher polynomial.

2756                               v. Use the best fit to define the mid-segment elevation. This  
2757                               parameter is **h\_te\_best\_fit** in Table 2.1.

2758                                       1. If h\_te\_best\_fit is farther than 3 m from h\_te\_interp (best  
2759                                       fit diff threshold), check if: there are terrain photons on  
2760                                       both sides of the mid-segment location; or the elevation  
2761                                       difference between weightedZ and h\_te\_interp is  
2762                                       greater than the best fit diff threshold; or the number of  
2763                                       ground photons in the segment is <= 5% of total  
2764                                       number of classified photons per segment. If any of  
2765                                       those cases are present, use h\_te\_interp as the corrected  
2766                                       h\_te\_best\_fit. Otherwise use weightedZ as the corrected  
2767                                       h\_te\_best\_fit.

2768                               i. Compute the difference of the median ground height from the  
2769                               reference DTM height. This parameter is **h\_dif\_ref** in Table 2.4.  
2770

2771                               2. If the number of ground photons in the segment <= 5% of total number of  
2772                               classified photons per segment,

2773                                       a. Report an invalid value for terrain products: **h\_te\_mean**,  
2774                                       **h\_te\_median**, **h\_te\_min**, **h\_te\_max**, **h\_te\_mode**, **h\_te\_skew**, **h\_te\_std**,  
2775                                       **and h\_te\_uncertainty** respectively as described in Table 2.1.

2776                                       b. If the number of ground photons in the segment is <= 5% of total  
2777                                       number of classified photons in the segment, compute **terrain\_slope**

2778 via a linear fit of the interpolated ground surface, FINALGROUND,  
2779 instead of the ground photons.  
2780 c. Report the mid-segment interpolated terrain surface, FinalGround, as  
2781 **h\_te\_interp** as described in Table 2.1, and report **h\_te\_best\_fit** as the  
2782 h\_te\_interp value.  
2783

#### 2784 **4.18 Compute segment parameters for the Canopy Products**

- 2785 1. For each 100 m segment, determine the classed photons (photons classified as  
2786 ground, canopy, or top of canopy).  
2787 a) If there are fewer than 50 classed photons (strong beam) or < 30  
2788 classed photons (weak beam) in a 100 m segment, do not calculate  
2789 land or canopy products.  
2790 b) If there are 50 or more classed photons in a 100 m segment (strong  
2791 beam) or 30 or more classed photons in a 100 m segment (weak beam),  
2792 extract all canopy photons (i.e., canopy and top of canopy; henceforth  
2793 referred to as “canopy” unless otherwise noted) to create the canopy  
2794 products.  
2795 2. Only compute canopy height products if the number of canopy photons is >  
2796 5% of the total number of classed photons within the segment (this control  
2797 value of 5% can be modified once on orbit).  
2798 a) If the number of ground photons is also > 5% of the total number of  
2799 classed photons within the segment, set **canopy\_rh\_conf** to 2.  
2800 b) If the number of ground photons is < 5% of the total number of classed  
2801 photons within the segment, continue with the relative canopy height  
2802 calculations, but set canopy\_rh\_conf to 1.  
2803 c) If the number of canopy photons is < 5% of the total number of classed  
2804 photons within the segment, regardless of ground percentage, set  
2805 canopy\_rh\_conf to 0 and report an invalid value for each canopy height  
2806 variable.



- 2807 d) Considering adding in a QC check for the absolute canopy height. If the  
 2808 height is below the reference DEM, disregard this ATL08 segment.
- 2809 3. Again, the relative heights (height above the interpolated ground surface,  
 2810 FINALGROUND) have been computed already. All parameters derived in the  
 2811 section are based on relative heights.
- 2812 4. Sort the heights and compute a cumulative distribution of the heights. Select  
 2813 the height associated with the 98% maximum height. This value is **h\_canopy**  
 2814 listed in Table 2.2.
- 2815 5. Compute statistics on the relative canopy heights. Min, Mean, Median, Max and  
 2816 standard deviation. These values are reported on the product as  
 2817 **h\_min\_canopy**, **h\_mean\_canopy**, **h\_max\_canopy**, and **canopy\_openness**  
 2818 respectively in Table 2.2.
- 2819 6. Using the cumulative distribution of relative canopy heights, select the heights  
 2820 associated with the **canopy\_h\_metrics** percentile distributions (10, 15, 20, 25,  
 2821 30, 35, 40, 45, 50, 55, 60, 65, 70, 75, 80, 85, 90, 95), and report as listed in Table  
 2822 2.2.
- 2823 7. Compute the difference between **h\_canopy** and **canopy\_h\_metrics(50)**. This  
 2824 parameter is **h\_dif\_canopy** reported in Table 2.2 and represents an amount of  
 2825 canopy depth.
- 2826 8. Compute the standard deviation of all photons that were labeled as Top of  
 2827 Canopy (flag 3) in the photon labeling portion. This value is reported on the  
 2828 data product as **toc\_roughness** listed in Table 2.2.
- 2829 9. The quadratic mean height, **h\_canopy\_quad** is computed by

2830 
$$qmh = \sqrt{\frac{\sum_{i=1}^{N_{ca}} h_i^2}{N_{ca}}}$$

2831 where  $N_{ca}$  is the number of canopy photons in the segment and  $h_i$  are the  
 2832 individual canopy heights.

2833

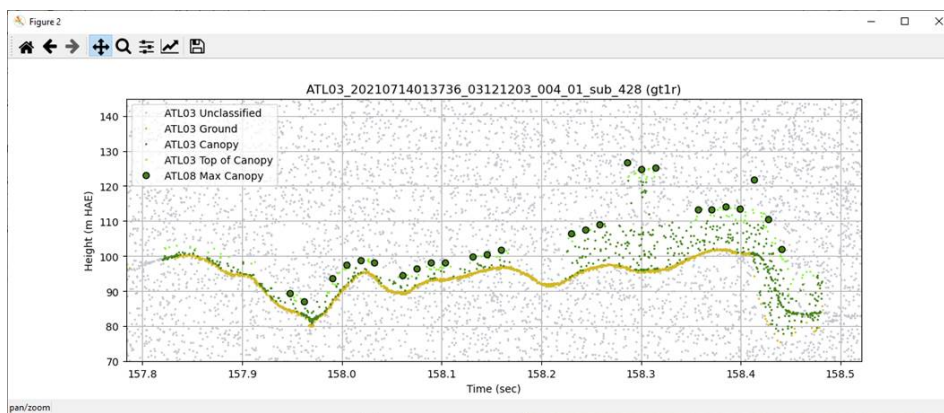
#### 4.18.1 Canopy Products calculated with absolute heights

1. The absolute canopy height products are calculated if the number of canopy photons is  $> 5\%$  of the total number of classed photons within the segment. No number of ground photons threshold is applied for these. Absolute canopy heights are first determined as the relative heights of individual photons above the estimated terrain surface. Once those cumulative distribution is made, the absolute heights are the relative heights plus the best fit terrain height ( $h_{te\_bestfit}$ ).
2. The **centroid\_height** parameter in Table 2.2 is represented by all the classed photons for the segment (canopy & ground). To determine the centroid height, compute a cumulative distribution of all absolute classified heights and select the median height.
3. Calculate **h\_canopy\_abs**, the 98<sup>th</sup> percentile of the absolute canopy heights.
4. Compute statistics on the absolute canopy heights: Min, Mean, Median, and Max. These values are reported on the product as **h\_min\_canopy\_abs**, **h\_mean\_canopy\_abs**, and **h\_max\_canopy\_abs**, respectively, as described in Table 2.2.
5. Again, using the cumulative distribution of relative canopy heights, select the heights associated with the **canopy\_h\_metrics\_abs** percentile distributions (10, 15, 20, 25, 30, 35, 40, 45, 50, 55, 60, 65, 70, 75, 80, 85, 90, 95) and then added to the  $h_{te\_bestfit}$ , and report as listed in Table 2.2.

#### 4.19 Segment Quality Check

1. Quality check is based on the radiometry rates,  $te\_photon\_rate$  and  $can\_photon\_rate$ . For the strong beams, if the  $total\_photon\_rate$  ( $te\_photon\_rate + can\_photon\_rate$ ) has a value of 16 or higher, reject all parameters in this ATL08 segment as invalid and reassign any labeled photons back to noise unless the saturation flag is on. For the weak beams, if the  $total\_photon\_rate$  ( $te\_photon\_rate + can\_photon\_rate$ ) has a value of 4 or higher, reject all parameters in this ATL08 segment as invalid and reassign any labeled photons back to noise unless the saturation flag is on.

2. If  $h\_canopy\_abs + 50 < ref\_dem$ , reject all parameters in this ATL08 segment as these height are likely noise points that were mislabeled. Reassign any labeled (ground or canopy) photons back to noise.
3. **THIS QA CHECK IS BEING IGNORED IN RELEASE 007.** Canopy Photon Background Rate QA check. The objective of this QA check is to utilize the calculated background noise and the calculated noise reduced canopy photon rate ( $photon\_rate\_can\_nr$ ) within each 100 m geosegment to relabel noise photons that may have incorrectly been labeled as canopy photons (see example below). The methodology for this step is as follows:
- For acquisitions where the  $solar\_elev > 20$  degrees, if canopy photons are within 1 m of the final interpolated ground line, ignore those canopy photons in this special canopy test. Thus, count only the canopy photons higher than 1 m above the final interpolated ground line.
  - Divide the special canopy count by the unique delta times to determine a special canopy rate.
  - If the background noise rate is  $> 99.5\%$  of the special canopy photon rate, reassign the canopy photons as noise (label value of 0).



2885    **4.20 Record final product without buffer**

2886        1. Now that all products have be determined via processing of the *L-km*  
2887            segment with the buffer included, remove the products that lie within the  
2888            buffer zone on each end of the *L-km* segment.

2889        2. Record the final *L-km* products and move on to process the next *L-km*  
2890            segment.

2891

2892

**5 DATA PRODUCT VALIDATION STRATEGY**

Although there are no Level-1 requirements related to the accuracy and precision of the ATL08 data products, we are presenting a methodology for validating terrain height, canopy height, and canopy cover once ATL08 data products are created. Parameters for the terrain and canopy will be provided at a fixed size of 100 m along the ground track referred to as a segment. Validation of the data parameters should occur at the 100 m segment scale and residuals of uncertainties are quantified (i.e. averaged) at the 5-km scale. This 5-km length scale will allow for quantification of errors and uncertainties at a local scale which should reflect uncertainties as a function of surface type and topography.

**5.1 Validation Data**

Swath mapping airborne lidar is the preferred source of validation data for the ICESat-2 mission due to the fact that it is widely available and the errors associated with most small-footprint, discrete return data sets are well understood and quantified. Profiling airborne lidar systems (such as MABEL) are more challenging to use for validation due to the low probability of exact overlap of flightlines between two profiling systems (e.g. ICESat-2 and MABEL). In order for the ICESat-2 validation exercise to be statistically relevant, the airborne data should meet the requirements listed in Table 5.1. Validation data sets should preferably have a minimum average point density of 5 pts/m<sup>2</sup>. In some instances, however, validation data sets with a lower point density that still meet the requirements in Table 5.1 may be utilized for validation to provide sufficient spatial coverage.

Table 5.1. Airborne lidar data vertical height (Z accuracy) requirements for validation data.

ICESat-2 ATL08 Parameter	Airborne lidar (rms)
Terrain height	<0.3 m over open ground (vertical)
	<0.5 m (horizontal)

Canopy height	<2 m temperate forest, < 3 m tropical forest
Canopy cover	n/a

2917

2918 Terrain and canopy heights will be validated by computing the residuals between the  
 2919 ATL08 terrain and canopy height value, respectively, for a given 100 m segment and  
 2920 the terrain height (or canopy height) of the validation data for that same  
 2921 representative distance. Canopy cover on the ATL08 data product shall be validated  
 2922 by computing the relative canopy cover ( $cc = \text{canopy returns} / \text{total returns}$ ) for the  
 2923 same representative distance in the airborne lidar data.

2924 It is recommended that the validation process include the use of ancillary data sets  
 2925 (i.e. Landsat-derived annual forest change maps) to ensure that the validation results  
 2926 are not errantly biased due to non-equivalent content between the data sets.

2927 Using a synergistic approach, we present two options for acquiring the required  
 2928 validation airborne lidar data sets.

2929

#### 2930 **Option 1:**

2931 We will identify and utilize freely available, open source airborne lidar data as the  
 2932 validation data. Potential repositories of this data include OpenTopo (a NSF  
 2933 repository or airborne lidar data), NEON (a NSF repository of ecological monitoring  
 2934 in the United States), and NASA GSFC (repository of G-LiHT data). In addition to  
 2935 small-footprint lidar data sets, NASA Mission data (i.e. ICESat and GEDI) can also be  
 2936 used in a validation effort for large scale calculations.

2937

#### 2938 **Option 2:**

2939 Option 2 will include Option 1 as well as the acquisition of additional airborne lidar  
 2940 data that will benefit multiple NASA efforts.

2941 GEDI: With the launch of the Global Ecosystems Dynamic Investigation  
2942 (GEDI) mission in 2018, there are tremendous synergistic activities for  
2943 data validation between both the ICESat-2 and GEDI missions. Since the  
2944 GEDI mission, housed on the International Space Station, has a  
2945 maximum latitude of 51.6 degrees, much of the Boreal zone will not be  
2946 mapped by GEDI. The density of GEDI data will increase as latitude  
2947 increases north to 51.6 degrees. Since the data density for GEDI would  
2948 be at its highest near 51.6 degrees, we would propose to acquire  
2949 airborne lidar data in a “GEDI overlap zone” that would ample  
2950 opportunity to have sufficient coverage of benefit to both ICESat-2 and  
2951 GEDI for calibration and validation.

2952 We recommend the acquisition of new airborne lidar collections that will meet our  
2953 requirements to best validate ICESat-2 as well as be beneficial for the GEDI mission.  
2954 In particular, we would like to obtain data over the following two areas:

- 2955 1) Boreal forest (as this forest type will NOT be mapped with GEDI)
- 2956 2) GEDI high density zone (between 50 to 51.6 degrees N). Airborne lidar data  
2957 in the GEDI/ICESat-2 overlap zone will ensure cross-calibration between  
2958 these two critical datasets which will allow for the creation of a global,  
2959 seamless terrain, canopy height, and canopy cover product for the  
2960 ecosystem community.

2961 In both cases, we would fly data with the following scenario:

2962 Small-footprint, full-waveform, dual wavelength (green and NIR), high point density  
2963 (>20 pts/m<sup>2</sup>) and, over low and high relief locations. In addition, the newly acquired  
2964 lidar data must meet the error accuracies listed in Table 5.1.

2965 Potential candidate acquisition areas include: Southern Canadian Rocky Mountains  
2966 (near Banff), Pacific Northwest mountains (Olympic National Park, Mt. Baker-  
2967 Snoqualmie National Forest), and Sweden/Norway. It is recommended that the

2968 airborne lidar acquisitions occur during the summer months to avoid snow cover in  
2969 either 2016 or 2017 prior to launch of ICESat-2.

2970

2971 **5.2 Internal QC Monitoring**

2972 In addition to the data product validation, internal monitoring of data  
2973 parameters and variables is required to ensure that the final ATL08 data quality  
2974 output is trustworthy. Table 5.2 lists a few of the computed parameters that should  
2975 provide insight into the performance of the surface finding algorithm within the  
2976 ATL08 processing chain.

2977 Table 5.2. ATL08 parameter monitoring.

Group	Description	Source	Monitor	Validate in Field
<b>h_te_median</b>	Median terrain height for segment	computed		Yes against airborne lidar data. The airborne lidar data should have an absolute accuracy of <30 cm rms.
<b>n_te_photons</b> <b>n_ca_photons</b> <b>n_toc_photons</b>	Number of classed (sum of terrain, canopy, and top of canopy) photons in a 100 m segment	computed	Yes. Build an internal counter for the number of segments in a row where there aren't enough photons (currently a minimum of 50 photons	



---

<b>h_te_interp</b>	Interpolated terrain surface height, FINALGROUND	computed	per 100 m segment is used) Difference h_te_interp and h_te_median and determine if the value is > a specified threshold. 2 m is suggested as the threshold value. This is an internal check to evaluate whether the median elevation for a segment is roughly the same as the interpolated surface height.	
<b>h_dif_ref</b>	Difference between h_te_median and ref_dem	computed	This value will be computed and flagged if the difference is > 25 m. The reference DEM is the onboard DEM.	
<b>h_canopy</b>	95% height of individual canopy heights for segment	computed	Yes, > a specified threshold (e.g. 60 m)	Yes against airborne lidar data. The

---

---

				canopy heights derived from airborne lidar data should have a relative accuracy <2 m in temperate forest, <3 m in tropical forest
<b>h_dif_canopy</b>	Difference between h_canopy and canopy_h_metrics(50)	computed	Yes, this is an internal check to make sure the calculations on canopy height are not suspect	
<b>psf_flag</b>	Flag is set if computed PSF exceeds 1m	computed	Yes, this is an internal check to make sure the calculations are not suspect	
<b>ph_removal_flag</b>	Flag is set if more than 50% of classified photons in a segment is removed during final QA check	computed		
<b>dem_removal_flag</b>	Flag is set if more than 20% of classified photons in a segment is removed due to a large distance from the reference DEM	computed	Yes, this will check if bad results are due to bad DEM values or because too much noise was labeled as signal	

---

In addition to the monitoring parameters listed in Table 5.2, a plot such as what is shown in Figure 5.1 would be helpful for internal monitoring and quality assessment of the ATL08 data product. Figure 5.1 illustrates in graphical form what the input point cloud look like in the along-track direction, the classifications of each photon, and the estimated ground surface (FINALGROUND).

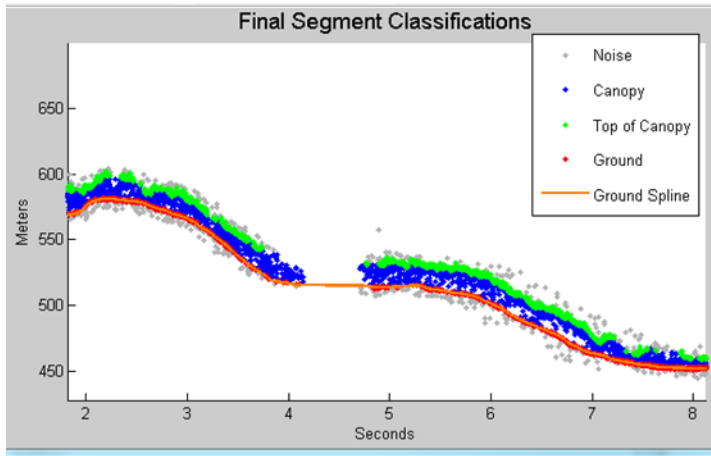


Figure 5.1. Example of  $L$ -km segment classifications and interpolated ground surface.

2987 The following parameters are to be calculated and placed in the QA/QC group on the  
 2988 HDF5 data file, based on Table 5.2 of the ATL08 ATBD. Statistics shall be computed  
 2989 on a per-granule basis and reported on the data product. If any parameter meets the  
 2990 QA trigger conditional, an alert will be sent to the ATL08 ATBD team for product  
 2991 review.

2992 Table 5.3. QA/QC trending and triggers.

QA/QC trending description	QA trigger conditional
Percentage of segments with > 50 classed photons	None
Max, median, and mean of the number of contiguous segments with < 50 classed photons	None
Number and percentage of segments with difference in $h_{te\_interp} - h_{te\_median}$ is greater than a specified threshold (2 m TBD)	> 50 segments in a row
Max, median, and mean of $h_{diff\_ref}$ over all segments	None
Percentage of segments where $h_{diff\_ref} > 25$ m	Percentage > 75%
Percentage of segments where the $h_{canopy}$ is > 60m	None
Max, median, and mean of $h_{diff}$	None
Percentage of segments where $psf\_flag$ is set	Percentage > 75%
Percentage of classified photons removed in a segment during final photon QA check	Percentage > 50% (i.e., $ph\_removal\_flag$ is set to true)
Percentage of classified photons removed in a segment during the reference DEM threshold removal process	Percentage > 20% (i.e., $dem\_removal\_flag$ is set to true)

2993  
2994

## 6 REFERENCES

- Carroll, M. L., Townshend, J. R., DiMiceli, C. M., Noojipady, P., & Sohlberg, R. A. (2009). A new global raster water mask at 250 m resolution. *International Journal of Digital Earth*, 2(4), 291–308. <http://doi.org/10.1080/17538940902951401>
- Channan, S., K. Collins, and W. R. Emanuel (2014). Global mosaics of the standard MODIS land cover type data. University of Maryland and the Pacific Northwest National Laboratory, College Park, Maryland, USA.
- Chauve, Adrien, et al. (2008). Processing full-waveform lidar data: modelling raw signals. *International archives of photogrammetry, remote sensing and spatial information sciences 2007*, 102-107.
- Cleveland, W. S. (1979). Robust Locally Weighted Regression and Smoothing Scatterplots. *Journal of the American Statistical Association*, 74(368), 829–836. <http://doi.org/10.2307/2286407>
- Friedl, M.A., D. Sulla-Menashe, B. Tan, A. Schneider, N. Ramankutty, A. Sibley and X. Huang (2010). MODIS Collection 5 global land cover: Algorithm refinements and characterization of new datasets, 2001-2012, Collection 5.1 IGBP Land Cover, Boston University, Boston, MA, USA.
- Fritsch, F.N., and Carlson, R.E. (1980). Monotone Piecewise Cubic Interpolation. *SIAM Journal on Numerical Analysis*, 17(2), 238–246. <http://doi.org/10.1137/0717021>
- Goshtasby, A., and O'Neill, W.D. (1994). Curve fitting by a Sum of Gaussians. *Graphical Models and Image Processing*, 56(4), 281-288.
- Goetz and Dubayah (2011). Advances in remote sensing technology and implications for measuring and monitoring forest carbon stocks and change. *Carbon Management*, 2(3), 231-244. doi:10.4155/cmt.11.18

3021 Hall, F.G., Bergen, K., Blair, J.B., Dubayah, R., Houghton, R., Hurtt, G., Kelldorfer, J.,  
 3022 Lefsky, M., Ranson, J., Saatchi, S., Shugart, H., Wickland, D. (2011). Characterizing 3D  
 3023 vegetation structure from space: Mission requirements. *Remote sensing of*  
 3024 *environment*, 115(11), 2753-2775

3025 Harding, D.J., (2009). Pulsed laser altimeter ranging techniques and implications for  
 3026 terrain mapping, in *Topographic Laser Ranging and Scanning: Principles and*  
 3027 *Processing*, Jie Shan and Charles Toth, eds., CRC Press, Taylor & Francis Group, 173-  
 3028 194.

3029 Neuenschwander, A.L. and Magruder, L.A. (2016). The potential impact of vertical  
 3030 sampling uncertainty on ICESat-2/ATLAS terrain and canopy height retrievals for  
 3031 multiple ecosystems. *Remote Sensing*, 8, 1039; doi:10.3390/rs8121039

3032 Neuenschwander, A.L. and Pitts, K. (2019). The ATL08 Land and Vegetation Product  
 3033 for the ICESat-2 Mission. *Remote Sensing of Environment*, 221, 247-259.  
 3034 <https://doi.org/10.1016/j.rse.2018.11.005>

3035 Neumann, T., Brenner, A., Hancock, D., Robbins, J., Saba, J., Harbeck, K. (2018). ICE,  
 3036 CLOUD, and Land Elevation Satellite – 2 (ICESat-2) Project Algorithm Theoretical  
 3037 Basis Document (ATBD) for Global Geolocated Photons (ATL03).

3038 Obu, J.; Westermann, S.; Barboux, C.; Bartsch, A.; Delaloye, R.; Grosse, G.; Heim, B.;  
 3039 Hugelius, G.; Irrgang, A.; Kääb, A.M.; Kroisleitner, C.; Matthes, H.; Nitze, I.; Pellet, C.;  
 3040 Seifert, F.M.; Strozzi, T.; Wegmüller, U.; Wieczorek, M.; Wiesmann, A. (2021): ESA  
 3041 Permafrost Climate Change Initiative (Permafrost\_cci): Permafrost version 3 data  
 3042 products. Centre for Environmental Data Analysis, *date of*  
 3043 *citation*. <http://catalogue.ceda.ac.uk/uuid/8239d5f6263f4551bf2bd100d3ecbead>.

3044 Olson, D. M., Dinerstein, E., Wikramanayake, E. D., Burgess, N. D., Powell, G. V. N.,  
 3045 Underwood, E. C., D'Amico, J. A., Itoua, I., Strand, H. E., Morrison, J. C., Loucks, C. J.,  
 3046 Allnutt, T. F., Ricketts, T. H., Kura, Y., Lamoreux, J. F., Wettengel, W. W., Hedao, P.,  
 3047 Kassem, K. R. (2001). Terrestrial ecoregions of the world: a new map of life on Earth.  
 3048 *Bioscience*, 51(11), 933-938.





## Appendix A

### DRAGANN Gaussian Deconstruction

John Robbins

20151021

Updates made by Katherine Pitts:

20170808

20181218

### Introduction

This document provides a verbal description of how the DRAGANN (Differential, Regressive, and Gaussian Adaptive Nearest Neighbor) filtering system deconstructs a histogram into Gaussian components, which can also be called *iteratively fitting a sum of Gaussian Curves*. The purpose is to provide enough detail for ASAS to create operational ICESat-2 code required for the production of the ATL08, Land and Vegetation product. This document covers the following Matlab functions within DRAGANN:

- mainGaussian\_dragann
- findpeaks\_dragann
- peakWidth\_dragann
- checkFit\_dragann

Components of the k-d tree nearest-neighbor search processing and histogram creation were covered in the document, *DRAGANN k-d Tree Investigations*, and have been determined to function consistently with UTexas DRAGANN Matlab software.

### Histogram Creation

Steps to produce a histogram of nearest-neighbor counts from a normalized photon cloud segment have been completed and confirmed. Figure A.1 provides an example of such a histogram. The development, below, is specific to the two-dimensional case and is provided as a review.

The histogram represents the frequency (count) of the number of nearby photons within a specified radius, as ascertained for each point within the photon cloud. The radius,  $R$ , is established by first normalizing the photon cloud in time (x-axis) and in height (y-axis), i.e., both sets of coordinates (time & height) run from 0 to 1; then an average radius for finding 20 points is determined based on forming the ratio of 20 to the total number of the photons in the cloud ( $N_{total}$ ):  $20/N_{total}$ .

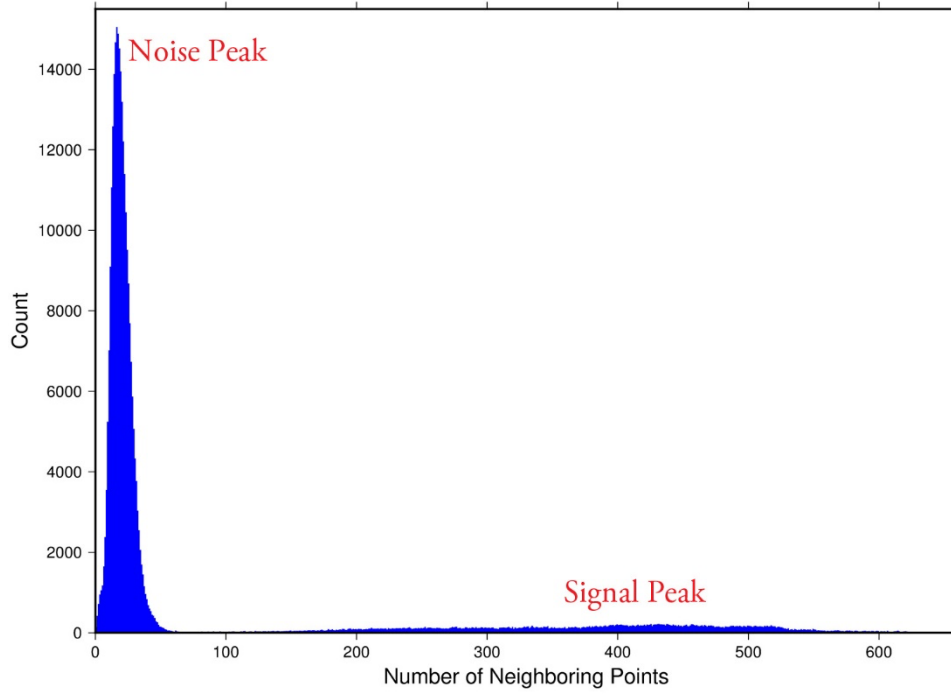


**Figure A.1.** Histogram for Mabel data, channel 43 from SE-AK flight on July 30, 2014 at 20:16.

Given that the total area of the normalized photon cloud is, by definition, 1, then this ratio gives the average area,  $A$ , in which to find 20 points. A corresponding radius is found by the square root of  $A/\pi$ . A single equation describing the radius, as a function of the total number of photons in the cloud (remembering that this is done in the cloud normalized, two-dimensional space), is given by

$$R = \sqrt{\frac{20/N_{total}}{\pi}} \quad (A.1)$$

For the example in Figure A.1,  $R$  was found to be 0.00447122. The number of photons falling into this radius, at each point in the photon cloud, is given along the x-axis; a count of their number (or frequency) is given along the y-axis.

### Gaussian Peak Removal

At this point, the function, `mainGaussian_dragann`, is called, which passes the histogram and the number of peaks to detect (typically set to 10).

This function essentially estimates (i.e., fits) a sequence of Gaussian curves, from larger to smaller. It determines a Gaussian fit for the highest histogram peak, then removes it before determining the fit for the next highest peak, etc. In concept, the process is an iterative sequential-removal of the ten largest Gaussian components within the histogram.

3110 In the process of *sequential least-squares*, parameters are re-estimated when input  
 3111 data is incrementally increased and/or improved. The present problem operates in  
 3112 a slightly reverse way: the data set is fixed (i.e., the histogram), but components  
 3113 within the histogram (independent Gaussian curve fits) are removed sequentially  
 3114 from the histogram. The paper by *Goshtasby & O'Neill* (1994) outlines the concepts.

3115 Recall that a Gaussian curve is typically written as

$$3116 \quad y = a \cdot \exp(-(x - b)^2 / 2c^2) \quad (A.2)$$

3117 where  $a$  = the height of the peak;  $b$  = position of the peak; and  $c$  = width of the bell  
 3118 curve.

3119 The function, `mainGaussian_dragann`, computes the  $[a, b, c]$  values for the ten  
 3120 highest peaks found in the histogram. At initialization, these  $[a, b, c]$  values are set to  
 3121 zero. The process begins by locating histogram peaks via the function,  
 3122 `findpeaks_dragann`.

3123

## 3124 **Peak Finding**

3125 As input arguments, the `findpeaks_dragann` function receives the histogram and a  
 3126 minimum peak size for consideration (typically set to zero, which means all peaks  
 3127 will be found). An array of index numbers (i.e., the “number of neighboring points”,  
 3128 values along x-axis of Figure A.1) for all peaks is returned and placed into the  
 3129 variable `peaks`.

3130 The methodology for locating each peak goes like this: The function first computes  
 3131 the derivatives of the histogram. In Matlab there is an intrinsic function, called `diff`,  
 3132 which creates an array of the derivatives. `Diff` essentially computes the differences  
 3133 along sequential, neighboring values. “ $Y = \text{diff}(X)$  calculates differences between  
 3134 adjacent elements of  $X$ .” [from Matlab Reference Guide] Once the derivatives are  
 3135 computed, then `findpeaks_dragann` enters a loop that looks for changes in the sign  
 3136 of the derivative (positive to negative). It skips any derivatives that equal zero.

3137 For the  $k$ th derivative, the “*next*” derivative is set to  $k+1$ . A test is made whereby if  
 3138 the  $k+1$  derivative equals zero and  $k+1$  is less than the total number of histogram  
 3139 values, then increment “*next*” to  $k+2$  (i.e., find the next negative derivative). The test  
 3140 is iterated until the start of the “down side” of the peak is found (i.e., these iterations  
 3141 handle cases when the peak has a flat top to it).

3142 When a sign change (positive to negative) is found, the function then computes an  
 3143 approximate index location (variable *maximum*) of the peak via

$$3144 \quad \text{maximum} = \text{round}\left(\frac{\text{next}-k}{2}\right) + k \quad (A.3)$$

3145 These values of *maximum* are retained in the peaks array (which can be *grown* in  
3146 Matlab) and returned to the function mainGaussian\_dragann.

3147 Next, back within mainGaussian\_dragann, there are two tests to determine whether  
3148 the first or last elements of the histogram are peaks. This is done since the  
3149 findpeaks\_dragann function will not detect peaks at the first or last elements, based  
3150 solely on derivatives. The tests are:

3151 If ( histogram(1) > histogram(2) && max(histogram)/histogram(1) < 20 ) then  
3152 insert a value of 1 to the very first element of the peaks array (again, Matlab can  
3153 easily “grow” arrays). Here, max(histogram) is the highest peak value across the  
3154 whole histogram.

3155 For the case of the last histogram value (say there are N-bins), we have

3156 If ( histogram(N) > histogram(N-1) && max(histogram)/histogram(N) < 4 ) then  
3157 insert a value of N to the very last element of the peaks array.

3158 One more test is made to determine whether there any peaks were actually found  
3159 for the whole histogram. If none were found, then the function,  
3160 mainGaussian\_dragann, merely exits.

3161

3162 **Identifying and Processing upon the Ten Highest Peaks**

3163 The function, mainGaussian\_dragann, now begins a loop to analyze the ten highest  
3164 peaks. It begins the  $n^{\text{th}}$  loop (where  $n$  goes from 1 to 10) by searching for the largest  
3165 peak among all remaining peaks. The index number, as well as the magnitude of the  
3166 peak, are retained in a variable, called maximum, with dimension 2.

3167 In each pass in the loop, the  $[a,b,c]$  values (see eq. 2) are retained as output of the  
3168 function. The values of  $a$  and  $b$  are set equal to the index number and peak  
3169 magnitude saved in maximum(1) and maximum(2), respectively. The  $c$ -value is  
3170 determined by calling the function, peakWidth\_dragann.

3171 *Determination of Gaussian Curve Width*

3172 The function, peakWidth\_dragann, receives the whole histogram and the index  
3173 number (maximum(1)) of the peak for which the value  $c$  is needed, as arguments.  
3174 For a specific peak, the function essentially searches for the point on the histogram  
3175 that is about  $\frac{1}{2}$  the size of the peak and that is furthest away from the peak being  
3176 investigated (left and right of the peak). If the two sides (left and right) are  
3177 equidistant from the peak, then the side with the smallest value is chosen ( $> \frac{1}{2}$   
3178 peak).

3179 Upon entry, it first initializes  $c$  to zero. Then it initializes the index values left, xL and  
3180 right, xR as index-1 and index+1, respectively (these will be used in a loop,

described below). It next checks whether the  $n^{\text{th}}$  peak is the first or last value in the histogram and treats it as a special case.

At initialization, first and last histogram values are treated as follows:

If first bin of histogram (peak = 1), set left = 1 and xL = 1.

If last bin of histogram, set right =  $m$  and xR =  $m$ , where  $m$  is the final index of the histogram.

Next, a search is made to the left of the peak for a nearby value that is smaller than the peak value, but larger than half of the peak value. A while-loop does this, with the following conditions: (a) left > 0, (b) histogram value at left is  $\geq$  half of histo value at peak and (c) histo value at left is  $\leq$  histo value at peak. When these conditions are all true, then xL is set to left and left is decremented by 1, so that the test can be made again. When the conditions are no longer met (i.e., we've moved to a bin in the histogram where the value drops below half of the peak value), then the program breaks out of the while loop.

This is followed by a similar search made upon values to the right of the peak. When these two while-loops are complete, we then have the index numbers from the histogram representing bins that are above half the peak value. This is shown in Figure A.2.

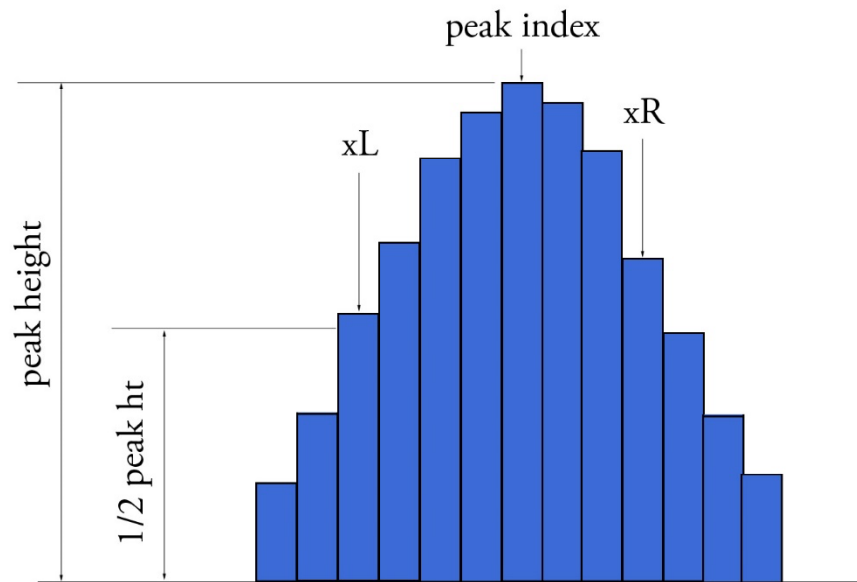


**Figure A.2.** Schematic representation of a histogram showing xL and xR parameters determined by the function peakWidth\_dragann.

A test is made to determine which of these is furthest from the middle of the peak. In Figure A.2, xL is furthest away and the variable x is set to equal xL. The histogram

3204 “height” at  $x$ , which we call  $V_x$ , is used (as well as  $x$ ) in an inversion of Equation A.2  
3205 to solve for  $c$ :

$$3206 \quad c = \sqrt{\frac{-(x-b)^2}{2\ln\left(\frac{V_x}{a}\right)}} \quad (\text{A.4})$$

3207 The function, `peakWidth_dragann`, now returns the value of  $c$  and control returns to  
3208 the function, `mainGaussian_dragann`.

3209 The `mainGaussian_dragann` function then picks-up with a test on whether the  
3210 returned value of  $c$  is zero. If so, then use a value of 4, which is based on an *a priori*  
3211 understanding that  $c$  usually falls between 4 and 6. If the value of  $c$  is not zero, then  
3212 add 0.5 to  $c$ .

3213 At this point, we have the  $[a,b,c]$  values of the Gaussian for the  $n^{th}$  peak. Based on  
3214 these values, the Gaussian curve is computed (via Equation A.2) and it is removed  
3215 (subtracted) from the current histogram (and put into a new variable called  
3216 `newWave`).

3217 After a Gaussian curve is removed from the current histogram, the following peak  
3218 width calculations could potentially have a  $V_x$  value less than 1 from  $a$ . This would  
3219 cause the width,  $c$ , to be calculated as unrealistically large. Therefore, a check is put  
3220 in place to determine if  $a - V_x < 1$ . If so,  $V_x$  is set to a value of  $a - 1$ .

#### 3221 *Numeric Optimization Steps*

3222 The first of the optimization steps utilizes a Full Width Half Max (*FWHM*) approach,  
3223 computed via

$$3224 \quad FWHM = 2c\sqrt{2\ln 2} \quad (\text{A.5})$$

3225 A left range,  $L_r$ , is computed by  $L_r = \text{round}(b - FWHM/2)$ . This tested to make sure it  
3226 doesn't go off the left edge of the histogram. If so, then it is set to 1.

3227 Similarly, a right range,  $R_r$ , is computed by  $R_r = \text{round}(b + FWHM/2)$ . This is also tested  
3228 to be sure that it doesn't go off the right edge of the histogram. If so, then it is set to  
3229 the index value for the right-most edge of the histogram.

3230 Using these new range values, create a temporary segment (between  $L_r$  and  $R_r$ ) of  
3231 the `newWave` histogram, this is called `errorWave`. Also, set three delta parameters  
3232 for further optimization:

3233  $\Delta C = 0.05;$        $\Delta B = 0.02;$        $\Delta A = 1$

3234 The temporary segment, `errorWave` is passed to the function `checkFit_dragann`,  
3235 along with a set of zero values having the same number of elements as `errorWave`,  
3236 the result, at this point, is saved into a variable called `oldError`. The function,  
3237 `checkFit_dragann`, computes the sum of the squares of the difference between two

3238 histogram segments (in this case, errorWave and zeros with the same number of  
3239 elements as errorWave). Hence, the result, oldError, is the sum of the squares of the  
3240 values of errorWave. This function is applied in optimization loops, to refine the  
3241 values of  $b$  and  $c$ , described below.

3242 *Optimization of the  $b$ -parameter.* The do-loop operates at a maximum of 1000 times.  
3243 It's purpose is to refine the value of  $b$ , in 0.02 increments. It increments the value of  
3244  $b$  by DeltaB, to the right, and computes a new Gaussian curve based on  $b+\Delta b$ , which  
3245 is then removed from the histogram with the result going into the variable  
3246 newWave. As before, checkFit\_dragann is called by passing the range-limited part of  
3247 newWave (errorWave) and returning a new estimate of the error (newError) which  
3248 is then checked against oldError to determine which is smaller. If newError is  $\geq$   
3249 oldError, then the value of  $b$  that produced oldError is retained, and the testing loop  
3250 is exited.

3251 *Optimization of the  $c$ -parameter.* Now the value of  $c$  is optimized, first to the left,  
3252 then to the right. It is performed independently of, but similarly, to the  $b$ -parameter,  
3253 using do-loops with a maximum of 1000 passes. These loops increment (to right) or  
3254 decrement (to left) by a value of 0.05 (DeltaC) and use checkFit\_dragann to, again,  
3255 check the quality of the fit. The loops (right and left) kick-out when the fit is found to  
3256 be smallest.

3257 The final, optimized Gaussian curve is now removed (subtracted) from the  
3258 histogram. After removal, a statement "corrects" any histogram values that may  
3259 drop below zero, by setting them to zero. This could happen due to any mis-fit of the  
3260 Gaussian.

3261 The  $n^{\text{th}}$  loop is concluded by examining the peaks remaining in the histogram  
3262 without the peak just processed by sending the  $n^{\text{th}}$ -residual histogram back into the  
3263 function findpeaks\_dragann. If the return of peak index numbers from  
3264 findpeaks\_dragann reveals more than 1 peak remaining, then the index numbers for  
3265 peaks that meet these three criteria are retained in an array variable called these:

- 3266 1. The peak must be located above  $b(n)-2*c(n)$ , and
- 3267 2. The peak must be located below  $b(n)+2*c(n)$ , and
- 3268 3. The height of the peak must be  $< a(n)/5$ .

3269

3270 The peaks meeting all three of these criteria are to be eliminated from further  
3271 consideration. What this accomplishes is eliminate the nearby peaks that have a size  
3272 lower than the peak just previously analyzed; thus, after their elimination, only  
3273 leaving peaks that are further away from the peak just processed and are  
3274 presumably "real" peaks. The  $n^{\text{th}}$  iteration ends here, and processing begins with the  
3275 revised histogram (after having removed the peak just analyzed).

3276



## 3277 Gaussian Rejection

3278 The function `mainGaussian_dragann` returns the  $[a,b,c]$  parameters for the ten  
3279 highest peaks from the original histogram. The remaining code in `dragann` examines  
3280 each of the ten Gaussian peaks and eliminates the ones that fail to meet a variety of  
3281 conditions. This section details how this is accomplished.

3282 First, an approximate area,  $\text{area1}=a*c$ , is computed for each found peak and  $b$ , for all  
3283 ten peaks, being the index of the peaks, are converted to an actual value via  
3284  $b+\text{min}(\text{numptsinrad})-1$  (call this  $\text{allb}$ ).

3285 Next, a rejection is made for all peaks that have any component of  $[a,b,c]$  that are  
3286 imaginary (Matlab `isreal` function is used to confirm that all three components are  
3287 real, in which case it passes).

3288 To check for a narrow noise peak at the beginning of the histogram in cases of low  
3289 noise rates, such as during nighttime passes, a check is made to first determine if the  
3290 highest Gaussian amplitude,  $a$ , within the first 5% of the histogram is  $\geq 1/10$  \* the  
3291 maximum amplitude of all Gaussians. If so, that peak's Gaussian width,  $c$ , is checked  
3292 to determine if it is  $\leq 4$  bins. If neither of those conditions are met in the first 5%,  
3293 the conditions are rechecked for the first 10% of the histogram. This process is  
3294 repeated up to 30% of the histogram, in 5% intervals. Once a narrow noise peak is  
3295 found, the process breaks out of the incremental 5% histogram checks, and the  
3296 noise peak values are returned as  $[a0, b0, c0]$ .

3297 If a narrow noise peak was found, the remaining peak area values,  $\text{area1}$  ( $a*c$ ), then  
3298 pass through a descending sort; if no narrow noise peak was found, all peak areas go  
3299 through the descending sort. So now, the  $[a,\text{allb},c]$ -values are sorted from largest  
3300 "area" to smallest, these are placed in arrays  $[a1, b1, c1]$ . If a narrow noise peak was  
3301 found, it is then appended to the beginning of the  $[a1, b1, c1]$  arrays, such that  $a1 =$   
3302  $[a0\ a1]$ ,  $b1 = [b0\ b1]$ ,  $c1 = [c0\ c1]$ .

3303 In the case that a narrow noise peak was not found, a test is made to check that at  
3304 least one of the peaks is within the first 10% of the whole histogram. It is done  
3305 inside a loop that works from peak 1 to the number of peaks left at this point. This  
3306 loop first tests whether the first (sorted) peak is within the first 10% of the  
3307 histogram; if so, then it simply kicks out of the loop. If not, then it places the loop's  
3308 current peak into a holder (`ihold`) variable, increments the loop to the next peak and  
3309 runs the same test on the second peak, etc. Here's a Matlab code snippet:

```
3310 inds = 1:length(a1);  
3311 for i = 1:length(b1)  
3312     if b1(i) <= min(numptsinrad) + 1/10*max(numptsinrad)  
3313         if i==1  
3314             break;  
3315         end  
3316         ihold = inds(i);  
3317         for j = i:-1:2  
3318             inds(j) = inds(j-1);  
3319         end  
3320         inds(1) = ihold;
```



```

3321         break
3322     end
3323 end
3324

```

3325 The j-loop expression gives the init\_val:step\_val:final\_val. The semi-colon at the end  
3326 of statements causes Matlab to execute the expression without printout to the user's  
3327 screen. When this loop is complete, then the indexes (inds) are re-ordered and  
3328 placed back into the [a1,b1,c1] and area1 arrays.

3329 Next, are tests to reject any Gaussian peak that is entirely encompassed by another  
3330 peak. A Matlab code snippet helps to describe the processing.

```

3331 % reject any gaussian if it is fully contained within another
3332 isR = true(1,length(a1));
3333 for i = 1:length(a1)
3334     ai = a1(i);
3335     bi = b1(i);
3336     ci = c1(i);
3337     aset = (1-(c1/ci).^2);
3338     bset = ((c1/ci).^2*2*bi - 2*b1);
3339     cset = -(2*c1.^2.*log(a1/ai)-b1.^2+(c1/ci).^2*bi^2);
3340     realset = (bset.^2 - 4*aset.*cset >= 0) | (a1 > ai);
3341     isR = isR & realset;
3342 end
3343 a2 = a1(isR);
3344 b2 = b1(isR);
3345 c2 = c1(isR);
3346

```

3347 The logical array isR is initialized to all be true. The i-do-loop will run through all  
3348 peaks. The computations are done in array form with the variables aset,bset,cset all  
3349 being arrays of length(a1). At the bottom of the loop, isR remains "true" when  
3350 either of the conditions in the expression for realset is met (the single "|" is a logical  
3351 "or"). Also, the nomenclature, ".\*" and ".^", denote element-by-element array  
3352 operations (not matrix operations). Upon exiting the i-loop, the array variables  
3353 [a2,b2,c2] are set to the [a1,b1,c1] that remain as "true." [At this point, in our test  
3354 case from channel 43 of East-AK Mable flight on 20140730 @ 20:16, six peaks are  
3355 still retained: 18, 433, 252, 33, 44.4 and 54.]

3356 Next, reject Gaussian peaks whose centers lay within  $3\sigma$  of another peak, unless only  
3357 two peaks remain. The code snippet looks like this:

```

3358 isR = true(1, length(a2));
3359 for i = 1:length(a2)
3360     ai = a2(i);
3361     bi = b2(i);
3362     ci = c2(i);
3363     realset = (b2 > bi+3*ci | b2 < bi-3*ci | b2 == bi);
3364     realset = realset | a2 > ai;
3365     isR = isR & realset;
3366 end
3367 if length(a2) == 2
3368     isR = true(1, 2);
3369 end

```

```

3370     a3 = a2(isR);
3371     b3 = b2(isR);
3372     c3 = c2(isR);
3373

```

3374 Once again, the is \R array is initially set to “true.” Now, the array, realset, is tested  
3375 twice. In the first line, one of three conditions must be true. In the second line, if  
3376 realset is true or  $a2 > a_i$ , then it remains true. At this point, we’ve pared down, from  
3377 ten Gaussian peaks, to two Gaussian peaks; one represents the noise part of the  
3378 histogram; the other represents the signal part.

3379 If there are less than two peaks left, a thresholding/histogram error message is  
3380 printed out. If the lastTryFlag is not set, DRAGANN ends its processing and an empty  
3381 IDX value is returned. The lastTryFlag is set in the preprocessing function which  
3382 calls DRAGANN, as multiple DRAGANN runs may be tried until sufficient signal is  
3383 found.

3384 If there are two peaks left, then set the array [a,b,c] to those two peaks. [At this  
3385 point, in our test case from channel 43 of East-AK Mable flight on 20140730 @  
3386 20:16, the two peaks are: 18 and 433.]

3387

### 3388 **Gaussian Thresholding**

3389 With the two Gaussian peaks identified as noise and signal, all that is left is to  
3390 compute the threshold value between the Gaussians.

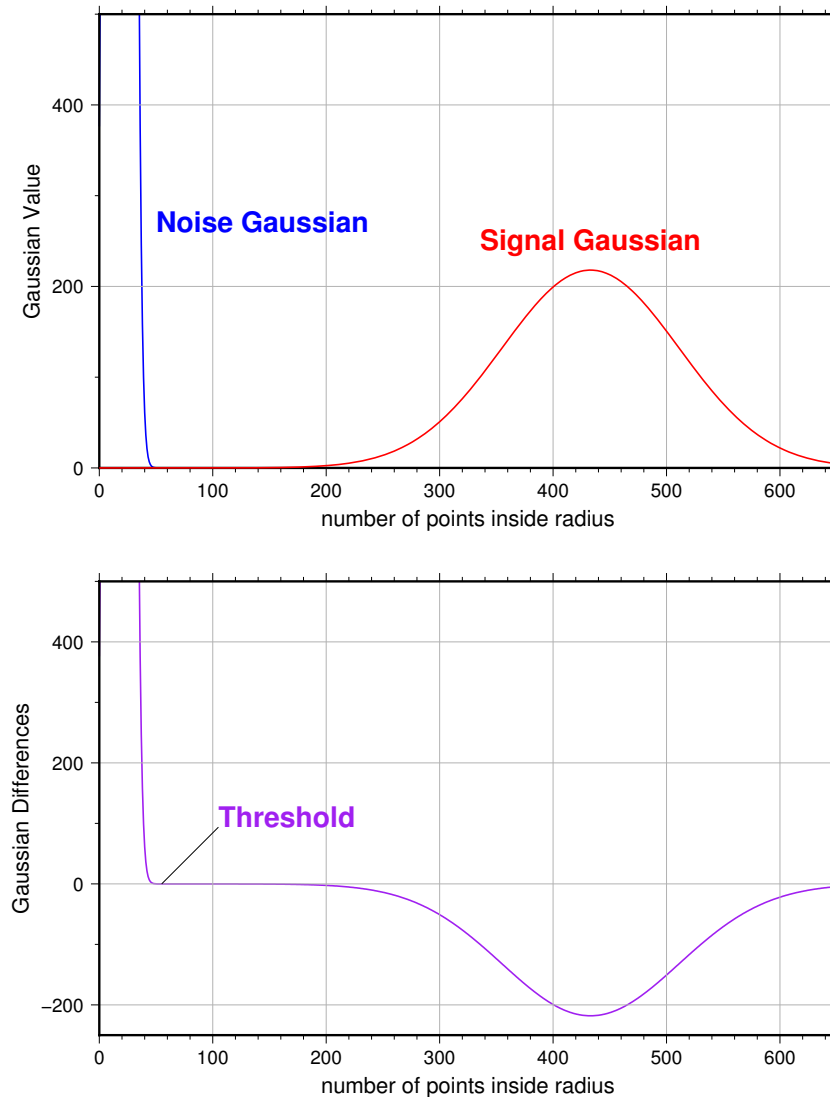
3391 An array of xvals is established running from min(numptsinrad) to  
3392 max(numptsinrad). In our example, xvals has indices between 0 and 653. For each  
3393 of these xvals, Gaussian curves (allGauss) are computed for the two Gaussian peaks  
3394 [a,b,c] determined at the end of the previous section. This computation is performed  
3395 via a function called gaussmaker which receives, as input, the xvals array and the  
3396 [a,b,c] parameters for the two Gaussian curves. An array of heights of the Gaussian  
3397 curves is returned by the function, computed with Equation A.2. In Matlab, the  
3398 allGauss array has dimension 2x654. An array, noiseGauss is set to be equal to the  
3399 1<sup>st</sup> column of allGauss.

3400 An if-statement checks whether the b array has more than 1 element (i.e., consisting  
3401 of two peaks), if so, then nextGauss is set to the 2<sup>nd</sup> column of allGauss, and a  
3402 difference, noiseGauss-nextGauss, is computed.

3403 The following steps are restricted to be between the two main peaks. First, the first  
3404 index of the absolute value of the difference that is near-zero (defined as 1e-8) is  
3405 found, if it exists, and put into the variable diffNearZero. This is expected to be found  
3406 if the two Gaussians are far away from each other in the histogram.

3407 Second, the point (i.e., index) is found of the minimum of the absolute value of the  
3408 difference; this index is put into variable, signchanges. This point is where the sign

3409 changes from positive to negative as one moves left-to-right, up the Gaussian curve  
 3410 differences (noise minus next will be positive under the peak of the noise curve, and  
 3411 negative under the next (signal) curve). Figure A.3 (top) shows the two Gaussian  
 3412 curves. The bottom plot shows their differences.



3413  
 3414 **Figure A.3.** Top: two remaining Gaussian curves representing the noise (blue) and  
 3415 signal (red) portions of the histogram in F1gure A.1. Bottom: difference noise –  
 3416 signal of the two Gaussian curves. The threshold is defined as the point where the  
 3417 sign of the differences change.

3418 If there is any value stored in diffNearZero, that value is now saved into the variable  
3419 threshNN. Else, the value of the threshold in signchanges is saved into threshNN,  
3420 concluding the if-statement for b having more than 1 element.

3421 An else clause ( $b \neq 1$ ), merely sets threshNN to  $b+c$ , i.e., 1-standard deviation away  
3422 from mean of the (presumably) noise peak.

3423 The final step is mask the signal part of the histogram where all indices above the  
3424 threshNN index are set to logical 1 (true). This is applied to the numptsinrad array,  
3425 which represents the photon cloud. After application, dragann returns the cloud  
3426 with points in the cloud identified as “signal” points.

3427 The Matlab code has a few debug statements that follow, along with about 40 lines  
3428 for plotting.

3429

## 3430 **References**

3431 Goshtasby, A & W. D. O'Neill, Curve Fitting by a Sum of Gaussians, *CVGIP: Graphical*  
3432 *Models and Image Processing*, V. 56, No. 4, 281-288, 1994.

3433 Ran, Y., Li, X., Cheng, G., Che, J., Aalto, J., Karjalainen, O., Hjort, J., Luoto, M., Jin, H.,  
3434 Obu, J., Hori, M., Yu, Q., and Chang, X.: New high-resolution estimates of the  
3435 permafrost thermal state and hydrothermal conditions over the Northern  
3436 Hemisphere, *Earth Syst. Sci. Data*, 14, 865–884, [https://doi.org/10.5194/essd-14-](https://doi.org/10.5194/essd-14-865-2022)  
3437 865-2022, 2022.